THE ROLE OF AUTOTRANSPORTER PROTEINS IN *BURKHOLDERIA PSEUDOMALLEI* PATHOGENESIS

Cristine Gomes Campos

A dissertation submitted to the faculty of the University of North Carolina at Chapel Hill in partial fulfillment of the requirements for the degree of Doctor of Philosophy in the Department of Microbiology and Immunology of the School of Medicine.

Chapel Hill
2013

Approved by:

Peggy Cotter, Ph.D.

Thomas Kawula, Ph.D.

Virginia Miller, Ph.D.

Anthony Richardson, Ph.D.

Rita Tamayo, Ph.D.

ABSTRACT

CRISTINE GOMES CAMPOS: The Role of Autotransporter proteins in *Burkholderia pseudomallei* Pathogenesis
(Under the direction of Peggy A. Cotter, Ph.D.)

Burkholderia pseudomallei is a tier 1 select agent, and the causative agent of melioidosis, a disease that ranges from chronic abscesses to fulminant pneumonia and septic shock, which can be rapidly fatal. Autotransporters (ATs) are outer membrane proteins belonging to the Type V Secretion System family, and many have been shown to play crucial roles in pathogenesis in other bacterial species. The genome of *B. pseudomallei* strain 1026b encodes two putative classical ATs, and nine putative trimeric AT proteins.

The open reading frame *bcaA* in *B. pseudomallei* strain 1026b is predicted to encode a classical autotransporter protein with a passenger domain that contains a subtilisin-related domain. Immediately 3′ to *bcaA* is *bcaB*, which encodes a putative prolyl 4-hydroxylase. To investigate the role of these genes in pathogenesis, large in-frame deletion mutations of *bcaA* and *bcaB* were constructed in strain Bp340, an efflux pump mutant derivative of the melioidosis clinical isolate 1026b. Comparison of Bp340Δ*bcaA* and Bp340Δ*bcaB* to wild type *B. pseudomallei in vitro* demonstrated similar adherence to A549 lung epithelial cells, but the mutant strains were defective in their ability to invade these cells and to form plaques. In a BALB/c mouse model of intranasal infection, a similar bacterial burden was observed after 48 hours in the lungs and liver of mice infected with Bp340Δ*bcaA*, Bp340Δ*bcaB* and wild type bacteria.

However, significantly fewer bacteria were recovered from the spleen of Bp340Δ*bcaA*-infected mice, supporting a role for this AT in dissemination or in survival from the site of infection to the spleen.

Using a bioinformatics approach, we annotated eight putative domains within each trimeric AT protein, excluding the well-studied BimA, and found short repeated sequences unique to *Burkholderia* species, as well as an unexpectedly high proportion of ATs with extended signal peptide regions (ESPRs). To characterize the role of trimeric ATs in pathogenesis, we constructed disruption or deletion mutations in each of eight AT-encoding genes and evaluated the resulting strains for adherence, invasion, and plaque formation in A549 cells. Five of the ATs, BoaA, BoaB, BpaA, BpaC, and BpaD, contribute to adherence, and four of the ATs, BpaA, BpaC, BpaE, and BpaF, are necessary for efficient internalization in A549 cells. Using a BALB/c mouse model of infection, we then determined the contribution of each AT to bacterial burden in lungs, liver, and spleen. At 48 hours post-inoculation, only one strain, Bp340::pD*bpaC*, demonstrated a defect in dissemination and/or survival in the liver, indicating that BpaC is required for wild-type virulence in this model.

ACKNOWLEGEMENTS

I would like to thank Dr. Peggy A. Cotter, my graduate student advisor, for generously providing me with the opportunity to work under her supervision, and for all she taught me. From sterile technique to infection models, you have provided me with the foundation to all of my microbiology knowledge. I will always be thankful.

I would like to thank present and past member of the Cotter laboratory for all of their help, especially Brandt Burgess, Sabrina Adelaine, Robin Hulbert, Matthew Byrd, and Eliza Mason for the countless hours of scientific and non-scientific conversation that were so instrumental in getting me through graduate school.

I would also like to thank Dr. Herbert Schweizer and Dr. Tung Hoang, as well as their graduate students, for all of their help. Without you this project would not have been possible. My heartfelt thanks also goes to Dr. Todd French and Dr. Erin Folchi for helping me through this journey. Dr. Sharon Taft-Benz, thank you for teaching me so much in the BSL-3, and for all your help. Your kindness and patience will never be forgotten.

Finally I must thank my family, especially my mom Fatima Gomes and my dad Ivan Campos for all of their encouragement and patience through the challenging times. A special thanks to my Krav Maga family for allowing me to punch my way to sanity so many times, and to all of my friends (you know who you are) who stuck around even though I was always too busy. You are all in my heart, thank you for seeing me through this.

TABLE OF CONTENTS

LIST OF TABLES

LIST OF FIGURES

LIST OF ABBREVIATIONS

aa	amino acid
AT	autotransporter
Bca	*Burkholderia* classical autotransporter
Boa	*Burkholderia* oligomeric coiled-coil adhesin
Bpa	*Burkholderia pseudomallei* autotransporter
CFU	colony forming unit
ESPR	extended signal peptide region
LPS	lipopolysaccharides
Mb	megabase pair
MNGC	multinucleated giant cells
MOI	multiplicity of infection
ORF	open reading frame
T3SS	Type III Secretion System
T6SS	Type Six Secretion System

CHAPTER I

Introduction

BURKHOLDERIA CLASSIFICATION AND EPIDEMIOLOGY

Burkholderia pseudomallei is a Gram-negative, rod-shaped, non-spore forming, motile saprotrophic bacterium with a 7.24 megabase pair (Mb) genome divided into two chromosomes (90). The large 4.07 Mb chromosome (chromosome 1) contains a high proportion of coding sequences related to metabolic functions, such as macromolecule biosynthesis and amino acid (aa) metabolism, and the small 3.17 Mb chromosome (chromosome 2) contains coding sequences for accessory proteins and a vast number of coding sequences predicted to encode proteins of unknown function (37). *B. pseudomallei* often forms dry, wrinkly colonies on Ash-down's agar, but colony morphology can vary considerably (15). Seven major colony morphotypes have been described, and morphology switching appears to occur in response to different environmental cues, including stress and interactions with epithelial cells or macrophages. Morphology switching has also been proposed to influence intracellular survival, and antibiotic resistance (79). *B. pseudomallei* is a hardy organism capable of surviving harsh environmental conditions including, but not limited to wide temperature changes and dehydration (18), prolonged nutritional deficiency (91), antiseptics and detergents (30), as well as acidic environments (23).

B. pseudomallei infects a wide-variety of organisms, including human and non-human mammals (19, 72). It causes Melioidosis, a disease that can range from chronic abscesses to fulminant pneumonia and septic shock and which can be rapidly fatal. First described by Dr. Whitmore, an army pathologist working in Burma, in 1912 (88), it has often been called the "great mimicker", because it can present a vast array of clinical signs and symptoms. The disease can vary from an acute septic illness to a chronic infection with the persistence of symptoms for over two months. Primary clinical presentation varies from pneumonia to genitourinary infection, skin infections, bacteremia without focus, septic arthritis, internal-organ abcesses, suppurative parotitis and brain stem encephalitis (89). Infections can be a result of percutaneous inoculation, inhalation, or ingestion. Melioidosis primarily affects people who have been exposed to environments containing *B. pseudomallei* (90); no reports of transmission between animals and humans have been described so far (9). Several conditions have been correlated with predisposition to *B. pseudomallei* infection in humans, including diabetes mellitus, impaired cellular immunity, leukemia/lymphomas, HIV infection, renal disease, and afflictions such as alcoholism and perenteral drug abuse (9). Melioidosis cases spike during the rainy season in the tropics, being highest during monsoonal rain season. Recurrence of disease is common, especially in the first year after the initial clinical presentation. Several of the reoccurrence cases are due to reinfection, while the remainder due to relapse from a persistent focus of infection (50). The period between exposure and clinical manifestation can be as long as 62 years (56). *B. pseudomallei* is resistant to most antibiotics, succesptible only to chloramphenicol, trimethroprim-sulfamethoxazole and a few others, which makes treatment of melioidosis difficult and eradication of the

disease without a vaccine (none has been developed to date) nearly impossible (87). Studies suggest that the intracellular nature of *B. pseudomallei* when infecting eukaryotic cells means that a vaccine will most likely not provide complete immunological protection, unless T-cell immunity could be engaged (40), which makes the task of developing the vaccine even more difficult. Endemic to southeast Asia, and northern Australia, sporadic cases and clusters have been reported in Brazil (64), the Caribbean, Africa, the Middle East and even in the United States (22).

BURKHOLDERIA PATHOGENESIS

A protein microarray containing over a thousand *B. pseudomallei* surface exposed proteins was probed with sera from several melioidosis patients, and 170 immunoreactive proteins were identified. Amongst these were autotransporter proteins, lipoproteins, flagellin, and stress response proteins (27). To date only a limited number of virulence regulators and factors have been characterized for *B. pseudomallei* including quorum sensing and two-component regulatory system regulators, capsular polysaccharides, Type III Secretion System (T3SS), Type VI Secretion System (T6SS), lipopolysaccharides (LPS), flagella, Type IV pilli, and one Type V Secretion System protein named BimA. How these proteins are involved in pathogenesis is unclear and still under investigation.

PUTATIVE *BURKHOLDERIA* VIRULENCE REGULATORS

Quorum sensing

Quorum sensing is a form of cell to cell communication that is population density mediated, and depends on the release and therefore detection of signaling molecules such as *N-decanoyl*-homoserine-lactone (90). The *B. pseudomallei* genome encodes three LuxI, and five LuxR quorum-sensing homologues. Disruption of these genes in *B.*

pseudomallei led to decrease virulence in the Syrian hamster and BALB/c models of infection (81). Quorum sensing is known to regulate the expression of several genes. Metalloproteases, phospholipases, and siderophores are among a few genes that were affected by *luxI* and *luxR* mutations in *B. pseudomallei* (82). The BpeAB-OprB multidrug efflux system found in *B. pseudomallei* is also involved in quorum sensing, since it is responsible for the extracellular secretion of homoserine-lactones. Deletion of the system caused reduced levels of cell invasion, and cytotoxicity for both epithelial and macrophage cell lines, and the same were partially restored by addition of homoserine-lactones (14). A second quorum sensing system using 4-hydroxy-3-methyl-2-alkylquinolone signaling molecules has also been described (83), however its function is yet to be determined.

Two-component regulatory system

A complex two-component transcriptional regulatory system (VirAG) is found in *B. pseudomallei*, but little is known about the role this system has in this bacterium pathogenesis (11, 78). Two-component regulatory systems allow bacteria to sense and respond to changes in may different environmental conditions. Typically, they consist of a membrane-bound histidine kinase that senses an environmental stimulus, and a corresponding response regulator that mediates expression of target genes (52). VirAG is encoded immediately upstream of T6SS-1 gene cluster in *B. pseudomallei*, and it has been shown to transcriptionally activate T6SS-1 genes while inside a macrophage prior to escape from the phagosome (11, 78). It also induces expression and export to the extracellular millieu of Hcp1, a protein that is an integral surface-associated component of the T6SS apparatus commonly found in the supernatants of bacteria that express a

functional T6SS (11). T6SS-1 is a virulence factor in the Syrian hamster model of melioidosis, however the environmental cues sensed by the VirAG system is still unknown, and whether transcription activation of T6SS-1 genes occurs directly or indirectly via VirAG is still under investigation (11).

PUTATIVE *BURKHOLDERIA* VIRULENCE FACTORS

Capsular polysaccharides

B. pseudomallei has an extracellular capsular polysaccharide, -3)-2-*O*-acetyl-6-deoxy-β-$_{D}$-*manno*-heptopyranose-(1-, that has been shown to be required for virulence in animal models (61). Although three other morphologically distinct variants have been observed by electron microscopy, little is known about these variants or their role in disease (58). In the presence of serum, capsule expression is increased, and the addition of purified *B. pseudomallei* capsule to serum bactericidal assays will increase the survival of a serum-sensitive strain (SLR5). Phagocytosis is also increased for capsule-deficient mutants when compared to wild type in the presence of human serum (62). Deposition of the complement C3b is enhanced in capsule mutants, suggesting that the persistence of *B. psedomallei* in the blood may be due to prevention of opsonization by complement in the blood (47).

Type III Secretion System

T3SS is a syringe-like secretion apparatus that when triggered by contact with host cells, translocates effector proteins into these host cells. Three T3SS have been identified in *B. pseudomallei* (3, 60, 77). T3SS-1 and T3SS-2 are both similar to plant pathogens T3SS, while T3SS-3 or T3SS$_{Bsa}$, is similar to the *Shigella* Mxi-Spa and

Salmonella SPI-1 T3SS, and highly conserved across *Burkholderia* species. T3SS can translocate multiple effectors into the host cell cytosol, where these effectors can subvert cell signaling to the benefit of the bacterium (31). $T3SS_{Bsa}$ has been implicated in invasion, escape from endosomes, intracellular survival, and evasion of autophagy (32) in *B. pseudomallei*. $T3SS_{Bsa}$ is required for virulence in hamster and mouse infection models (75, 86), but the complete repertoire of Bsa effectors remain largely unknown. Recently, the $T3SS_{Bsa}$ has been shown to be required for plaque formation and endosome escape, but dispensable for invasion (29).

Type VI Secretion System

Genes encoding a fairly recently discovered secretion system named T6SS have been identified in over one-fourth of all sequenced Gram-negative bacteria. T6SS function appears to be diverse and to be involved in interbacterial competition (67), increasing bacterial fitness in the environment, as well as being involved in pathogenesis (41). *B. pseudomallei* has six T6SSs. T6SS-1 has been shown to be necessary for virulence in an acute model of melioidosis and contributes to lethality in hamsters in *Burkholderia mallei* (a clonal descendent of *B. pseudomallei* that has undergone genome decay losing its capability for environmental survival) (66, 67). T6SS-1 has also recently been shown to be responsible for multinucleated giant cell (MNGC) formation in RAW264 cells (11), and wild-type levels of cell invasion and intracellular survival was observed in the same cell line when T6SS-1 was mutated (68).

Lipopolysaccharides

Lipopolysaccharides (LPS) are endotoxins found in the outer membrane of Gram-negative bacteria that can elicit strong immune responses (59). *B. pseudomallei* LPS

differ from other LPS, for it exibits weaker murine pyrogenic activity when compared to enterobacterial LPS but stronger mitogenic activity in murine splenocytes (53). Recognition of LPS by the host is crucial for innate immune response to Gram-negative bacteria through activation of the pattern-recognition receptor Toll-like receptor (TLR) 4 (8). *B. pseudomallei* infections have been shown to not elicit a TLR4 response, and little is known about how *B. pseudomallei* LPS plays a role in pathogenesis. *B. thailandensis*, a non-pathogenic bacterium (sometimes associated with human disease) that has a highly similar genome to *B. pseudomallei* (44), has a nearly identical LPS to *B. pseudomallei*. Both bacteria have a similar immunoblot profile against pooled sera from patients with melioidosis, and also similar LPS shedding profile, suggesting that LPS may not be involved in virulence and pathogenesis (1, 2).

Flagella and Type IV pili

B. pseudomallei is flagellated and motile. No difference was seen in the ability of wild type and aflagellate mutant *B. pseudomallei* to invade and replicate in human cells *in vitro* (20). In a diabetic rat and Syrian hamster infection study no difference between wild type and the aflagellate mutant was seen (24), however another study suggested that the aflagellate mutant was less virulent in a BALB/c intranasal model of infection (20).

Type IV pili have been shown to function as adhesins, and have an important role in virulence in many Gram-negative bacteria. Electron microscopy has shown the presence of flagella and variable expression of pili on *B. pseudomallei (85)*. Bioinformatic analysis has shown 13 gene clusters believed to be involved in fimbriae and type IV pili expression (37) in the *B. pseudomallei* clinical strain K96243. Currently there are conflicting data on the importance of flagella in virulence (24, 39), but one of

the eight type IV pili associated loci found in *B. pseudomallei*, which encodes *pilA*, when mutated was shown to cause decreased adhesion to epithelial cells, and reduced virulence in an intranasal route of infection BALB/c model (26).

BURKHOLDERIA PUTATIVE AUTOTRANSPORTER PROTEINS

Autotransporters (ATs) are outer membrane proteins belonging to the Type V Secretion System family, the largest family of extracellular proteins in Gram-negative bacteria (34). The AT secretion mechanism is remarkably simple, comprising a signal sequence, which targets the protein for secretion across the inner membrane through the Sec-system, a passenger domain (the secreted mature protein), and a C-terminal β-barrel domain that forms the pore in the outer membrane through which the passenger domain passes to the cell surface (33). Secretion of AT proteins have long been believed to be an energy independent, self- sufficient process (35). Many ATs have been shown to be virulence factors playing crucial roles in how bacteria cause disease (6, 10, 43).

Classical and trimeric autotransporter protein secretion

The AT family is divided into classical and trimeric autotransporter proteins. The C-terminal domain of classical ATs consist of 250 to 300 aa residues that form the β-barrel that is inserted into the outer membrane and facilitates the translocation of the N-terminal passenger domain to the surface (35). Once at the bacterial surface, classical ATs may be processed and released into the extracellular milieu (e.g. the serine protease Esp^P from *Escherichia coli*) (10), or cleaved but remain in contact with the bacterial surface through noncovalent interactions with the β-domain or cell surface (e.g. Pertactin

from *Bordetella* and the adhesin involved in diffuse adherence of *E. coli* (AIDA-I)) (6, 48).

Trimeric ATs require three proteins to form a functional unit, with the C-terminal 67 to 76 aa of each monomer contributing one-third of the β-barrel (21). Once at the bacterial surface, trimeric AT passenger domains remain intact as a large protein with a membrane bound C-terminus, and an N-terminal domain extending into the extracellular millieu (e.g. the adhesin protein from *Yiersinia* species YadA, and the adhesin from *Haemophilus influenzae* Hia) (63, 73). Oligomerization of the passenger domains occurs via a coiled-coil domain believed to be ~70 to 100 residues from the C-terminal end of the protein (36).

The mechanism of classical and trimeric AT translocation across the outer membrane has been the focus of constant intense debate. According to the initial model, the β-barrel domain is inserted into the outer membrane, and mediates the translocation of the passenger domain covalently linked to it without the aid of any other proteins (54, 57). Recently several autotransporters (e.g. AIDA-I, and the *Nisseria meningitides* immunoglobin A1 (IgA1)) have been shown to require the Bam complex for biogenesis (55, 84); depletion of BamA abrogates secretion of mature AT passenger domains to the exterior of the cell, and BamD has also been implicated in autotransporter biogenesis (65). How BamA and BamD are involved in inserting the autotransporter β-barrel into the outer membrane is still unknown, but models involving periplasmic chaperones have been proposed (45).

Once the β-barrel is inserted into the outer membrane, secretion of the passenger domain occurs. Several different models have been described for the mechanism of

passenger domain secretion, but the hairpin model holds the largest amount of supporting evidence currently. A hairpin structure is formed at the most C-terminal portion of the passenger domain, and maintained until the N-terminus of the passenger domain passes through the β-barrel (42, 49).

Following passenger domain secretion, some classical autotransporters are cleaved and released from their β-domain. Some mechanisms of passenger domain proteolysis have been elucidated. For example, the autotransporter IcsA required for intra- and inter-cellular motility in *Shigella flexneri* is cleaved by an exogenous protease (69). AIDA-I on the other hand is processed by autoproteolysis by two acidic residues that are contained within the passenger domain (16).

Classical autotransporter passenger domains

Although the β-domains generally show aa sequence conservation, which is consistent with their conserved function, passenger domains can vary widely reflecting their many roles. The IgA1 protease from *N. meningitides* for example is a serine protease, with a trypsin-like active domain (57) that is responsible for outer membrane release of this classical autotransporter protein. The mature protein is then capable of cleaving human-IgA1, and has a role in human mucosal colonization (43). IgA1 has also been shown to aid in trans-epithelial trafficking in T84 (human colon epithelial cells) monolayers, and to cleave LAMP1 (major integral glycoprotein of lysosomes) contributing to intracellular reproduction of the bacteria (38, 51).

Pertactin, an AT of a few *Bordetella* species, has a cleaved mature passenger domain that remains noncovalently associated with its β-barrel (17). Although a function has not been clearly defined for pertactin, it has been implicated in adhesion (48),

inhibition of bacterial uptake in human tracheal epithelial cells (5), and cytotoxicity in phagocytic cells (28). AIDA-I, an adhesin found in some diffusely adherent *E. coli* strains (7), like pertactin remains associated with its β-barrel, and electron microscopy has shown it to be evenly distributed around the cell surface. AIDA-I (α-domain), which mediates the specific attachment of bacteria to target cells, in order to be fully functional, needs to be post-translationally modified by heptose residues at multiple sites (46). Also found in *E. coli* is EspP, an autotransporter protein of the enterohaemorrhagic (EHEC) O157:H7 strain. This AT is a protease capable of cleaving pepsin A and human coagulation factor V, and is believed to contribute to the mucosal haemorrhage observed in patients with haemorrhagic colitis (10).

Trimeric autotransporter passenger domains

The trimeric AT *Yersinia* adhesin A (YadA) found in some *Yersinia* species was first described because of its capacity to promote auto-agglutination of *Y. enterocolitica* and *Y. pseudotuberculosis*, as well as adherence to many substrates including epithelial cells, extracellular matrix, collagen, cellular but not plasma fibronectin, and laminin (36). The main function of Yad-A is believed to lie in its ability to confer resistance to bactericidal activity of human serum by binding factor H (13). Non-typeable and encapsulated *Haemophilus influenzae* have Hia (*H. influenzae* adhesin), a trimeric autotransporter that has been shown to contribute to adherence to epithelial cells, and also to have two binding domains that interact with an as yet unknown host receptor with different affinities (71).

B. pseudomallei putative autotransporter proteins

B. pseudomallei strain K96243 contains genes predicted to encode nine trimeric ATs and two classical ATs. These are conserved across other *B. pseudomallei* genomes and some homologues are found in *B. mallei*, *B. thailandensis*, and *B. gladioli* strains. BPSS0962 (*bcaA*) and BPSL2237 are putative classical autotransporters predicted to function as a putative serine protease (12) and a lipase/esterase, respectively (UniProtKB/TrEMBL). BPSL1631, BPSL1705 (*boaB*), BPSL2063, BPSS0088, BPSS0796 (*boaA*), BPSS0908, BPSS1434 (*bpaA*), BPSS1439 and BPSS1492 (*bimA*) are all putative trimeric autotransporters.

The only well characterized of these genes is *bimA*, which encodes *Burkholderia* intracellular motility A (BimA), a trimeric autotransporter that is localized at the pole of the bacterium and binds monomeric actin, stimulating actin polymerization and the formation of actin tails (74). *bimA* is the last gene in an operon, and is preceded by a gene encoding a glycosyl-transferase, which has been proposed to post-translationally modify BimA, and perhaps to be required for full activity of the protein (76). Mutation of *bimA* abolishes actin-mediated motility of intracellular bacteria, as well as actin tail formation. BimA contains proline-rich motifs and Wiskott-Aldrich syndrome protein homology-2 (WASP-2) domains, which are associated with actin-binding and motility (76). A 13 aa repeat region in BimA has been shown to be required for intracellular spread, but not for actin binding and polymerization. Regions of BimA necessary for for actin binding and actin polymerization have also been well defined, and characterized (70). To date no studies have shown if BimA contributes to pathogenesis in murine models of melioidosis.

Two trimeric ATs BoaA and BoaB have been expressed in *E. coli* and shown to be displayed on the bacterial surface and promote attachment to epithelial cell lines. *B. pseudomallei* strains with mutations in *boaA* and *boaB* exhibited reduced adherence to epithelial cells, but no growth defect in phagocytic cell lines (4). Although this suggests these genes have a role in virulence, animal studies are required to establish the role of BoaA and BoaB in pathogenesis. The trimeric AT BpaA head domain crystal structure has been resolved (25), but its function remains to be elucidated.

Serum from 21 *B. pseudomallei* infected patients were used to probe a K96243 expression library, and five autotransporter proteins (BPSL2036, BPSS0908, BoaA, BPSS1439 and BimA) were shown to be potentially immunogenic during human melioidosis (80). A protein microarray probed with pooled melioidosis patients sera identified BPSS0088, BoaA, BpaA and BimA as also having the ability to interact with melioidosis-specific antibodies (27), further suggesting that *B. pseudomallei* autotransporters play a role in pathogenesis.

Little is known about how *B. pseudomallei* causes disease. The bacterium is able to invade and replicate in phagocytic, and non-phagocytic cells, and following T3SS-mediated endosomal escape, replicates in the cytoplasm of eukaryotic cells and spreads from cell-to-cell without ever leaving the cytoplasm (29, 75). One *B. pseudomallei* T6SS has been shown to mediate MNGC formation, allowing the bacteria to freely spread form cell to cell using BimA for actin-mediated motility (76). The overall goal of this study was to determine the role of putative autotransporters encoded by *B. pseudomallei* in pathogenesis.

References

1. **Anuntagool, N., P. Intachote, V. Wuthiekanun, N. J. White, and S. Sirisinha. 1998. Lipopolysaccharide from nonvirulent Ara+ Burkholderia pseudomallei isolates is immunologically indistinguishable from lipopolysaccharide from virulent Ara- clinical isolates. Clin Diagn Lab Immunol 5:225-229.**

2. **Anuntagool, N., T. Panichakul, P. Aramsri, and S. Sirisinha. 2000. Shedding of lipopolysaccharide and 200-kDa surface antigen during the in vitro growth of virulent Ara- and avirulent Ara+ Burkholderia pseudomallei. Acta tropica 74:221-228.**

3. **Attree, O., and I. Attree. 2001. A second type III secretion system in Burkholderia pseudomallei: who is the real culprit? Microbiology 147:3197-3199.**

4. **Balder, R., S. Lipski, J. J. Lazarus, W. Grose, R. M. Wooten, R. J. Hogan, D. E. Woods, and E. R. Lafontaine. Identification of Burkholderia mallei and Burkholderia pseudomallei adhesins for human respiratory epithelial cells. BMC microbiology 10:250.**

5. **Bassinet, L., P. Gueirard, B. Maitre, B. Housset, P. Gounon, and N. Guiso. 2000. Role of adhesins and toxins in invasion of human tracheal epithelial cells by Bordetella pertussis. Infection and immunity 68:1934-1941.**

6. **Benz, I., and M. A. Schmidt. 1992. AIDA-I, the adhesin involved in diffuse adherence of the diarrhoeagenic Escherichia coli strain 2787 (O126:H27), is synthesized via a precursor molecule. Mol Microbiol 6:1539-1546.**

7. **Benz, I., and M. A. Schmidt. 1989. Cloning and expression of an adhesin (AIDA-I) involved in diffuse adherence of enteropathogenic Escherichia coli. Infection and immunity 57:1506-1511.**

8. **Beutler, B., and E. T. Rietschel. 2003. Innate immune sensing and its roots: the story of endotoxin. Nat Rev Immunol 3:169-176.**
9. **Brett, P. J., and D. E. Woods. 2000. Pathogenesis of and immunity to melioidosis. Acta tropica 74:201-210.**

10. **Brunder, W., H. Schmidt, and H. Karch. 1997. EspP, a novel extracellular serine protease of enterohaemorrhagic Escherichia coli O157:H7 cleaves human coagulation factor V. Mol Microbiol 24:767-778.**

11. **Burtnick, M. N., P. J. Brett, S. V. Harding, S. A. Ngugi, W. J. Ribot, N. Chantratita, A. Scorpio, T. S. Milne, R. E. Dean, D. L. Fritz, S. J. Peacock, J. L. Prior, T. P. Atkins, and D. Deshazer. The cluster 1 type VI secretion system is a major virulence determinant in Burkholderia pseudomallei. Infection and immunity 79:1512-1525.**

12. **Campos, C. G., L. Borst, and P. A. Cotter. Characterization of BcaA, a putative classical autotransporter protein in Burkholderia pseudomallei. Infection and immunity.**

13. **Casutt-Meyer, S., F. Renzi, M. Schmaler, N. J. Jann, M. Amstutz, and G. R. Cornelis. Oligomeric coiled-coil adhesin YadA is a double-edged sword. PLoS One 5:e15159.**

14. **Chan, Y. Y., and K. L. Chua. 2005. The Burkholderia pseudomallei BpeAB-OprB efflux pump: expression and impact on quorum sensing and virulence. J Bacteriol 187:4707-4719.**

15. **Chantratita, N., V. Wuthiekanun, K. Boonbumrung, R. Tiyawisutsri, M. Vesaratchavest, D. Limmathurotsakul, W. Chierakul, S. Wongratanacheewin, S. Pukritiyakamee, N. J. White, N. P. Day, and S. J. Peacock. 2007. Biological relevance of colony morphology and phenotypic switching by Burkholderia pseudomallei. J Bacteriol 189:807-817.**

16. **Charbonneau, M. E., J. Janvore, and M. Mourez. 2009. Autoprocessing of the Escherichia coli AIDA-I autotransporter: a new mechanism involving acidic residues in the junction region. J Biol Chem 284:17340-17351.**

17. **Charles, I., N. Fairweather, D. Pickard, J. Beesley, R. Anderson, G. Dougan, and M. Roberts. 1994. Expression of the Bordetella pertussis P.69 pertactin adhesin in Escherichia coli: fate of the carboxy-terminal domain. Microbiology 140 (Pt 12):3301-3308.**

18. **Chen, Y. S., S. C. Chen, C. M. Kao, and Y. L. Chen. 2003. Effects of soil pH, temperature and water content on the growth of Burkholderia pseudomallei. Folia Microbiol (Praha) 48:253-256.**

19. **Cheng, A. C., and B. J. Currie. 2005. Melioidosis: epidemiology, pathophysiology, and management. Clinical microbiology reviews 18:383-416.**

20. **Chua, K. L., Y. Y. Chan, and Y. H. Gan. 2003. Flagella are virulence determinants of Burkholderia pseudomallei. Infection and immunity 71:1622-1629.**

21. Cotter, S. E., N. K. Surana, and J. W. St Geme, 3rd. 2005. Trimeric autotransporters: a distinct subfamily of autotransporter proteins. Trends Microbiol 13:199-205.

22. Currie, B. J., D. A. Dance, and A. C. Cheng. 2008. The global distribution of Burkholderia pseudomallei and melioidosis: an update. Trans R Soc Trop Med Hyg 102 Suppl 1:S1-4.

23. Dejsirilert, S., E. Kondo, D. Chiewsilp, and K. Kanai. 1991. Growth and survival of Pseudomonas pseudomallei in acidic environments. Jpn J Med Sci Biol 44:63-74.

24. DeShazer, D., P. J. Brett, R. Carlyon, and D. E. Woods. 1997. Mutagenesis of Burkholderia pseudomallei with Tn5-OT182: isolation of motility mutants and molecular characterization of the flagellin structural gene. J Bacteriol 179:2116-2125.

25. Edwards, T. E., I. Phan, J. Abendroth, S. H. Dieterich, A. Masoudi, W. Guo, S. N. Hewitt, A. Kelley, D. Leibly, M. J. Brittnacher, B. L. Staker, S. I. Miller, W. C. Van Voorhis, P. J. Myler, and L. J. Stewart. Structure of a Burkholderia pseudomallei trimeric autotransporter adhesin head. PLoS One 5.

26. Essex-Lopresti, A. E., J. A. Boddey, R. Thomas, M. P. Smith, M. G. Hartley, T. Atkins, N. F. Brown, C. H. Tsang, I. R. Peak, J. Hill, I. R. Beacham, and R. W. Titball. 2005. A type IV pilin, PilA, Contributes To Adherence of Burkholderia pseudomallei and virulence in vivo. Infection and immunity 73:1260-1264.

27. Felgner, P. L., M. A. Kayala, A. Vigil, C. Burk, R. Nakajima-Sasaki, J. Pablo, D. M. Molina, S. Hirst, J. S. Chew, D. Wang, G. Tan, M. Duffield, R. Yang, J. Neel, N. Chantratita, G. Bancroft, G. Lertmemongkolchai, D. H. Davies, P. Baldi, S. Peacock, and R. W. Titball. 2009. A Burkholderia pseudomallei protein microarray reveals serodiagnostic and cross-reactive antigens. Proceedings of the National Academy of Sciences of the United States of America 106:13499-13504.

28. Fleckenstein, J. M., D. J. Kopecko, R. L. Warren, and E. A. Elsinghorst. 1996. Molecular characterization of the tia invasion locus from enterotoxigenic Escherichia coli. Infection and immunity 64:2256-2265.

29. French, C. T., I. J. Toesca, T. H. Wu, T. Teslaa, S. M. Beaty, W. Wong, M. Liu, I. Schroder, P. Y. Chiou, M. A. Teitell, and J. F. Miller. Dissection of the Burkholderia intracellular life cycle using a photothermal nanoblade. Proceedings of the National Academy of Sciences of the United States of America 108:12095-12100.

30. Gal, D., M. Mayo, H. Smith-Vaughan, P. Dasari, M. McKinnon, S. P. Jacups, A. I. Urquhart, M. Hassell, and B. J. Currie. 2004. Contamination of hand wash detergent linked to occupationally acquired melioidosis. Am J Trop Med Hyg 71:360-362.

31. Galan, J. E., and H. Wolf-Watz. 2006. Protein delivery into eukaryotic cells by type III secretion machines. Nature 444:567-573.

32. Gong, L., M. Cullinane, P. Treerat, G. Ramm, M. Prescott, B. Adler, J. D. Boyce, and R. J. Devenish. The Burkholderia pseudomallei type III secretion system and BopA are required for evasion of LC3-associated phagocytosis. PLoS One 6:e17852.

33. Henderson, I. R., and J. P. Nataro. 2001. Virulence functions of autotransporter proteins. Infection and immunity 69:1231-1243.

34. Henderson, I. R., F. Navarro-Garcia, M. Desvaux, R. C. Fernandez, and D. Ala'Aldeen. 2004. Type V protein secretion pathway: the autotransporter story. Microbiol Mol Biol Rev 68:692-744.

35. Henderson, I. R., F. Navarro-Garcia, and J. P. Nataro. 1998. The great escape: structure and function of the autotransporter proteins. Trends Microbiol 6:370-378.

36. Hoiczyk, E., A. Roggenkamp, M. Reichenbecher, A. Lupas, and J. Heesemann. 2000. Structure and sequence analysis of Yersinia YadA and Moraxella UspAs reveal a novel class of adhesins. EMBO J 19:5989-5999.

37. Holden, M. T., R. W. Titball, S. J. Peacock, A. M. Cerdeno-Tarraga, T. Atkins, L. C. Crossman, T. Pitt, C. Churcher, K. Mungall, S. D. Bentley, M. Sebaihia, N. R. Thomson, N. Bason, I. R. Beacham, K. Brooks, K. A. Brown, N. F. Brown, G. L. Challis, I. Cherevach, T. Chillingworth, A. Cronin, B. Crossett, P. Davis, D. DeShazer, T. Feltwell, A. Fraser, Z. Hance, H. Hauser, S. Holroyd, K. Jagels, K. E. Keith, M. Maddison, S. Moule, C. Price, M. A. Quail, E. Rabbinowitsch, K. Rutherford, M. Sanders, M. Simmonds, S. Songsivilai, K. Stevens, S. Tumapa, M. Vesaratchavest, S. Whitehead, C. Yeats, B. G. Barrell, P. C. Oyston, and J. Parkhill. 2004. Genomic plasticity of the causative agent of melioidosis, Burkholderia pseudomallei. Proceedings of the National Academy of Sciences of the United States of America 101:14240-14245.

38. Hopper, S., B. Vasquez, A. Merz, S. Clary, J. S. Wilbur, and M. So. 2000. Effects of the immunoglobulin A1 protease on Neisseria gonorrhoeae trafficking across polarized T84 epithelial monolayers. Infection and immunity 68:906-911.

39. Inglis, T. J., T. Robertson, D. E. Woods, N. Dutton, and B. J. Chang. 2003. Flagellum-mediated adhesion by Burkholderia pseudomallei precedes

invasion of Acanthamoeba astronyxis. Infection and immunity 71:2280-2282.

40. Inglis, T. J., and J. L. Sagripanti. 2006. Environmental factors that affect the survival and persistence of Burkholderia pseudomallei. Appl Environ Microbiol 72:6865-6875.

41. Jani, A. J., and P. A. Cotter. Type VI secretion: not just for pathogenesis anymore. Cell Host Microbe 8:2-6.

42. Junker, M., R. N. Besingi, and P. L. Clark. 2009. Vectorial transport and folding of an autotransporter virulence protein during outer membrane secretion. Mol Microbiol 71:1323-1332.

43. Kilian, M., J. Reinholdt, H. Lomholt, K. Poulsen, and E. V. Frandsen. 1996. Biological significance of IgA1 proteases in bacterial colonization and pathogenesis: critical evaluation of experimental evidence. APMIS 104:321-338.

44. Kim, H. S., M. A. Schell, Y. Yu, R. L. Ulrich, S. H. Sarria, W. C. Nierman, and D. DeShazer. 2005. Bacterial genome adaptation to niches: divergence of the potential virulence genes in three Burkholderia species of different survival strategies. BMC Genomics 6:174.

45. Knowles, T. J., A. Scott-Tucker, M. Overduin, and I. R. Henderson. 2009. Membrane protein architects: the role of the BAM complex in outer membrane protein assembly. Nat Rev Microbiol 7:206-214.

46. Laarmann, S., and M. A. Schmidt. 2003. The Escherichia coli AIDA autotransporter adhesin recognizes an integral membrane glycoprotein as receptor. Microbiology 149:1871-1882.

47. Larsen, J. C., and N. H. Johnson. 2009. Pathogenesis of Burkholderia pseudomallei and Burkholderia mallei. Mil Med 174:647-651.

48. Leininger, E., M. Roberts, J. G. Kenimer, I. G. Charles, N. Fairweather, P. Novotny, and M. J. Brennan. 1991. Pertactin, an Arg-Gly-Asp-containing Bordetella pertussis surface protein that promotes adherence of mammalian cells. Proceedings of the National Academy of Sciences of the United States of America 88:345-349.

49. Leo, J. C., I. Grin, and D. Linke. Type V secretion: mechanism(s) of autotransport through the bacterial outer membrane. Philos Trans R Soc Lond B Biol Sci 367:1088-1101.

50. Limmathurotsakul, D., W. Chaowagul, W. Chierakul, K. Stepniewska, B. Maharjan, V. Wuthiekanun, N. J. White, N. P. Day, and S. J. Peacock. 2006.

Risk factors for recurrent melioidosis in northeast Thailand. Clin Infect Dis 43:979-986.

51. Lin, L., P. Ayala, J. Larson, M. Mulks, M. Fukuda, S. R. Carlsson, C. Enns, and M. So. 1997. The Neisseria type 2 IgA1 protease cleaves LAMP1 and promotes survival of bacteria within epithelial cells. Mol Microbiol 24:1083-1094.

52. Mascher, T., J. D. Helmann, and G. Unden. 2006. Stimulus perception in bacterial signal-transducing histidine kinases. Microbiol Mol Biol Rev 70:910-938.

53. Matsuura, M., K. Kawahara, T. Ezaki, and M. Nakano. 1996. Biological activities of lipopolysaccharide of Burkholderia (Pseudomonas) pseudomallei. FEMS Microbiol Lett 137:79-83.

54. Meng, G., N. K. Surana, J. W. St Geme, 3rd, and G. Waksman. 2006. Structure of the outer membrane translocator domain of the Haemophilus influenzae Hia trimeric autotransporter. EMBO J 25:2297-2304.

55. Mogensen, J. E., J. H. Kleinschmidt, M. A. Schmidt, and D. E. Otzen. 2005. Misfolding of a bacterial autotransporter. Protein Sci 14:2814-2827.

56. Ngauy, V., Y. Lemeshev, L. Sadkowski, and G. Crawford. 2005. Cutaneous melioidosis in a man who was taken as a prisoner of war by the Japanese during World War II. J Clin Microbiol 43:970-972.

57. Pohlner, J., R. Halter, K. Beyreuther, and T. F. Meyer. 1987. Gene structure and extracellular secretion of Neisseria gonorrhoeae IgA protease. Nature 325:458-462.

58. Puthucheary, S. D., and S. A. Nathan. 2006. Comparison by electron microscopy of intracellular events and survival of Burkholderia pseudomallei in monocytes from normal subjects and patients with melioidosis. Singapore Med J 47:697-703.

59. Raetz, C. R., and C. Whitfield. 2002. Lipopolysaccharide endotoxins. Annu Rev Biochem 71:635-700.

60. Rainbow, L., C. A. Hart, and C. Winstanley. 2002. Distribution of type III secretion gene clusters in Burkholderia pseudomallei, B. thailandensis and B. mallei. J Med Microbiol 51:374-384.

61. Reckseidler, S. L., D. DeShazer, P. A. Sokol, and D. E. Woods. 2001. Detection of bacterial virulence genes by subtractive hybridization:

identification of capsular polysaccharide of Burkholderia pseudomallei as a major virulence determinant. Infection and immunity 69:34-44.

62. Reckseidler-Zenteno, S. L., R. DeVinney, and D. E. Woods. 2005. The capsular polysaccharide of Burkholderia pseudomallei contributes to survival in serum by reducing complement factor C3b deposition. Infection and immunity 73:1106-1115.

63. Roggenkamp, A., N. Ackermann, C. A. Jacobi, K. Truelzsch, H. Hoffmann, and J. Heesemann. 2003. Molecular analysis of transport and oligomerization of the Yersinia enterocolitica adhesin YadA. J Bacteriol 185:3735-3744.

64. Rolim, D. B., D. C. Vilar, A. Q. Sousa, I. S. Miralles, D. C. de Oliveira, G. Harnett, L. O'Reilly, K. Howard, I. Sampson, and T. J. Inglis. 2005. Melioidosis, northeastern Brazil. Emerg Infect Dis 11:1458-1460.

65. Rossiter, A. E., D. L. Leyton, K. Tveen-Jensen, D. F. Browning, Y. Sevastsyanovich, T. J. Knowles, K. B. Nichols, A. F. Cunningham, M. Overduin, M. A. Schembri, and I. R. Henderson. The essential beta-barrel assembly machinery complex components BamD and BamA are required for autotransporter biogenesis. J Bacteriol 193:4250-4253.

66. Schell, M. A., R. L. Ulrich, W. J. Ribot, E. E. Brueggemann, H. B. Hines, D. Chen, L. Lipscomb, H. S. Kim, J. Mrazek, W. C. Nierman, and D. Deshazer. 2007. Type VI secretion is a major virulence determinant in Burkholderia mallei. Mol Microbiol 64:1466-1485.

67. Schwarz, S., T. E. West, F. Boyer, W. C. Chiang, M. A. Carl, R. D. Hood, L. Rohmer, T. Tolker-Nielsen, S. J. Skerrett, and J. D. Mougous. Burkholderia type VI secretion systems have distinct roles in eukaryotic and bacterial cell interactions. PLoS Pathog 6:e1001068.

68. Shalom, G., J. G. Shaw, and M. S. Thomas. 2007. In vivo expression technology identifies a type VI secretion system locus in Burkholderia pseudomallei that is induced upon invasion of macrophages. Microbiology 153:2689-2699.

69. Shere, K. D., S. Sallustio, A. Manessis, T. G. D'Aversa, and M. B. Goldberg. 1997. Disruption of IcsP, the major Shigella protease that cleaves IcsA, accelerates actin-based motility. Mol Microbiol 25:451-462.

70. Sitthidet, C., S. Korbsrisate, A. N. Layton, T. R. Field, M. P. Stevens, and J. M. Stevens. Identification of motifs of Burkholderia pseudomallei BimA required for intracellular motility, actin binding, and actin polymerization. J Bacteriol 193:1901-1910.

71. Spahich, N. A., and J. W. St Geme, 3rd. Structure and Function of the Haemophilus influenzae Autotransporters. Front Cell Infect Microbiol 1:5.

72. Sprague, L. D., and H. Neubauer. 2004. Melioidosis in animals: a review on epizootiology, diagnosis and clinical presentation. J Vet Med B Infect Dis Vet Public Health 51:305-320.

73. St Geme, J. W., 3rd, and D. Cutter. 2000. The Haemophilus influenzae Hia adhesin is an autotransporter protein that remains uncleaved at the C terminus and fully cell associated. J Bacteriol 182:6005-6013.

74. Stevens, J. M., R. L. Ulrich, L. A. Taylor, M. W. Wood, D. Deshazer, M. P. Stevens, and E. E. Galyov. 2005. Actin-binding proteins from Burkholderia mallei and Burkholderia thailandensis can functionally compensate for the actin-based motility defect of a Burkholderia pseudomallei bimA mutant. J Bacteriol 187:7857-7862.

75. Stevens, M. P., A. Haque, T. Atkins, J. Hill, M. W. Wood, A. Easton, M. Nelson, C. Underwood-Fowler, R. W. Titball, G. J. Bancroft, and E. E. Galyov. 2004. Attenuated virulence and protective efficacy of a Burkholderia pseudomallei bsa type III secretion mutant in murine models of melioidosis. Microbiology 150:2669-2676.

76. Stevens, M. P., J. M. Stevens, R. L. Jeng, L. A. Taylor, M. W. Wood, P. Hawes, P. Monaghan, M. D. Welch, and E. E. Galyov. 2005. Identification of a bacterial factor required for actin-based motility of Burkholderia pseudomallei. Mol Microbiol 56:40-53.

77. Stevens, M. P., M. W. Wood, L. A. Taylor, P. Monaghan, P. Hawes, P. W. Jones, T. S. Wallis, and E. E. Galyov. 2002. An Inv/Mxi-Spa-like type III protein secretion system in Burkholderia pseudomallei modulates intracellular behaviour of the pathogen. Mol Microbiol 46:649-659.

78. Sun, G. W., Y. Chen, Y. Liu, G. Y. Tan, C. Ong, P. Tan, and Y. H. Gan. Identification of a regulatory cascade controlling Type III Secretion System 3 gene expression in Burkholderia pseudomallei. Mol Microbiol 76:677-689.

79. Tandhavanant, S., A. Thanwisai, D. Limmathurotsakul, S. Korbsrisate, N. P. Day, S. J. Peacock, and N. Chantratita. Effect of colony morphology variation of Burkholderia pseudomallei on intracellular survival and resistance to antimicrobial environments in human macrophages in vitro. BMC microbiology 10:303.

80. Tiyawisutsri, R., M. T. Holden, S. Tumapa, S. Rengpipat, S. R. Clarke, S. J. Foster, W. C. Nierman, N. P. Day, and S. J. Peacock. 2007. Burkholderia Hep_Hag autotransporter (BuHA) proteins elicit a strong antibody response during experimental glanders but not human melioidosis. BMC microbiology 7:19.

81. Ulrich, R. L., D. Deshazer, E. E. Brueggemann, H. B. Hines, P. C. Oyston, and J. A. Jeddeloh. 2004. Role of quorum sensing in the pathogenicity of Burkholderia pseudomallei. J Med Microbiol 53:1053-1064.

82. Valade, E., F. M. Thibault, Y. P. Gauthier, M. Palencia, M. Y. Popoff, and D. R. Vidal. 2004. The PmlI-PmlR quorum-sensing system in Burkholderia pseudomallei plays a key role in virulence and modulates production of the MprA protease. J Bacteriol 186:2288-2294.

83. Vial, L., F. Lepine, S. Milot, M. C. Groleau, V. Dekimpe, D. E. Woods, and E. Deziel. 2008. Burkholderia pseudomallei, B. thailandensis, and B. ambifaria produce 4-hydroxy-2-alkylquinoline analogues with a methyl group at the 3 position that is required for quorum-sensing regulation. J Bacteriol 190:5339-5352.

84. Volokhina, E. B., J. Grijpstra, M. Stork, I. Schilders, J. Tommassen, and M. P. Bos. Role of the periplasmic chaperones Skp, SurA, and DegQ in outer membrane protein biogenesis in Neisseria meningitidis. J Bacteriol 193:1612-1621.

85. Vorachit, M., K. Lam, P. Jayanetra, and J. W. Costerton. 1995. Electron microscopy study of the mode of growth of Pseudomonas pseudomallei in vitro and in vivo. J Trop Med Hyg 98:379-391.

86. Warawa, J., and D. E. Woods. 2005. Type III secretion system cluster 3 is required for maximal virulence of Burkholderia pseudomallei in a hamster infection model. FEMS Microbiol Lett 242:101-108.

87. White, N. J. 2003. Melioidosis. Lancet 361:1715-1722.

88. Whitmore A, K. C. 1912. An account of the discovery of a hitherto undescribed infective disease occurring among the population of Rangoon. Indian Med Gaz 92:262-267.

89. Wiersinga, W. J., B. J. Currie, and S. J. Peacock. Melioidosis. N Engl J Med 367:1035-1044.

90. Wiersinga, W. J., T. van der Poll, N. J. White, N. P. Day, and S. J. Peacock. 2006. Melioidosis: insights into the pathogenicity of Burkholderia pseudomallei. Nat Rev Microbiol 4:272-282.

91. Wuthiekanun, V., M. D. Smith, and N. J. White. 1995. Survival of Burkholderia pseudomallei in the absence of nutrients. Trans R Soc Trop Med Hyg 89:491.

CHAPTER II

Characterization of BcaA, a putative classical autotransporter protein, in *Burkholderia pseudomallei*[1]

Introduction

Burkholderia pseudomallei is a Gram-negative saprotroph that causes melioidosis, a disease that ranges from chronic abscesses to fulminant pneumonia and septic shock and which can be rapidly fatal. *B. pseudomallei* has an approximately 7.2-megabase pair (Mb) genome divided into two chromosomes (19), affording this bacterium the metabolic repertoire necessary to adapt to and survive in a variety of different habitats, including soil, the rhizosphere of plants, and a wide variety of human and non-human mammals (36). Melioidosis, first reported by Dr. Whitmore, an army pathologist working in Burma, in 1912 (41), emerged as an infectious disease of serious public health concern in the latter part of the 20th century, manifesting as a rapidly progressing septicemia, with or without pneumonia; a localized soft-tissue infection; or a sub-clinical infection with delayed evidence of clinical infection (21, 42). *B. pseudomallei* is endemic to southeast Asia and northern Australia, however sporadic *B. pseudomallei* infections have been reported worldwide (4), including but not limited to the United States, Puerto Rico, El Salvador, and Brazil (10, 21, 34, 43). *B. pseudomallei*

[1] Adapted for this dissertation from: Cristine G. Campos, Luke Borst, and Peggy A. Cotter. Characterization of BcaA, a putative autotransporter protein in *Burkholderia pseudomallei*. 2013. Infection and Immunity. 81:4 1121-1128.

is classified as an NIH category B priority pathogen and select agent (40), and has recently been reclassified as a CDC Tier 1 select agent due to its virulence in animals, low infectious dose, robust environment stability, and possible delay in diagnosis since the bacterium is not endemic to the United States (http://www.selectagents.gov).

Autotransporters (ATs) are outer membrane proteins belonging to the Type V Secretion System family, the largest family of extracellular proteins in Gram-negative bacteria (18). These proteins have been shown to function as adhesins, degradative enzymes, and cytotoxins, as well as having roles in cell-to-cell spread and serum resistance (17). The AT family is divided into classical and trimeric proteins. The C-terminal 250 to 300 amino acids of classical ATs form a β-barrel that is inserted into the outer membrane where it facilitates the translocation of the N-terminal passenger domain to the cell surface. Trimeric ATs require three proteins to form a functional unit, with the C-terminal 67 to 76 C-terminal amino acids of each monomer contributing one-third of the barrel (7). The β-barrel domains of AT proteins are well conserved, while the passenger domains can vary substantially and have distinct functions (31).

To date, little is known about how *B. pseudomallei* causes disease (25). It is able to invade and replicate in phagocytic and non-phagocytic cells, and following Type III Secretion System (T3SS)-mediated endosomal escape, *B. pseudomallei* replicates in the cytoplasm of eukaryotic cells and spreads from cell-to-cell without leaving the cytoplasm (12, 37). One *B. pseudomallei* Type Six Secretion System (T6SS) has been shown to mediate multinucleated giant cell (MNGC) formation (3), allowing the bacteria to freely spread from cell to cell by actin-mediated motility, similar to *Shigella flexneri* and *Listeria monocytogenes* (33). *B. pseudomallei* actin-dependent motility requires the

trimeric autotransporter BimA, which contains proline-rich motifs and WH2-like domains that are believed to be responsible for actin polymerization at the pole of the bacterial cell where BimA is localized (38).

The genome of *B. pseudomallei* strain 1026b contains genes predicted to encode nine trimeric ATs and two classical ATs. The purpose of this study was to determine the role of the predicted classical AT encoded by Bp1026b_II1054 in pathogenesis.

Materials and Methods

Bacterial Strains. All manipulations of *B. pseudomallei* were conducted in a CDC/USDA-approved animal biosafety level 3 (ABSL3) facility at the University of North Carolina at Chapel Hill. The bacterial strains used in this study are listed in Table 1. *B. pseudomallei* strains were cultured in Low Salt Lysogeny Broth (LSLB), or on Low Salt Lysogeny Broth Agar (LSLBA) (Sigma-Aldrich, St. Louis, MO) for 24 hours at 37ºC. *Escherichia coli* strains were cultured on LB or LBA. When appropriate, culture media were supplemented with Kanamycin (Km, 125 μg/ml for *B. pseudomallei* and 50 μg/ml for *E. coli*), or Zeocin (Zeo, 100 μg/ml for *B. pseudomallei*, and 35 μg/ml for *E. coli*). LB agar was supplemented with 400 μg/ml of diaminopimelic acid (DAP; LL-, DD-, and meso-isomers; (Sigma-Aldrich, St. Louis, MO) to support growth of RHO3 cells. Yeast extract-tryptone (YT) medium containing 10 g/l of yeast extract (Difco, Detroit, MI) and 10 g/l of tryptone (Fisher Scientific, Fairlawn, NJ) supplemented with 15% sucrose and X-Gluc (GoldBio, St. Louis, MO) was used for counter-selection during the construction of *B. pseudomallei* deletion mutation strains.

Construction of *B. pseudomallei bcaA* and *bcaB* mutant strains and plasmids. Deletion of the *bcaA* and *bcaB* genes from *B. pseudomallei* strain Bp340 (a derivative of strain1026b containing a Δ(*amrRAB-oprA*) mutation. Strain was shown by Dr. Herbert Schweizer to be as virulent as 1026b in the BALB/c acute model of infection) (14, 30) was carried out by allelic exchange using pEXKm5 (28) derivatives. The DNA fragments used to construct pCCX1 and pCCX2 (Table 1) were generated using a two-step, overlap polymerase chain reaction (PCR) method and cloned into pEXKm5. DNA fragments contained approximately 500 bp 5′ to the gene including the first three codons and 500 bp 3′ to the gene including the last three codons. pCCX1 and pCCX2 were transformed into *E. coli* RHO3 cells, and were delivered to Bp340 by conjugation. For Bp340Δ*bcaA* and Bp340Δ*bcaB* complementation strains, the gene and promoter region was cloned into pUC18T-mini-Tn7-Zeo and delivered as previously described (5). All plasmids were verified to be correct and contain no unintended nucleotide changes by DNA sequence analysis.

Bacterial conjugations. Matings between *B. pseudomallei* and *E. coli* strain RHO3 were performed by incubating Bp340 with RHO3 cells carrying the appropriate allelic exchange plasmid (Table 1) on LSLB-DAP agar plates overnight. Cointegrants were selected on LSLB-Km. PCR-confirmed cointegrants were grown overnight in LSLB without selection, allowing for a second recombination event and the loss of the allelic exchange plasmid. Colonies were selected on YT agar supplemented with 15% sucrose and X-Gluc (28), as previously described. Colonies were screened by PCR for the deletion mutation, and the strains were confirmed by DNA sequencing. To generate the complementation strains, RHO3 cells harboring pCCZ1 or pCCZ2 (Table 1) were mated

with Bp340Δ*bcaA* and Bp340Δ*bcaB*, respectively, and cointegrants were selected on LSLB-Zeo (5). Integration at the correct location was confirmed by PCR. All DNA regions encompassing about 2 Kb across the deletion junction were PCR amplified and verified to be correct and to contain no unintended nucleotide changes by DNA sequence analysis. DNA sequence inserted in the *att* Tn7 site in complementation strains were also PCR amplified and verified by DNA sequence analysis.

Total RNA isolation and cDNA synthesis. Total RNA was isolated in Trizol (Invitrogen, Grand Island, NY) from Bp340 grown overnight in LSLB at 37ºC according to the manufacturer's protocol. For the reverse transcription step, 5 ng of total RNA was transcribed using Super Script III reverse transcriptase (Invitrogen, Grand Island, NY) with oligo(dT) and random primers according to the manufacturer's instructions. Transcripts were determined by PCR primers described in Table 2.

Immunoblot analysis. Strain Bp340::pCCS12HA1 was constructed using pCCS12HA1, a suicide plasmid containing the constitutively active ribosomal S12 subunit promoter (P_{S12}) up to and including the S12 ribosomal binding site fused to the first 329 codons of *bcaA*, starting at the ATG. The hemagglutinin (HA) epitope-encoding sequence was introduced between codons 58 and 59. The plasmid was verified by PCR and sequence analysis to have integrated into the Bp340 strain 3′ to the HA epitope-encoding sequence, yielding a chromosomal HA-tagged copy of *bcaA* driven by the S12 promoter. Whole cell lysates were prepared from overnight cultures grown in LSLB-Km. SDS-PAGE was performed by the method of Laemmli (24) using denaturing 10% SDS polyacrylamide gels. Gels were transferred to a nitrocellulose membrane (Scheleicher and Schuell Bioscience, Dassel, Germany) and were probed with an anti-HA antibody

(diluted 1:5,000) followed by an IR800-conjugated secondary antibody (diluted 1:20,000) (Rockland, Gilbertsville, PA). Antigen-antibody complexes were visualized using the Odyssey infrared imaging system (Li-Cor Biosciences, Lincoln, NE).

Plaque Assay. *B. pseudomallei* strains were grown overnight in LSLB at 37ºC. Each well of a 6-well plate was seeded with A549 human lung cells such that confluent monolayers contained approximately $1x10^6$ cells per well. Cells were incubated in F12K (Cellgro, Circle Westwood, MA) supplemented with 10% fetal bovine serum (Gibco, Grand Island, NY) at 37ºC with 5% CO_2. Bacterial strains were diluted to an OD_{600} of 0.1 in fresh tissue culture medium, further diluted 1:10, and 25 µl of the diluted culture was added to each well (MOI of 0.1). Plates were incubated for 2 hours and each well was washed thoroughly with fresh culture medium and overlayed with a mixture containing 1.2% low-melting agarose (Fisher Scientific, Fairlawn, NJ), F12K with 10% FBS, and 0.01% Neutral red (Fischer Scientific, Waltham, MA). Plates were incubated for 24 hours at 37ºC with 5% CO_2, and plaques were enumerated in each well. Experiments were performed three times in duplicate, and the results were combined. The combined results were analyzed using a one-way analysis of variance (ANOVA) with Tukey's post-test at a 95% confidence interval.

Adherence and invasion assay. Bacterial strains and A549 cells were grown as described above. Bacteria were diluted to an OD_{600} of 0.1 in fresh tissue culture medium, and 250µL of the diluted cultures added to each well (MOI of 100). Plates were incubated for 2 hours, and each well was washed thoroughly with fresh culture medium. For the adherence assay, cells were immediately lysed using 1% Triton X-100 (Sigma-Aldrich, St. Louis, MO) and were diluted and plated to determine the total colony

forming units (CFU) in each well. For the invasion assay, cells were incubated an additional hour and a half with Gentamicin (90 μg/ml), washed with fresh culture medium, and were lysed using 1% Triton X-100. Lysates were diluted and plated to determine the total CFU in each well. To calculate the percentage of adherent or invading bacteria, the number of adherent or invading bacteria was divided by the total number of bacteria in the inoculum and multiplied by 100. Experiments were performed three times in duplicate, and the results were combined. The combined results were analyzed using a one-way ANOVA with Tukey's post-test at a 95% confidence interval.

Animal experiments. All animal experiments were approved by the Animal Studies Committee of the University of North Carolina at Chapel Hill (protocol 10-165). Six- to eight-week-old female BALB/c mice (The Jackson Laboratory, Bar Harbor, ME) were allowed free access to sterilized food and water. Animals were anesthetized prior to infection with Avertin (140mg/Kg) by intraperitoneal injection. For all infections, the desired inoculum of *B. pseudomallei* was suspended in sterile phosphate buffered saline (PBS). Mice were inoculated intranasally with 500 CFU (LD_{50} for 1026b has been determined to be around 900 CFU (14)), and at the indicated time points were euthanized by CO_2 overdose. Organs were aseptically harvested, homogenized, and the bacterial burden of each organ was determined by plating serial dilutions of the homogenates. Animal experiments were performed twice, with three to four animals per strain per time point and the results combined. Animal experiments were terminated at 48 hours at which time all animals had become moribund.

Pathology. Lungs, livers and spleens of six- to eight-week-old female BALB/c mice intranasally infected with 500 CFU of Bp340 or Bp340Δ*bcaA* were harvested, fixed

in 10% neutral buffered formalin for 24 hours. Samples were stored in 70% ethanol until processed into paraffin using routine methods. Paraffin embedded tissues were sectioned 3 to 5 microns thick, captured onto glass slides and stained with hematoxylin and eosin (HE). Sections of liver, spleen and lung were analyzed using light microscopy by a single pathologist (LB) who was blinded to group. Microscopic lesions consisting primarily of necrosis and acute inflammation (neutrophils, macrophages, apoptotic bodies, and fibrin) were quantified as follows: In the lung, the affected bronchi per 20 bronchiolar profiles were counted starting with an affected bronchiole. In the liver and spleen, inflammatory foci were enumerated in 10 consecutive fields at 20x magnification starting on an area of inflammation identified on low magnification.

Results

Bioinformatic analysis of the *bcaA* and *bcaB* genes of *B. pseudomallei* strain 1026b

Bp1026b_II1054 is a 3393 base pair (bp) gene predicted to encode a classical AT that we named *bcaA* for *Burkholderia* classical autotransporter A. Forty base pairs 3′ to *bcaA* is Bp11026_II1055 (which we named *bcaB*), a 687 bp gene predicted to encode a hypothetical protein. There is a 480 bp gene predicted to encode a hypothetical protein 1522 bp 5′ to *bcaA*, and 198 bp 3′ to *bcaB* is a 1593 bp gene oriented in the opposite direction, predicted to encode a periplasmic solute-binding protein (Fig. 1A).

SignalP identified a signal peptide and a cleavage site on the predicted 1133 amino acid (aa) BcaA protein between aa 40 and 41 (2). Simple Modular Architecture Research Tool

(SMART) predicts BcaA to have a serine protease domain, from aa 64 to 380, belonging to the Peptidase S8 or Subtilase family, and a classical AT β-domain from aa 857 to 1121. BcaB, is a 255 aa protein predicted to contain a prolyl 4-hydroxylase domain from aa 41 to 225 (Fig.1B) (27).

BLAST indicated that homologues of *bcaA* are present in *B. pseudomallei*, *B. mallei, B. thailandensis,* and *B. gladioli* strains but not in *Ralstonia* or *Cupriavidus* species, close relatives of the *Burkholderia* genus. All *B. pseudomallei* and *B. mallei* strains for which genome sequence is available are predicted to encode proteins with 99% identity with BcaA, 89% identity is found in *B. thailandensis* and 82% identity in *B. oklahomensis*. Predicted homologues are not found in bacteria outside of the *Burkholderia* genus, suggesting this gene is unique to *Burkholderia*.

To investigate the role of *bcaA* and *bcaB* in the pathogenesis of *B. pseudomallei*, we constructed strains of Bp340 containing in-frame deletion mutations in each gene (Fig. 1A) by allelic exchange (28). Complementation of these deletion mutations was accomplished by delivering a full-length copy of the gene, along with its presumed promoter region (the approximately 1 Kb region immediately 5′ to the *bcaA* translation start site) to Tn7 *att* sites in the respective deletion strain using pUC18T-mini-Tn7-Zeo (5). The same presumed promoter region, approximately 1 Kb preceding the translation start site of *bcaA* was fused to the full-length copy of *bcaB* for the construction of the complementation of Bp340Δ*bcaB*.

bcaA and *bcaB* appear to form an operon

RT-PCR was used to determine if *bcaA* and *bcaB* are cotranscribed. cDNA was prepared from Bp340 grown overnight at 37°C in LSLB, and used as template for PCR using the primer pairs (Table 2) shown in Figure 1A. Products of expected sizes were obtained for each primer pair (Fig. 1C), including the pair spanning the intergenic region between *bcaA* and *bcaB*, suggesting that these genes are cotranscribed. No product was observed in the mock RT samples demonstrating the lack of DNA contamination in the isolated RNA samples, and consequently the cDNA samples.

BcaA appears to be proteolyzed to smaller polypeptides

To visualize the production of BcaA protein, we constructed Bp340 derivatives in which nucleotides encoding HA epitopes were inserted either immediately following the protein's predicted signal sequence cleavage site or between codons 58 and 59. Both strains were grown overnight in LSLB at 37°C but no polypeptide was recognized by Western blotting using an anti-HA antibody. After several unsuccessful attempts to visualize the BcaA protein when the gene was expressed from its native promoter, we constructed a strain in which *bcaA* was expressed from a strong, constitutively active promoter (the promoter for the *rpsL* gene from *Burkholderia pseudomallei* 1026b). First, we inserted the HA epitope-encoding codons immediately following the predicted signal sequence cleavage site, but again were unsuccessful at visualizing BcaA. Finally, we inserted the HA epitope-encoding codons between codons 58 and 59 (Bp340::pCCS12HA1) and the protein was then successfully visualized by western blot analysis. Polypeptides approximately 21 kDa and 28 kDa in size as well as a large smear

between 250 and 75 kDa were observed in whole cell lysates of Bp340::pCC12HA1, but not in whole cell lysates of the wild-type strain lacking the HA epitope tag (Figure 2). These data suggest that BcaA is proteolyzed to smaller polypeptides. The smaller polypeptides were not detected in western blots of concentrated supernatant fractions (data not shown), suggesting that they remain associated with the bacterial cell.

bcaA and *bcaB* are required for efficient plaque formation

B. pseudomallei can spread from cell to cell without exiting the cytoplasm and can form plaques in a cell monolayer (22). To determine if *bcaA* or *bcaB* contribute to plaque formation, A549 respiratory epithelial cell monolayers were infected at an MOI of 0.1 and plaques were counted after 24 hours. Bp340 formed an average of 100 plaques/well, while Bp340Δ*bcaA* (Fig. 3A) and Bp340Δ*bcaB* (Fig. 3B) each formed only about 50 to 60 plaques/well. Complementation of both mutations restored plaque-forming ability to wild type levels, indicating that both *bcaA* and *bcaB* are required for efficient plaque formation.

bcaA and *bcaB* are required for efficient invasion of A549 cells

The plaques formed by Bp340Δ*bcaA* and Bp340Δ*bcaB* strains appeared to be of similar sizes to those formed by wild type bacteria, suggesting that *bcaA* and *bcaB* are involved in the first steps of plaque formation, and therefore required for either adhesion or invasion. To determine if *bcaA* and *bcaB* are required for efficient adhesion or invasion, A549 cell monolayers were infected at an MOI of 100, and following a 2-hour incubation, cells were either washed, lysed, serially diluted, and plated to determine

percent adhesion, or were washed, incubated with 90μg/mL of Gentamicin for an additional hour and a half, then lysed, serially diluted, and plated to determine percent invasion. No difference was observed in adhesion between Bp340 and Bp340Δ*bcaA* or Bp340 and Bp340Δ*bcaB* (Fig. 4A). However, Bp340Δ*bcaA*, and Bp340Δ*bcaB* demonstrated significantly decreased invasion compared to Bp340 (Fig. 4B), suggesting that *bcaA* and *bcaB* are required for efficient invasion of A549 cells. Complementation of Δ*bcaA* and Δ*bcaB* at the Tn7 *att* site restored invasion to wild type levels. C57BL/6 bone marrow-derived macrophages were also used in similar experiments, but no difference was observed between Bp340, Bp340Δ*bcaA*, and Bp340Δ*bcaB* (data not shown). *bcaA* and *bcaB*, therefore, are required for invasion of non-phagocytic cells, but do not appear to affect uptake by phagocytic cells.

***bcaA* is required for efficient dissemination to or survival in the spleen**

To determine the contribution of *bcaA* and *bcaB* to *B. pseudomallei* pathogenesis we used an acute intranasal (i.n.) mouse model of infection. Bp340 has been shown to have the same LD_{50} as 1026b (14) when delivered by the i.n. route, so 6- to 8-week-old female BALB/c mice were inoculated with 500 CFU of *B. pseudomallei* delivered in a 25 μL volume to the nose. All animals showed signs of respiratory distress by 48 hours post inoculation, becoming moribund and marking the end point of our experiments. The number of CFU in the lungs, liver, and spleen was determined at 48 hours post-inoculation. The number of CFU recovered from the lungs and livers of animals inoculated with Bp340 and Bp340Δ*bcaA* was not significantly different. The number of CFU recovered from the spleen of Bp340Δ*bcaA*-infected mice, however, was

significantly lower than the number recovered from mice infected with Bp340 (Fig. 5A). Complementation of Δ*bcaA* at the Tn7 *att* site restored bacterial numbers in the spleen to wild type levels, suggesting that *bcaA* is required for efficient dissemination to or survival of *B. pseudomallei* in the spleen in this model. The number of bacteria recovered from the lungs, liver and spleen of animals inoculated with Bp340Δ*bcaB* was not significantly different from those infected with Bp340 (Figure 5B).

bcaA does not appear to contribute to *B. pseudomallei*-induced organ pathology

To determine if *bcaA* contributes to tissue pathology, lungs, livers and spleens were harvested at 48 hours post-intranasal inoculation, Hematoxylin and Eosin (H&E)-stained sections were prepared, coded for blind scoring, and examined for histopathological changes. Inflammation was observed in the lungs, livers and spleens of all mice infected with Bp340 and Bp340Δ*bcaA*, varying only in the degree of severity. Approximately the same number of affected bronchi per bronchiolar profile was found in the mice infected with both strains, and the number of inflammatory foci found in the livers and spleens was also similar.

Lungs showed suppurative bronchointerstitial pneumonia, with small airways partially to completely filled with mostly degenerative neutrophils. Adjacent and randomly scattered alveolar septa were moderately expanded by degenerative neutrophils and fibrin (microthrombi). Livers showed multifocoal necrosuppurative hepatitis with random hepatocellular necrosis and inflammatory infiltrate (neutrophils), as well as fibrin hemorrhage. Spleens showed multifocoal necrosuppurative splenitis with scattered (red

pulp) areas of necrosis and inflammatory infiltrate (neutrophilic predominant, rare macrophages, apoptotic bodies), as well as mild fibrin hemorrhage.

The overall histological picture was of bronchopneumonia followed by acute sepsis as evidenced by interstitial pulmonary involvement and multifocal distribution of inflammation and necrosis in the spleens and livers, however there was no significant difference in histological scoring between organs harvested from animals inoculated with Bp340 and Bp340Δ*bcaA*.

Discussion

The sequenced genome of *B. pseudomallei* contains eleven genes predicted to encode AT proteins. Only the trimeric AT BimA (38) has been well characterized and it has been shown to play a role in pathogenesis. This work focused on the characterization of *bcaA*, a gene predicted to encode a classical AT. Our data indicate that *bcaA* and *bcaB* contribute to non-phagocytic cell invasion and *bcaA* to dissemination to or survival of *B. pseudomallei* in the spleen in a BALB/c intranasal model of infection.

The *bcaA* and *bcaB* genes appear to form an operon. RT-PCR supports this hypothesis by showing that *bcaA* and *bcaB* are cotranscribed from a common promoter upstream of *bcaA*. Our data do not rule out the presence of an additional *bcaB* promoter located within the *bcaA* gene. However, the DNA fragment used to complement the Δ*bcaB* strain contained approximately 1 Kb preceding the translation start site of *bcaA* fused directly to the full-length copy of *bcaB* and this DNA fragment restored invasion of

the Δ*bcaB* strain to wild type levels, further suggesting that *bcaA* and *bcaB* are transcribed from a promoter 5′ to *bcaA*.

BcaA is predicted to be a 113 kDa classical AT protein with an approximately 80 kDa passenger domain containing a serine protease domain belonging to the Peptidase S8 or Subtilase family and a 30 kDa β-domain. Subtilisins are the second largest family of serine proteases, characterized by a conserved catalytic triad that functions in a charge relay system much like trypsin family proteases (23). Subtilisins use well conserved Asp, Ser and His catalytic residues for their protease activity (35) and their functions include contributing to cellular nutrition, mediating host cell invasion, and the maturation of other polypeptides (39). A few AT subtilases have been described, including Ssp from *Serratia marcescens,* a 112 kDa protein with an approximately 80 kDa passenger domain that is auto-proteolyzed into a 41 KDa polypeptide that is released into the medium (32), and AasP from *Actinobacillus pleuropneumoniae,* a 104 kDa protein that cleaves another outer membrane protein OmlA into smaller polypeptides of about 30 kDa that are released into the medium (1). BcaA contains the same well-conserved catalytic triad found in other subtilisins (Asp 90, His 124 and Ser 329). Western Blot characterization studies using a HA-tagged BcaA detected 21kDa and 28 kDa polypeptides that were present in whole cell lysates but not in supernatants. Much like Ssp from *S. marcescens*, the BcaA 80kDa passenger domain appears to be proteolyzed into smaller polypeptides, however, these small polypeptides do not appear to be released into the extracellular environment in the case of BcaA. Further studies will include characterization of these polypeptides and determining if these polypeptides are generated by auto-proteolysis or if another protein is involved in processing.

We showed that *bcaA* and *bcaB* are required for invasion and plaque formation in epithelial cells, but did not affect uptake in phagocytic cells. *B. pseudomallei* has been shown to invade and replicate in both phagocytic and non-phagocytic cells, and to spread from cell to cell without leaving the cytoplasm (37). Although a substantial amount has been learned about the intracellular life cycle of *B. pseudomallei*, no proteins responsible for the initial invasion step have been identified previously. BcaA, therefore, represents the first identified invasin in *B. pseudomallei.*

In vivo, *bcaA* is required for efficient dissemination to or survival of *B. pseudomallei* in the spleen in a BALB/c intranasal model of infection. Although histology showed no difference in the amount of inflammatory foci found in the spleens of animals infected with Bp340Δ*bcaA* and the wild-type strain, significantly fewer bacteria were recovered from the spleens of animals infected with Bp340Δ*bcaA*. How the invasion phenotype *in vitro* relates to the spleen dissemination or survival defect *in vivo* is unknown. *Yersinia enterocolitica* has been shown to have both invasin-dependent and invasin-independent routes of spleen colonization from the intestine of C57BL/6 mice; Handley *et al.* showed that a *Y. enterocolitica* invasin mutant was attenuated in its ability to disseminate from the intestine to the spleen (16). The same phenotype has also been described for *Y. pseudotuberculosis* after oral inoculation (29). It had been proposed that enteropathogenic *Yersinia* colonize the Peyer's patch, then drain into the mesenteric lymph nodes, and in turn enter tissues such as the spleen. The studies by Marra *et al.* and Handley *et al.*, however, showed that there are several routes of spread, and how initial colonization of one site leads to the colonization of another appears to be more

complicated than initially appreciated. To date, little is known about how *B. pseudomallei* disseminates from the initial site of infection (13). Inhalation, ingestion, and via soft tissue abrasions or lacerations are routes of infection (4, 9), however the steps the bacteria follow after the inoculation are still unknown. It is possible that *bcaA* functions like the *Y. enterocolitica* invasin, specifically aiding dissemination to the spleen. Further studies will include determining the route of spleen colonization, as well as studies to determine if *bcaA* and *bcaB* affect survival once the bacteria have reached the spleen.

bcaB is predicted to encode a hypothetical protein with a prolyl 4-hydroxylase domain. Bacterial prolyl 4-hydroxylases are believed to hydroxylate peptidyl prolines, and although some such hydroxylases have been identified in bacteria, their substrates and therefore their function remain unknown (15). Prolyl 4-hydroxylase, which catalyzes the most prevalent posttranslational modification in humans has as substrate collagen functioning by stabilizing collagen triple helix structure (20), elastin where it affects the formation of elastin fibrils (11) and even prion proteins although its consequence is unknown (15). In bacteria, a *Bacillus anthracis* enzyme, designated anthrax-P4H has been shown to hydroxylate peptidyl prolines, however although it binds to collagen-like peptides *in vitro* its physiological substrate and role remain unknown (8). Further studies should include determining if *bcaB* plays a role in hydroxylating any of the fifty-two prolines found in BcaA since it is possible that BcaA is the physiological substrate for BcaB, which would be consistent with their operon structure.

Both *bcaA* and *bcaB* are required for invasion and plaque formation, consistent with the idea that they function together. However, only *bcaA* showed a phenotype *in vivo*. It is possible that this simply reflects the limitations of the tools we used. Although

the BALB/c model has been broadly used as an acute model for *B. pseudomallei* infection (26), it may not be sensitive enough to reveal phenotypes for all factors that contribute to disease, depending on the step and stage of disease in which they function. Our future experiments will include the development of additional animal models that will expand the repertoire of *B. pseudomallei* disease processes that we are able to study in the laboratory.

Table 1. Strains and plasmids used in this study

Strain or plasmid	Description	Reference or source
RHO3	Km^s; SM10(λ*pir*)Δ*asd*::*FRT*Δ*aphA*::*FRT*	(28)
Bp340	1026b with Δ(*amrRAB-oprA*)	(30)
Bp340Δ*bcaA*	Bp340 with Δ*bcaA*	This study
Bp340Δ*bcaB*	Bp340 with Δ*bcaB*	This study
Bp340Δ*bcaA*::*att*Tn7*bcaA*	Bp340 with Δ*bcaA::att*Tn7*bcaA*	This study
Bp340Δ*bcaB*::*att*Tn7*bcaB*	Bp340 with Δ*bcaB::att*Tn7*bcaB*	This study
Bp340::pCCS12HA1	Bp340 with pCCS12HA1::*bcaA*	This study
pCCX1	Km^r; pEXKm5 derivative	(28)
pCCX2	Km^r; pEXKm5 derivative	(28)
pCCZ1	Amp^r, Km^r; pUC18T-mini-Tn7-Zeo derivative	(6)
pMBZ2	Amp^r, Km^r; pUC18T-mini-Tn7-Zeo derivative	(6)
pTNS2	Ap^r; plasmid expressing *tnsABCD* from P_{lac}	(6)
pCCS12HA1	Km^r; pCC derivative (pRE118 derivative), suicide plasmid for *B. pseudomallei*.	This study

Table 2. Primers used in this study

CBcaART_F:	TTC GACAGC TTC CAT CTC GGC
CBcaART_R:	GTT CTT CAG ATG CAC ATA CGC GAC
CBcaBRT_F:	TTT CGC AGA CGT ACT TGA CGC AGC
CBcaBRT_R:	TTG AAC ATC AGC GTG ATC CGC ATC GTC
CBcaA/BRT_F:	CTC GGC AAG AAC GGA TGG CTG
CBcaA/BRT_R:	CAG AAA CCG GTG GAT CTG CGC

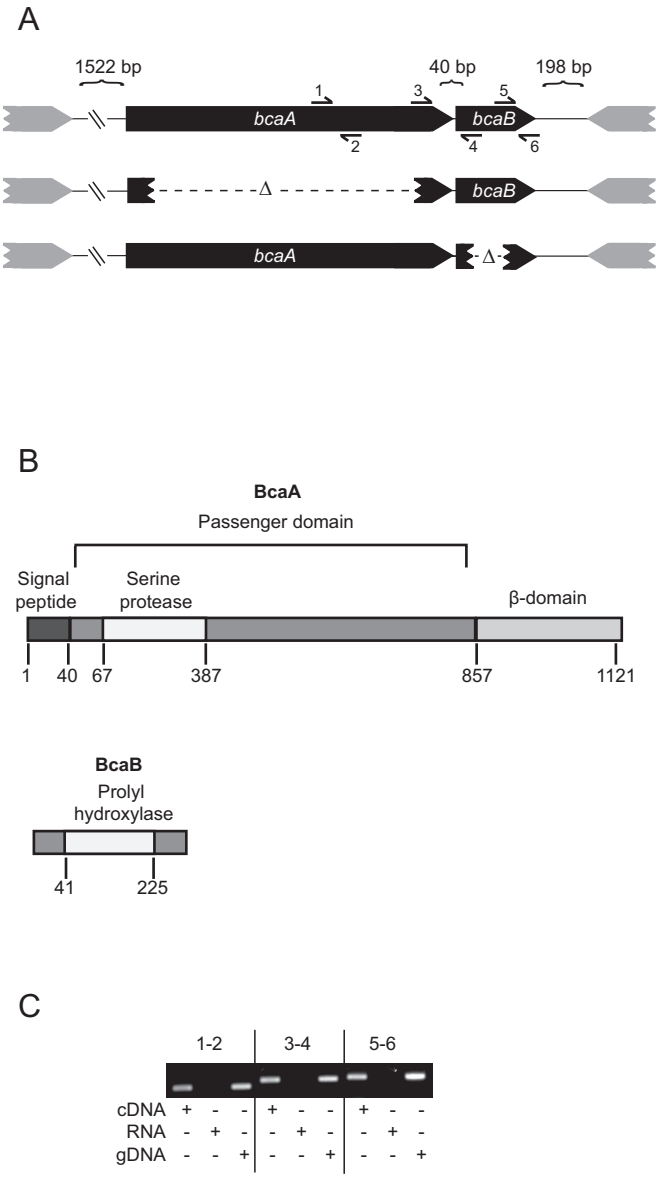

Fig. 1. *bcaA* and *bcaB* appear to form an operon. **(**A) Genetic organization of the *bcaA* and *bcaB* locus and description of the strains used in this study. Visual representation of the primer pairs used for RT-PCR. (B) The putative domains of BcaA and BcaB proteins drawn to scale. (C) RT-PCR analysis of the operon structure of *bcaA* and *bcaB*. Primer pairs 1-2, 3-4 and 5-6 were used, as indicated in 1A.

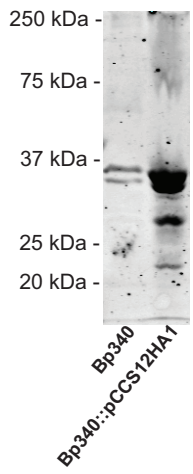

Fig. 2. Immunoblot of whole cell lysates of Bp340 with no tag, and Bp340::pCCS12HA1, strains were separated by SDS-PAGE and stained with anti-HA antibody.

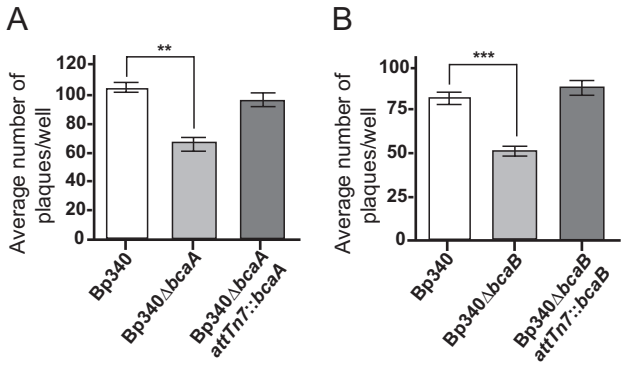

Fig. 3. Average number of plaques formed in an A549 monolayer by Bp340, Bp340Δ*bcaA* (A), Bp340Δ*bcaB* (B) and respective complementation strains. Assays were performed three times in duplicate, and the results were combined. Data are mean ± SEM. $^{**}p<0.0080$ and $^{***}p<0.0001$, by one-way ANOVA with Tukey's post-test at a 95% confidence interval.

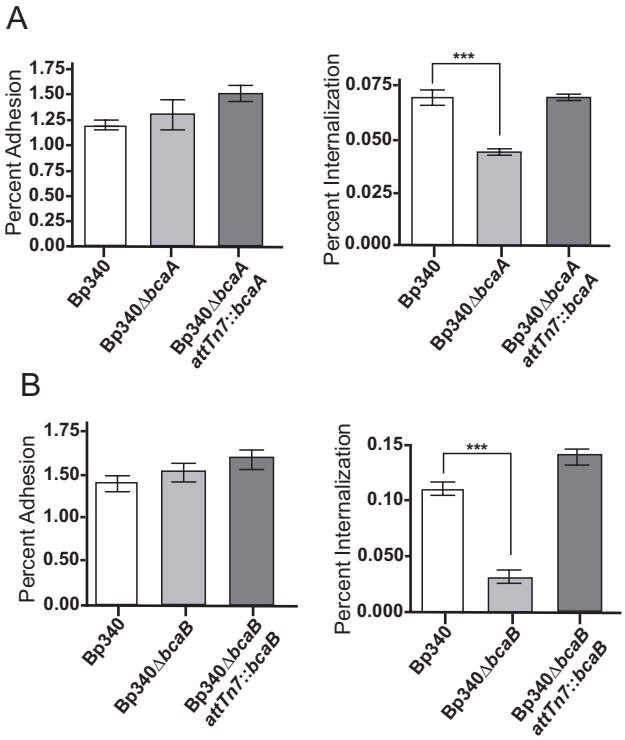

Fig. 4. Colony forming units (CFU) recovered after two-hour adherence and invasion assays with Bp340, Bp340Δ*bcaA* (A), Bp340Δ*bcaB* (B) and respective complementation strains. Assays were performed in three times in duplicate, and the results were combined. Data are mean ± SEM. $^{***}p<0.0001$, by one-way ANOVA with Tukey's post-test at a 95% confidence interval.

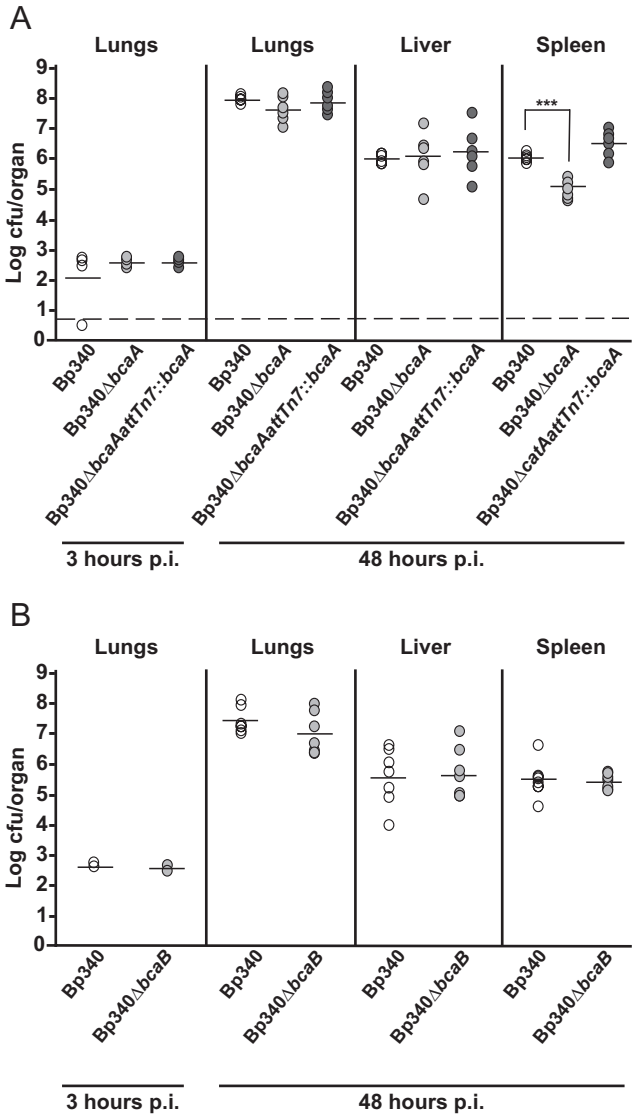

Fig. 5. Six- to 8-week-old female BALB/c mice were inoculated with 500 CFU of *B. pseudomallei* Bp340 (white circles), Bp340Δ*bcaA* (A), Bp340Δ*bcaB* (B) (light grey circles) and respective complementation strains (dark grey circles). Each circle represents the number of CFU recovered from a mouse. The horizontal line represents the average number of CFU. The dotted line represents the lower limit of detection. $^{***}p<0.0001$. Animal experiments were performed twice for each strain, and results combined.

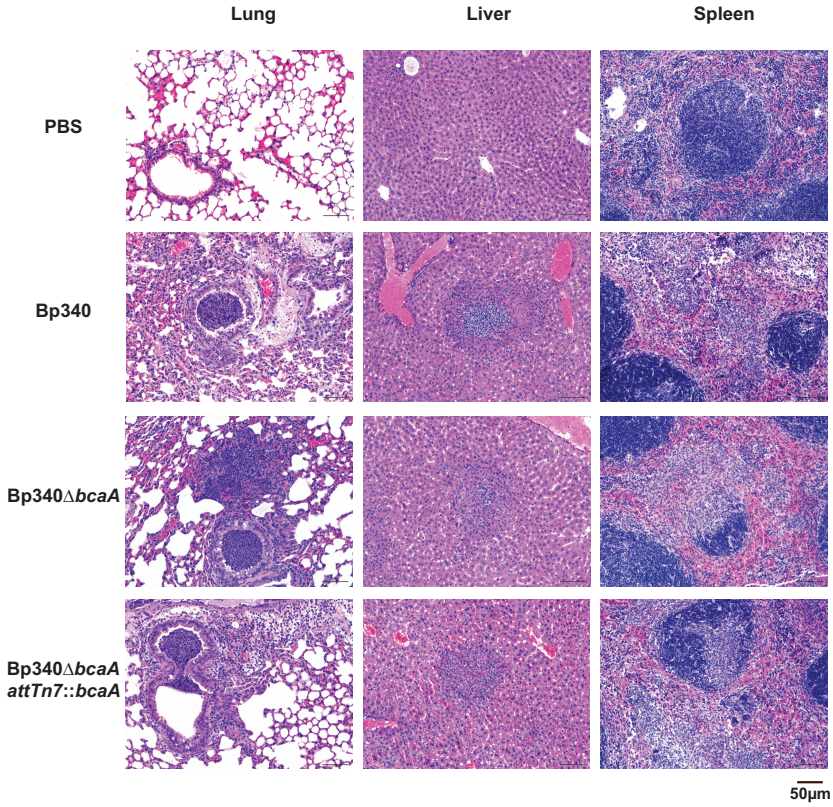

Fig. 6. Histological analysis of *B. pseudomallei*-infected tissues. Representative tissue samples from BALB/c infected mice i.n. with Bp340, Bp340Δ*bcaA* and Bp340Δ*bcaA*::*att*Tn7*bcaA* (~500 CFU), or PBS mock-infected control animals.

References

1. **Ali, T., N. J. Oldfield, K. G. Wooldridge, D. P. Turner, and D. A. Ala'Aldeen. 2008. Functional characterization of AasP, a maturation protease autotransporter protein of Actinobacillus pleuropneumoniae. Infect Immun 76:5608-5614.**

2. **Bendtsen, J. D., H. Nielsen, G. von Heijne, and S. Brunak. 2004. Improved prediction of signal peptides: SignalP 3.0. J Mol Biol 340:783-795.**

3. **Burtnick, M. N., P. J. Brett, S. V. Harding, S. A. Ngugi, W. J. Ribot, N. Chantratita, A. Scorpio, T. S. Milne, R. E. Dean, D. L. Fritz, S. J. Peacock, J. L. Prior, T. P. Atkins, and D. Deshazer. The cluster 1 type VI secretion system is a major virulence determinant in Burkholderia pseudomallei. Infection and immunity 79:1512-1525.**

4. **Cheng, A. C., and B. J. Currie. 2005. Melioidosis: epidemiology, pathophysiology, and management. Clin Microbiol Rev 18:383-416.**
5. **Choi, K. H., D. DeShazer, and H. P. Schweizer. 2006. mini-Tn7 insertion in bacteria with multiple glmS-linked attTn7 sites: example Burkholderia mallei ATCC 23344. Nat Protoc 1:162-169.**

6. **Choi, K. H., T. Mima, Y. Casart, D. Rholl, A. Kumar, I. R. Beacham, and H. P. Schweizer. 2008. Genetic tools for select-agent-compliant manipulation of Burkholderia pseudomallei. Appl Environ Microbiol 74:1064-1075.**
7. **Cotter, S. E., N. K. Surana, and J. W. St Geme, 3rd. 2005. Trimeric autotransporters: a distinct subfamily of autotransporter proteins. Trends Microbiol 13:199-205.**

8. **Culpepper, M. A., E. E. Scott, and J. Limburg. Crystal structure of prolyl 4-hydroxylase from Bacillus anthracis. Biochemistry 49:124-133.**
9. **Dance, D. A. 2000. Ecology of Burkholderia pseudomallei and the interactions between environmental Burkholderia spp. and human-animal hosts. Acta Trop 74:159-168.**

10. **Dorman, S. E., V. J. Gill, J. I. Gallin, and S. M. Holland. 1998. Burkholderia pseudomallei infection in a Puerto Rican patient with chronic granulomatous disease: case report and review of occurrences in the Americas. Clin Infect Dis 26:889-894.**

11. **Dunn, D. M., and C. Franzblau. 1982. Effects of ascorbate on insoluble elastin accumulation and cross-link formation in rabbit pulmonary artery smooth muscle cultures. Biochemistry 21:4195-4202.**

12. **French, C. T., I. J. Toesca, T. H. Wu, T. Teslaa, S. M. Beaty, W. Wong, M. Liu, I. Schroder, P. Y. Chiou, M. A. Teitell, and J. F. Miller. Dissection of the**

Burkholderia intracellular life cycle using a photothermal nanoblade. Proceedings of the National Academy of Sciences of the United States of America 108:12095-12100.

13. **Goodyear, A., H. Bielefeldt-Ohmann, H. Schweizer, and S. Dow. Persistent gastric colonization with Burkholderia pseudomallei and dissemination from the gastrointestinal tract following mucosal inoculation of mice. PLoS One 7:e37324.**

14. **Goodyear, A., L. Kellihan, H. Bielefeldt-Ohmann, R. Troyer, K. Propst, and S. Dow. 2009. Protection from pneumonic infection with burkholderia species by inhalational immunotherapy. Infection and immunity 77:1579-1588.**

15. **Gorres, K. L., and R. T. Raines. Prolyl 4-hydroxylase. Crit Rev Biochem Mol Biol 45:106-124.**

16. **Handley, S. A., R. D. Newberry, and V. L. Miller. 2005. Yersinia enterocolitica invasin-dependent and invasin-independent mechanisms of systemic dissemination. Infect Immun 73:8453-8455.**

17. **Henderson, I. R., and J. P. Nataro. 2001. Virulence functions of autotransporter proteins. Infection and immunity 69:1231-1243.**
18. **Henderson, I. R., F. Navarro-Garcia, M. Desvaux, R. C. Fernandez, and D. Ala'Aldeen. 2004. Type V protein secretion pathway: the autotransporter story. Microbiol Mol Biol Rev 68:692-744.**

19. **Holden, M. T., R. W. Titball, S. J. Peacock, A. M. Cerdeno-Tarraga, T. Atkins, L. C. Crossman, T. Pitt, C. Churcher, K. Mungall, S. D. Bentley, M. Sebaihia, N. R. Thomson, N. Bason, I. R. Beacham, K. Brooks, K. A. Brown, N. F. Brown, G. L. Challis, I. Cherevach, T. Chillingworth, A. Cronin, B. Crossett, P. Davis, D. DeShazer, T. Feltwell, A. Fraser, Z. Hance, H. Hauser, S. Holroyd, K. Jagels, K. E. Keith, M. Maddison, S. Moule, C. Price, M. A. Quail, E. Rabbinowitsch, K. Rutherford, M. Sanders, M. Simmonds, S. Songsivilai, K. Stevens, S. Tumapa, M. Vesaratchavest, S. Whitehead, C. Yeats, B. G. Barrell, P. C. Oyston, and J. Parkhill. 2004. Genomic plasticity of the causative agent of melioidosis, Burkholderia pseudomallei. Proceedings of the National Academy of Sciences of the United States of America 101:14240-14245.**

20. **Holmgren, S. K., L. E. Bretscher, K. M. Taylor, and R. T. Raines. 1999. A hyperstable collagen mimic. Chem Biol 6:63-70.**

21. **Inglis, T. J., and J. L. Sagripanti. 2006. Environmental factors that affect the survival and persistence of Burkholderia pseudomallei. Appl Environ Microbiol 72:6865-6875.**

22. Kespichayawattana, W., P. Intachote, P. Utaisincharoen, and S. Sirisinha. 2004. Virulent Burkholderia pseudomallei is more efficient than avirulent Burkholderia thailandensis in invasion of and adherence to cultured human epithelial cells. Microb Pathog 36:287-292.

23. Krem, M. M., and E. Di Cera. 2001. Molecular markers of serine protease evolution. EMBO J 20:3036-3045.

24. Laemmli, U. K. 1970. Cleavage of structural proteins during the assembly of the head of bacteriophage T4. Nature 227:680-685.

25. Lazar Adler, N. R., B. Govan, M. Cullinane, M. Harper, B. Adler, and J. D. Boyce. 2009. The molecular and cellular basis of pathogenesis in melioidosis: how does Burkholderia pseudomallei cause disease? FEMS Microbiol Rev 33:1079-1099.

26. Leakey, A. K., G. C. Ulett, and R. G. Hirst. 1998. BALB/c and C57Bl/6 mice infected with virulent Burkholderia pseudomallei provide contrasting animal models for the acute and chronic forms of human melioidosis. Microb Pathog 24:269-275.

27. Letunic, I., T. Doerks, and P. Bork. SMART 7: recent updates to the protein domain annotation resource. Nucleic Acids Res 40:D302-305.

28. Lopez, C. M., D. A. Rholl, L. A. Trunck, and H. P. Schweizer. 2009. Versatile dual-technology system for markerless allele replacement in Burkholderia pseudomallei. Appl Environ Microbiol 75:6496-6503.

29. Marra, A., and R. R. Isberg. 1997. Invasin-dependent and invasin-independent pathways for translocation of Yersinia pseudotuberculosis across the Peyer's patch intestinal epithelium. Infection and immunity 65:3412-3421.

30. Mima, T., and H. P. Schweizer. The BpeAB-OprB efflux pump of Burkholderia pseudomallei 1026b does not play a role in quorum sensing, virulence factor production, or extrusion of aminoglycosides but is a broad-spectrum drug efflux system. Antimicrob Agents Chemother 54:3113-3120.

31. Nishimura, K., N. Tajima, Y. H. Yoon, S. Y. Park, and J. R. Tame. Autotransporter passenger proteins: virulence factors with common structural themes. J Mol Med (Berl) 88:451-458.

32. Ohnishi, Y., and S. Horinouchi. 1996. Extracellular production of a Serratia marcescens serine protease in Escherichia coli. Biosci Biotechnol Biochem 60:1551-1558.

33. Pantaloni, D., C. Le Clainche, and M. F. Carlier. 2001. Mechanism of actin-based motility. Science 292:1502-1506.

34. Rolim, D. B., D. C. Vilar, A. Q. Sousa, I. S. Miralles, D. C. de Oliveira, G. Harnett, L. O'Reilly, K. Howard, I. Sampson, and T. J. Inglis. 2005. Melioidosis, northeastern Brazil. Emerg Infect Dis 11:1458-1460.

35. Siezen, R. J., and J. A. Leunissen. 1997. Subtilases: the superfamily of subtilisin-like serine proteases. Protein Sci 6:501-523.

36. Sprague, L. D., and H. Neubauer. 2004. Melioidosis in animals: a review on epizootiology, diagnosis and clinical presentation. J Vet Med B Infect Dis Vet Public Health 51:305-320.

37. Stevens, M. P., A. Haque, T. Atkins, J. Hill, M. W. Wood, A. Easton, M. Nelson, C. Underwood-Fowler, R. W. Titball, G. J. Bancroft, and E. E. Galyov. 2004. Attenuated virulence and protective efficacy of a Burkholderia pseudomallei bsa type III secretion mutant in murine models of melioidosis. Microbiology 150:2669-2676.

38. Stevens, M. P., J. M. Stevens, R. L. Jeng, L. A. Taylor, M. W. Wood, P. Hawes, P. Monaghan, M. D. Welch, and E. E. Galyov. 2005. Identification of a bacterial factor required for actin-based motility of Burkholderia pseudomallei. Mol Microbiol 56:40-53.

39. Tripathi, L. P., and R. Sowdhamini. 2008. Genome-wide survey of prokaryotic serine proteases: analysis of distribution and domain architectures of five serine protease families in prokaryotes. BMC Genomics 9:549.

40. Valvano, M. A., K. E. Keith, and S. T. Cardona. 2005. Survival and persistence of opportunistic Burkholderia species in host cells. Current opinion in microbiology 8:99-105.

41. Whitmore, A., and C.S. Krisnaswami. 1912. An account f the discovery of a hitherto undescribed infective disease occurring among the population of Rangoon. Ind. Med. Gaz.:262-267.

42. Wiersinga, W. J., B. J. Currie, and S. J. Peacock. Melioidosis. N Engl J Med 367:1035-1044.

43. Yabuuchi, E., Y. Kosako, M. Arakawa, H. Hotta, and I. Yano. 1992. Identification of Oklahoma isolate as a strain of Pseudomonas pseudomallei. Microbiol Immunol 36:1239-1249.

CHAPTER III

Functional characterization of *Burkholderia pseudomallei* trimeric autotransporters[2]

Introduction

Burkholderia pseudomallei is a Gram-negative soil saprotroph and the causative agent of melioidosis, a severe and often systemic infection that can occur in both chronic and acute forms (1, 2). Acute pulmonary melioidosis is characterized by high fever, respiratory distress, and the formation of visceral abscesses, while chronic pulmonary melioidosis is characterized by prolonged pneumonia and abscess formation in lungs, liver, and spleen (2). Overall mortality due to melioidosis is high, approaching 50% in Thailand and 20% in Australia (2, 3). *B. pseudomallei* is endemic to Southeast Asia and Northern Australia, but has also been identified in Africa, South and Central America, India, and the Middle East (4, 5). Intrinsic resistance to clinically important antibiotics, including beta-lactams and many macrolides and aminoglycosides (6, 7), as well as the ability to invade and persist in phagocytic cells (8, 9), contributes to the difficulty of successfully treating *B. pseudomallei* infections. Intense antibiotic therapy over several months is often required to eliminate the bacteria, but despite a robust treatment regimen, relapse occurs with high frequency (10).

B. pseudomallei is able to adhere to and invade a variety of epithelial cell lines, and has also been shown to invade and survive within macrophage-like cells (8, 11-14).

---

[1]Authored by: Cristine G. Campos, Matthew Byrd, and Peggy A. Cotter.

Following uptake by a eukaryotic cell, *B. pseudomallei* is able to escape the endocytic compartment using one of its Type III Secretion Systems (T3SS) and enter the cytoplasm. Once in the cytoplasm, the bacterium polymerizes host actin using the surface protein BimA to move within host cells, avoiding exposure to the extracellular space (9, 15), *B. pseudomallei* can induce fusion of neighboring host cell membranes leading to the formation of multinucleated giant cells (MNGC) in a process that depends on one of its Type VI Secretion Systems (T6SS) (9, 16-18). Although several putative *B. pseudomallei* adhesins have been identified by genomic screens and protein microarrays (19, 20), only a few have been characterized, including Type IV pili and two putative autotransporter (AT) proteins BoaA and BoaB (21, 22).

AT proteins are secreted via the Type V Secretion System pathway, the largest family of secreted proteins amongst Gram-negative bacteria. AT proteins share three common features: an N-terminal signal sequence for Sec-dependent translocation into the periplasm, a central passenger region containing the functional domain(s), and a highly conserved, outer membrane channel-forming β-barrel domain at the C-terminus that is required for export of the passenger domain to the surface (23). The two subfamilies of AT proteins, classical and trimeric, are distinguished by the mechanism of β-barrel assembly and by the processing and localization of the passenger domain (24). The C-terminal β-domains of classical ATs are sufficient to form a channel, while trimeric ATs require three polypeptides to form the outer membrane channel, with each β-domain contributing one-third of the channel (23, 25, 26). In addition, classical AT proteins function as monomers and cleavage of the passenger domain usually occurs at or near the junction of the β-barrel domain and the passenger domain. Once cleaved, classical ATs

remain non-covalently associated with the cell surface or are released into the extracellular environment (23, 24). In contrast, trimeric AT passenger domains remain covalently linked to the β-domain, with the N-terminus located distal to the cell surface (23, 25).

AT proteins have been implicated in virulence in numerous Gram-negative bacterial pathogens. Two prototypical trimeric ATs, YadA (from *Yersinia enterocolitica*) and Hia (from *Haemophilus influenzae*), function as adhesins, and YadA also confers serum resistance by interfering with complement activation (27, 28). *B. pseudomallei* strain 1026b, isolated from a melioidosis patient in Thailand, encodes eleven putative AT proteins (two classical and nine trimeric) (29). Apart from the host actin-polymerizing BimA, only three *B. pseudomallei* trimeric AT proteins have been described. BoaA and BoaB have been reported to function as adhesins *in vitro* and contribute to *B. pseudomallei* replication inside macrophage-like cells (21). A portion of the passenger domain of a third AT protein, encoded by *bpaA*, has been crystallized, and the structure of its tightly woven trimeric head region resembles that of other trimeric ATs, including YadA, Hia, and BadA from *Bartonella henselae* (30).

In this study, we investigated eight *B. pseudomallei* trimeric ATs and evaluated their role in adherence, invasion, and plaque formation *in vitro*. We also performed the first animal experiments using any *B. pseudomallei* strains defective for production of trimeric ATs and found that one trimeric AT, BpaC, is required for efficient dissemination of bacteria to or survival within the liver in a BALB/c respiratory infection model.

Materials and Methods

Bacterial Strains. All manipulations of *B. pseudomallei* were conducted in a CDC/USDA-approved animal biosafety level 3 (ABSL3) facility at the University of North Carolina at Chapel Hill. The bacterial strains used in this study are listed in Table 1. *B. pseudomallei* strains were cultured in low salt lysogeny broth (LSLB; 10 g/l tryptone, 5 g/l yeast extract, 2.5 g/l NaCl), or on LSLB agar (Sigma-Aldrich, St. Louis, MO) for 24 h at 37ºC. *Escherichia coli* strains were grown in LB (10 g/l tryptone, 5 g/l yeast extract, 10 g/l NaCl) or on LB agar. When appropriate, culture media were supplemented with kanamycin (Km, 125 μg/ml for *B. pseudomallei* and 50 μg/ml for *E. coli*). LB agar was supplemented with 400 μg/ml of diaminopimelic acid (DAP; LL-, DD-, and meso-isomers; Sigma-Aldrich, St. Louis, MO) to support growth of RHO3 cells (31). Yeast extract-tryptone (YT; 10 g/l of yeast extract and 10 g/l of tryptone) medium supplemented with 15% sucrose and X-Gluc (GoldBio, St. Louis, MO) was used for counter-selection during the construction of *B. pseudomallei* deletion mutation strains (31).

Construction of *B. pseudomallei* mutant strains and plasmids. Deletion of *boaB*, *bpaE*, *bpaF*, and *bpaFds1/2* genes from *B. pseudomallei* strain Bp340 (a derivative of strain 1026b containing a Δ*amrRAB-oprA* mutation (32)) was carried out by allelic exchange using pEXKm5 derivatives (31). DNA fragments containing approximately 500 bp 5′ to the gene(s) (including the first three codons) and 500 bp 3′ to the gene (including the last three codons) were generated using a two-step, overlap PCR approach and were cloned into pEXKm5, resulting in plasmids pMBX3, pCCX3, pMBX1, and pMBX2. Plasmids were transformed into *E. coli* RHO3 cells and were delivered to Bp340 by

conjugation (31). Disruption strains were constructed by amplifying 300 bp from within each gene and ligating this fragment into the suicide vector pCC (a derivative of pRE118 (33) created by digesting the plasmid with EcoRI, and religating the backbone without the *sacB1* gene). Plasmids were transformed into *E. coli* RHO3 cells, and were delivered to Bp340 by conjugation.

Bacterial conjugations. Matings between *B. pseudomallei* and *E. coli* strain RHO3 were performed by incubating Bp340 with RHO3 cells carrying the appropriate allelic exchange plasmid or disruption plasmid (Table 1) on LSLB-DAP agar plates overnight. Cointegrants were selected on LSLB-Km. For deletion strains, cointegrants confirmed for plasmid insertion by PCR were grown overnight in LSLB without selection, allowing for a second recombination event to occur and for the plasmid to be lost. An aliquot of cells were plated on YT agar supplemented with 15% sucrose and X-Gluc, as previously described (31). Colonies arising from the counterselection were screened by PCR for the deletion mutation and/or disruption mutation, and all strains were confirmed by DNA sequencing.

Plaque assay. *B. pseudomallei* strains were grown overnight in LSLB at 37ºC. Each well of a 6-well plate was seeded with A549 human lung epithelial cells such that confluent monolayers contained approximately 1×10^6 cells per well. Cells were incubated in F12K medium (Cellgro, Circle Westwood, MA) supplemented with 10% fetal bovine serum (Gibco, Grand Island, NY) at 37ºC with 5% CO_2. Bacterial suspensions were diluted to an OD_{600} of 0.1 in fresh tissue culture medium, further diluted 1:10, and 25 μl of the diluted culture was added to each well (MOI of 0.1). Plates were incubated for 2 h and each well was washed thoroughly with fresh culture medium

and overlaid with a mixture containing 1.2% low-melting agarose (Fisher Scientific, Fairlawn, NJ), F12K with 10% FBS, gentamicin (Gm, 90 μg/ml), and 0.01% neutral red (Fischer Scientific, Waltham, MA). Plates were incubated for 24 h at 37ºC with 5% CO_2, and plaques were enumerated in each well.

Adherence and invasion assays. Bacterial strains and A549 cells were grown as described above. Bacteria were diluted to an OD_{600} of 0.1 in fresh tissue culture medium, and 250 μL of the diluted culture was added to each well of a 6-well plate (MOI of 100). Plates were incubated for 2 h, and each well was washed thoroughly with fresh culture medium. For the adherence assay, cells were immediately lysed using 1% Triton X-100 (Sigma-Aldrich, St. Louis, MO), and lysates were diluted and plated to determine the total colony forming units (CFU) in each well. For the invasion assay, cells were incubated an additional 90 min. in the presence of gentamicin (Gm, 90 μg/ml), washed with fresh culture medium, and lysed using 1% Triton X-100. Lysates were diluted and plated to determine the total CFU in each well. To calculate the percentage of adherent or internalized bacteria, the number of adherent or internalized bacteria was divided by the total number of bacteria in the inoculum and multiplied by 100.

Animal experiments. All animal experiments were approved by the Animal Studies Committee of the University of North Carolina at Chapel Hill (protocol 10-165). Six- to eight-week-old female BALB/c mice (The Jackson Laboratory, Bar Harbor, ME) were allowed free access to sterilized food and water. Animals were anesthetized with Avertin (140 mg/kg; Sigma-Aldrich, St. Louis, MO) by intraperitoneal injection prior to infection. For all infections, the desired inoculum of *B. pseudomallei* was suspended in phosphate buffered saline (PBS). Mice were inoculated intranasally with 500 CFU of *B.*

pseudomallei and were euthanized by CO_2 overdose at the indicated time points. At least three animals per strain were infected, and some experiments were performed twice and the results were combined. Animal experiments were terminated at 48 h, at which time all animals had become moribund. Organs were aseptically harvested and homogenized, and the bacterial burden in each organ was determined by plating serial dilutions of the homogenates.

Results

Bioinformatic characterization of putative trimeric AT-encoding gene loci. Nine putative trimeric AT-encoding genes were identified in the genome of the *B. pseudomallei* clinical isolate 1026b based on sequences at the 3′ ends of the open reading frames that are predicted to encode the characteristic β-domain. The trimeric AT-encoding gene *bimA*, which has been extensively characterized (15, 34), was not included in our analysis. Three of the remaining eight genes have been annotated previously as *boaA*, *boaB* (for *B*urkholderia *o*ligomeric coiled-coil *a*dhesin) (21), and *bpaA* (for B*urkholderia* p*seudomallei a*utotransporter) (30). For simplicity, we have named the remaining five uncharacterized genes *bpaB–F*. The trimeric AT-encoding genes are distributed between the two *B. pseudomallei* chromosomes: *boaB*, *bpaB*, and *bpaC* are on chromosome I, while *boaA*, *bpaA*, and *bpaD–F* are on chromosome II (Fig. 1).

One or more additional open reading frames (ORFs) with unknown function are present 3′ to and in the same orientation as four of the predicted AT genes (*bpaA*, *bpaB*, *bpaE*, and *bpaF*) (Fig. 1). The ORF BP1026B_II1528, 3′ to *bpaA*, is predicted to contain a consensus N-terminal lipobox sequence LAGC but lacks a Lol avoidance signal

necessary for retention at the inner membrane, suggesting that this protein is a lipoprotein that is localized to the inner leaflet of the outer membrane (35, 36). The ORFs 3′ to *bpaB* and *bpaE* (BP1026B_I2045 or *bpaBds1* and BP1026B_II0997 or *bpaEds1*, respectively) are predicted to encode OmpA family proteins and share 29% amino acid sequence identity. Like the BP1026B_II1528 gene product, the proteins encoded by *bpaBds1* and *bpaEds1* possess a lipobox sequence (LGAC and LTGC, respectively), and are likely localized to the inner leaflet of the outer membrane given the lack of a Lol avoidance signal. Immediately 3′ to *bpaF* is an ORF (BP1026B_II1531) that encodes a hypothetical protein containing the domain of unknown function (DUF) 2827. DUF2827 proteins are well conserved amongst *Burkholderia* species, and though a second DUF2827-encoding ORF (BP1026B_II1532) immediately follows the first, these two proteins share only 48% amino acid sequence identity. To distinguish these DUF2827-encoding genes in later analyses, we refer to them as *bpaF*ds1 and *bpaF*ds2.

The first fully sequenced *B. pseudomallei* strain, K92643, was isolated from a patient in Thailand, and is the strain in which the eleven autotransporter-encoding genes were first identified (21, 37, 38). Although genes predicted to encode trimeric ATs are conserved amongst *B. pseudomallei* strains, two of the eight putative AT-encoding genes in our study are annotated differently in strain 1026b compared to K92643. *boaA* (BPSS0796 in K92643) is unannotated in the 1026b genome, but an alignment of the region expected to contain *boaA* with the corresponding region of the K92643 genome shows that *boaA* is indeed present in 1026b and is 91.5% identical to BPSS0796 at the nucleotide level. Similarly, *bpaD* (BPSS0088 in K92643) is annotated as a pseudogene of

1833 bp in 1026b; however, aligning the sequences 5′ to *bpaD* with BPSS0088 reveals a full-length *bpaD* gene that is 84.6% identical to BPSS0088 at the nucleotide level.

Bioinformatic characterization of putative trimeric AT proteins. The predicted proteins encoded by *boaA*, *boaB*, and *bpaA–F* range in size from 72.3 kDa (BpaD, 782 aa) to 241.5 kDa (BpaA, 2575 aa) and share features common to all trimeric ATs, including a 70–80 aa C-terminal β-barrel domain and a passenger domain containing numerous short repeated sequences (Fig. 2). Interestingly, seven of the eight trimeric AT proteins (all but BpaD) have a well-conserved 23-aa extended signal peptide region (ESPR, black region in Fig. 2) preceding a typical N-terminal signal sequence (dark blue region, Fig. 2); these regions begin with the sequence MN(K/R) and resemble the ESPRs of other trimeric AT and two-partner secretion proteins (Fig. 3). ESPRs can be found in ~10% of ATs and may be involved in regulating the translocation of ATs across the inner membrane into the periplasm (23, 39). Although, as annotated, BpaD does not contain an ESPR, manually translating the sequence immediately 5′ to the *bpaD* ORF reveals an MNR consensus sequence beginning 14 amino acids N-terminal to the predicted valine start codon. However, between the MNR and the initial valine are two UGA stop codons, preventing the ESPR-like region from being translated. Therefore, it appears that BpaD, predicted to be the smallest of the trimeric ATs in *B. pseudomallei*, may have had an ESPR earlier in its evolutionary history (Fig. 3).

We used the domain annotation of trimeric autotransporter adhesins (daTAA) software to predict motifs within the passenger domain of *B. pseudomallei* trimeric AT proteins that have been previously described for other trimeric ATs (40). One particular repeated sequence, the YadA-like head motif (also known as the NSVAIG--S motif), is

present in all eight proteins, making up the majority of the passenger domains of BpaC and BpaD (Fig. 2). This motif has been implicated in YadA-dependent collagen binding in *Yersinia enterocolitica*, though its role in *B. pseudomallei* adherence and/or virulence has not been assessed (41).

Five of the putative trimeric AT proteins (BoaA, BoaB, BpaA, BpaB, and BpaF) possess repeat regions in the passenger domain that are not common outside of *Burkholderia* species and share the N-terminal amino acid sequence SLST. These repeats are 11, 14, and 18 amino acids in length with consensus sequences of SLSTSTSTGTG, SLSTGLSTTNS(N/T/S)(V/L)(A/T), and SLSTSTSTGLSSA(N/T/Q)SS(I/V)A, respectively. A large portion of the passenger domains of BoaA and BoaB and nearly the entire passenger domains of BpaA and BpaF are composed of SLST repeats; however, searches for both primary amino acid sequence and secondary structure homology fail to suggest a structure or function for these repeats. In 1026b, BoaA and BoaB are 63.1% identical and share similarly annotated regions within their passenger domains, perhaps suggesting that BoaA and BoaB are the result of a gene duplication event.

Construction of mutant strains. To evaluate the contribution of putative trimeric ATs to *B. pseudomallei* virulence, we constructed strains containing plasmid disruption and/or deletion mutations in each AT-encoding gene, as well as in the ORF(s) 3′ to two AT-encoding gene loci (Fig. 4). Plasmid disruptions were made such that the suicide plasmid pCC, carrying a 300-bp internal fragment of the AT-encoding gene (or of the gene 3′ to *bpaE*), integrated at approximately the midpoint of the coding region of each gene via single-crossover homologous recombination. The presence of *nptII* (encoding a Km resistance protein) on the plasmid allowed for selection of cointegrants, and plating

the strains on selective and non-selective media provided a means to assess plasmid loss. We grew the disruption mutation strains in LSLB without Km and determined the percent of cells that were Km^r and Km^s after 48 h incubation at 37°C. There was no significant plasmid loss for seven out of eight AT-encoding gene disruption mutants or for Bp340::pD*bpaEds1*; however, nearly all Bp340::pD*boaB* cells had lost the plasmid after 24 h, suggesting either that *boaB* is indispensible for growth *in vitro* or that the plasmid is simply unstable in this location (data not shown).

As the plasmid instability observed for Bp340::pD*boaB* would prevent the use of this strain in subsequent assays, we constructed an unmarked, in-frame deletion mutation of *boaB* using the allelic exchange plasmid pEXKm5, which has been used previously in *Burkholderia* spp. (31). We also created strains with in-frame deletion mutations in *bpaE*, *bpaF*, and in a region encompassing both genes 3′ to *bpaF* (Fig. 4). We chose to delete the two genes 3′ to *bpaF* due to their unique presence in *Burkholderia* and their predicted function as glycosyltransferases, as glycosylation is a critical post-translational modification of certain ATs (42).

One *B. pseudomallei* trimeric AT, BpaE, contributes to plaque formation in A549 cells. *B. pseudomallei* can spread from cell to cell without exiting the cytoplasm and can form plaques in a cell monolayer (34, 43, 44). *In vitro*, this process can be quantified by assessing the ability of *B. pseudomallei* to form plaques in a monolayer of cultured cells. We evaluated strains containing disruption mutations in seven of the eight putative trimeric AT-encoding genes (all but BoaB) for plaque formation compared to the wild-type strain Bp340 (Fig. 5A). Six of the seven disruption mutants formed plaques at a frequency similar to Bp340, which formed approximately 75 plaques per well.

Bp340::pD*bpaE*, however, formed significantly fewer plaques compared to Bp340 (15.5 ± 3.26 compared to 78.5 ± 4.39, $p < 0.01$). We likewise evaluated plaque formation by the *boaB* deletion mutant but did not observe a difference compared to Bp340 (Fig. 5B). Our results suggest that BpaE is required for one or more steps in the plaque formation process, which includes adherence, invasion, intracellular survival, and cell-cell fusion.

BoaA, BoaB, BpaA, BpaC, and BpaD contribute to *B. pseudomallei* adherence to A549 cells. The plaques formed by Bp340::pD*bpaE* appeared to be of similar size to those formed by Bp340, suggesting that *bpaE* might be involved in plaque formation at a step prior to cell-cell fusion. We evaluated all seven disruption mutants and Bp340Δ*boaB* for adherence to A549 cells as described in Materials and Methods, and we observed a significant decrease in CFU recovered for four of the seven disruption mutants when lysates were plated on LSLB agar, and for six of the seven disruption mutants when lysates were plated on LSLB agar containing Km (Fig. 6A). Bp340Δ*boaB* likewise displayed a significant decrease in recovered CFU compared to Bp340 (Fig. 6B). Bp340::pD*bpaE* did not show a decrease in CFU recovered when plated on LSLB, and the decrease in CFU recovered when plated on LSLB with Km was only weakly significant compared to Bp340. Interestingly, for mutants with *bpaC*, *bpaE*, or *bpaF* disrupted, there were significantly fewer bacteria recovered when plated on LSLB containing Km compared to LSLB alone, suggesting that these strains had undergone substantial plasmid loss during the two-hour incubation period. In the most extreme case, 97% of Bp340::pD*bpaC* bacteria had lost the disruption plasmid during the experiment, indicating that there is strong selective pressure for maintaining an intact *bpaC* gene in the context of the adherence assay.

BpaA, BpaC, BpaE, and BpaF are required for efficient internalization in A549 cells. Some trimeric AT proteins are known to be multi-functional, including *P. mirabilis* AipA and *Y. pseudotuberculosis* YadA, both of which function as adhesins and mediate entry into eukaryotic cells (45-47). To address the contribution of *B. pseudomallei* 1026b trimeric ATs to A549 cell internalization, we performed invasion assays with the seven disruption mutants and the *boaB* deletion mutant. We observed a significant decrease in the number of CFU recovered compared to the inoculum for four of the disruption mutation strains when plated on LSLB, and for all seven strains when plated on LSLB containing Km (Fig. 6C). Two of the strains with fewer CFU recovered when plated without selection, Bp340::pD*bpaA* and Bp340::pD*bpaC*, also exhibited a decrease in CFU recovered in the adherence assay, which could influence internalization by decreasing the ability of the bacteria to associate with the A549 cell monolayer. The other two strains deficient in internalization, Bp340::pD*bpaE*, and Bp340::pD*bpaF*, were not deficient for adherence, suggesting that the observed phenotype is due to BpaE and BpaF promoting internalization and not simply preventing intimate association with the A549 monolayer. Three disruption strains, Bp340::pD*boaA*, Bp340::pD*bpaB*, and Bp340::pD*bpaD*, exhibited significant plasmid loss during the internalization assay, though these three strains were not those that had lost the plasmid in the adherence assay. The one deletion strain, Bp340Δ*boaB*, was recovered at a level similar to Bp340 (Fig. 5D).

Evaluation of *B. pseudomallei* trimeric ATs in a mouse model of acute infection. The *B. pseudomallei* trimeric AT proteins BoaA and BoaB have been implicated in adherence and invasion of host cells ((21) and Fig. 6), but there has been no

characterization of BoaA, BoaB, or BpaA-F in an animal model of *B. pseudomallei* infection. We hypothesized that one or more trimeric ATs would be required for *B. pseudomallei* virulence, consistent with the role of other trimeric ATs in virulence in a variety of Gram-negative pathogens (47-51). We infected BALB/c mice intranasally with 500 CFU of Bp340 or one of the trimeric AT-encoding gene disruption or deletion strains, and sacrificed the mice at 48 h post-inoculation and determined bacterial burden in the lungs, liver, and spleen. Mutants with plasmid disruptions of trimeric AT genes were plated on both LSLB and LSLB with 125 μg/ml Km to assess plasmid loss *in vivo*.

At 48 h, the lungs of mice infected with Bp340 contained approximately 10^6–10^8 CFU, while the liver and spleen contained approximately 10^5–10^6 CFU of *B. pseudomallei* (Fig. 7). There was no significant difference in the bacterial burden in any of the three organs for Bp340::pD*boaA* and Bp340Δ*boaB* compared to Bp340 (Fig. 7A and B). Likewise, the burden of Bp340::pD*bpaA*, Bp340::pD*bpaB*, and Bp340::pD*bpaD* was not different from Bp340 in any of the organs (Fig. 7C, D, and F). Although the burden of Bp340::pD*bpaC* was not different from Bp340 when plated on LSLB in the absence of selection, there was significant plasmid loss in the liver, suggesting that this strain was defective in its ability to disseminate to or survive in this organ (Fig. 7). We did not observe any plasmid loss in the other disruption mutation strains, suggesting that the lack of single trimeric AT genes, other than *bpaC*, was not detrimental to bacterial survival in the host.

To account for possible polar effects on the gene(s) 3′ to *bpaE* and *bpaF* due to plasmid disruption of the trimeric AT-encoding genes, we constructed in-frame deletion mutations in *bpaE* and *bpaF* in anticipation that one or both ATs would contribute to *B.*

pseudomallei pathogenesis. We also constructed a strain with a disruption mutation in the gene 3′ to *bpaE* (*bpaEds1*), and a strain with an in-frame deletion in the genes 3′ to *bpaF* (*bpaFds1* and *bpaFds2*). Both Bp340Δ*bpaE* and Bp340Δ*bpaF* were able to establish an infection in the lung and disseminate to the liver and spleen similar to Bp340 (Fig. 7G and H). Additionally, neither Bp340::pD*bpaEds1* nor Bp340Δ*bpaFds1/2* had a virulence defect (Fig. 7I and data not shown), suggesting that these highly conserved genes 3′ to *bpaE* and *bpaF* are not required in the BALB/c intranasal model of infection.

Discussion

In this study, we identified nine putative trimeric AT-encoding gene loci in the genome of *B. pseudomallei* clinical isolate 1026b, and described the predicted domains of eight out of the nine corresponding proteins (BimA excluded). We constructed strains containing disruption and/or deletion mutations in each of the AT-encoding genes, and in genes immediately 3′ to certain AT-encoding genes, and compared them with wild-type *B. pseudomallei* for plaque formation, adherence, and internalization in respiratory epithelial cells. Our characterization of eight trimeric ATs revealed a diverse set of phenotypes *in vitro*, with BpaA and BpaC contributing to both adherence and internalization in A549 cells, while BoaA, BoaB, and BpaD appeared to function solely in adhesion and BpaE and BpaF in invasion. Surprisingly, perhaps, only BpaC played a role in virulence in the BALB/c mouse model of *B. pseudomallei* respiratory infection.

Nearly all AT proteins characterized so far have been shown to play roles in pathogenesis *in vivo* or in virulence-associated assays (24, 28, 47, 49, 52-54). Protein microarray and expression library studies have provided evidence that the majority of *B.*

pseudomallei trimeric ATs are produced during human melioidosis (37, 55). A *B. pseudomallei* phage library expressed in *E. coli* revealed five AT proteins, BoaA, BpaB, BpaE, BpaF, and BimA, that reacted with convalescent melioidosis patient sera, indicating that these proteins were expressed at a level high enough to elicit an antibody response during infection (37). However, the occurrence of clones harboring trimeric AT-encoding genes was relatively low compared to the total number of sera-reactive clones, suggesting that these five genes may not be expressed in all instances of melioidosis, or that the overall expression of the genes is low. Additionally, a protein microarray study of potential antigens serodiagnostic for *B. pseudomallei* infection found that BpaA, BpaE, and BimA were significantly more reactive with melioidosis-positive patient sera compared to melioidosis-negative controls (55). These studies, along with the data presented here, suggest that the expression of trimeric AT-encoding genes in *B. pseudomallei* may be more complex and conditional than we had hypothesized.

The *bpaBds1* and *bpaEds1* genes are located 3′ to two of the AT-encoding genes characterized in this study, *bpaB* and *bpaE*, and are predicted to encode OmpA family proteins, while the *bpaAds1* gene is located 3′ to *bpaA* and encodes a protein of unknown function. Interestingly, all three of these proteins are predicted to be lipidated and localized to the outer membrane, suggesting that they may function as accessory proteins for their corresponding ATs (and potentially for other ATs as well). The requirement of accessory proteins for translocation of ATs across the periplasm and insertion into the outer membrane has recently been established as a general feature of AT biology (39, 56). The Bam complex, comprising the integral β-barrel protein BamA and the associated lipoproteins BamBCDE, is necessary for trimeric AT insertion in the outer membrane

through an unknown mechanism, while various periplasmic chaperones, such as SurA, Skp, and DegP, are required for AT passage through the periplasm (39). Further characterization of the putative accessory proteins identified in our study will be necessary to determine their role, if any, in trimeric AT production and function.

Seven of the eight trimeric ATs included in our study possess ESPRs (Fig. 3). ESPRs were initially thought to function in cotranslational targeting of large Type V family proteins to the periplasm; however, recent studies suggest that the region serves a more subtle function by regulating the rate of translocation across the inner membrane to avoid an accumulation of misfolded proteins in the periplasm (39, 57, 58). Bioinformatic analyses have revealed that ESPRs appear to be restricted to Type V proteins greater than approximately 100 kDa in *Beta-* and *Gammaproteobacteria*, and that they are present in approximately 10% of AT proteins (23, 24, 39, 59). In *B. pseudomallei* 1026b, an uncharacteristically high 78% (seven out of nine) of the trimeric ATs possess ESPRs, and the only two that lack such a feature are the two smallest trimeric ATs: BpaD and BimA. However, the fact that BpaD has what appears to be an ESPR remnant (Fig. 3) leads us to speculate that the ESPR is not necessary to regulate the secretion of proteins of this size and has thus been lost as BpaD evolved.

In addition to the presence of ESPRs in the majority of trimeric ATs in *B. pseudomallei* 1026b, five of these proteins contain "SLST" repeats of 11, 14, or 18 aa that are unique to *Burkholderia* species and have no predicted structure or function. Not surprisingly, variation in the length of BoaA, BoaB, BpaA, BpaB, and BpaF homologs amongst *B. pseudomallei* strains is largely due to different numbers of SLST repeats in the passenger domain. It is possible, therefore, that within 1026b, the addition or loss of

these repeats is used by the cell to regulate the length of the passenger domain and is perhaps related to AT function. Another possibility is that the serine- and threonine-rich repeats are glycosylation sites. Though initially thought to be a post-translational modification restricted to eukaryotes, protein glycosylation in prokaryotes has been extensively documented and is important for the function of several virulence factors, including the classical ATs Ag43 and AIDA-I in pathogenic *E. coli* (24, 42, 60, 61). For Ag43, it has been shown that serine- and threonine-rich regions of the passenger domain are multiply glycosylated with heptose residues, and that the addition of these sugars is essential for binding human-derived HEp-2 cells (61). In 1026b, the proteins encoded by *bpaFds1* and *bpaFds2*, which are located immediately 3′ to *bpaF*, have no predicted function based on homology searches of primary aa sequence, but structural homology searches reveal the greatest similarity to an *N*-acetylglucosamine transferase from the plant pathogen *Xanthomonas campestris*. Although we did not observe a phenotype *in vivo* for the mutant lacking both *bpaFds1* and *bpaFds2*, we are currently investigating the glycosylation state of BpaF and other AT proteins containing SLST repeats, as these genes may be important for AT function in other models.

In our study, we observed a significant decrease in the number of plaques formed in an A549 cell monolayer for only one trimeric AT-encoding gene disruption strain, Bp340::pD*bpaE*, compared to the wild-type strain. Though fewer in number, plaques formed by Bp340::pD*bpaE* were the same size as those formed by Bp340, indicating that, once inside the host cell, movement between cells was not hindered by loss of *bpaE*. The fact that six of the seven disruption mutants did not show a plaque formation defect suggests that either these genes are not important for any step in plaque formation

(adherence, invasion, intracellular survival, and cell-cell fusion), or that the disruption plasmid was lost due to selective pressure to maintain an intact trimeric AT-encoding gene. Plasmid loss could occur in the plaque assay, as it was performed in the absence of Km (Gm was added to the medium to kill extracellular bacteria, and once inside the A549 cells, Km would be ineffective because it does not cross the cell membrane). It is difficult to recover bacteria from plaques (especially in a BSL3 laboratory) to determine the amount of plasmid loss—therefore, we performed adherence and invasion assays both to assess the contribution of trimeric ATs to individual steps in the plaque formation process and to evaluate plasmid loss.

When we evaluated adherence and internalization of trimeric AT-encoding gene disruption or deletion mutants, we found that the eight trimeric ATs fell into one of four categories: having a phenotype in adherence only (BoaA, BoaB, and BpaD), in internalization only (BpaE and BpaF), in both adherence and internalization (BpaA and BpaC), or in neither adherence nor invasion (BpaB). In addition, the three strains that underwent significant plasmid loss in the adherence assay (Bp340::pD*bpaC*, Bp340::pD*bpaE*, and Bp340::pD*bpaF*) were not the same strains as those that showed significant plasmid loss in the internalization assay (Bp340::pD*boaA*, Bp340::pD*bpaB*, and Bp340::pD*bpaD*). The distinct contribution of each trimeric AT to adherence and/or internalization, as well as the variability in plasmid loss, indicates that these proteins have disparate functions and that the selective pressure to maintain certain trimeric AT-encoding genes intact is different in the context of internalization compared to adherence. Future studies will include the construction of strains containing in-frame deletion mutations to determine definitively the role of these genes in virulence

Given the array of phenotypes in the plaque, adherence, and invasion assays, we expected to observe a role in pathogenesis for more than one trimeric AT using a BALB/c mouse model of infection. Neither BoaA nor BoaB, which are reported to function in adherence by us and others (21), were required for growth or dissemination within the mouse. Similarly, the *bpaD* disruption mutant was deficient in adherence yet did not have a phenotype in the mouse model. Though defective for both adherence and internalization, Bp340::pD*bpaA* achieved the same burden in the lungs, liver, and spleen as Bp340. One disruption mutation strain, Bp340::pD*bpaB*, was not deficient in any assay *in vitro* or *in vivo*. Finally, neither Bp340Δ*bpaE* nor Bp340Δ*bpaF* generated a phenotype in the mouse, despite being significantly defective in internalization. However, Bp340::pD*bpaC* was deficient in adherence and subsequent internalization, and demonstrated significant plasmid loss in the liver, suggesting that BpaC is a general virulence factor that may function as an adhesin and/or invasin *in vivo*. Although our results do not demonstrate a correlation between *in vitro* and *in vivo* assays, the fact that six of the trimeric ATs are produced during human *B. pseudomallei* infections suggests that they do play a role in pathogenesis (37, 55), but additional animal models will be required to fully evaluate the contribution of trimeric ATs to disease.

The use of different model systems has proven to yield substantially different results with regard to flagella, one of the few *B. pseudomallei* virulence factors that has been examined in detail. DeShazer *et al*. initially characterized the *fliC* gene, encoding the flagellum structural protein, in *B. pseudomallei* 1026b and reported no difference in virulence for a *fliC* transposon mutant compared to the wild-type strain in either diabetic rat or Syrian hamster models (29). However, the authors were careful to note that their

results only applied to the two models they tested. In a more recent study, a Δ*fliC* mutant strain was evaluated in BALB/c mice inoculated by the intranasal route, and the mutant strain was dramatically attenuated for virulence compared to the wild-type strain, though it did not show a phenotype in an *in vitro* cell invasion assay or in the *Caenorhabditis elegans* model (62). Even within the same species, the choice of host strain can have profound consequences on the course of infection with *B. pseudomallei*. A study analyzing *B. pseudomallei* virulence in two mouse backgrounds, BALB/c and C57Bl/6, found the difference in the ten-day LD_{50} values between the backgrounds to be nearly four orders of magnitude (63). When infected at the same dose, all BALB/c mice had to be sacrificed after five days, whereas all C57Bl/6 mice survived until the experiment was terminated at four weeks (63). With these data in mind, repeating our animal experiments with C57Bl/6 mice may reveal a phenotype for AT proteins that we were not able to observe in BALB/c mice due to their extreme sensitivity to *B. pseudomallei*.

Our study is the first to systematically evaluate a class of genes (those encoding trimeric ATs) in *B. pseudomallei* both *in vitro* and *in vivo*. While we demonstrated that nearly all ATs tested have a function in adherence and/or invasion and that BpaC is important for efficient dissemination to or survival in the liver, we only evaluated strains containing a single trimeric AT-encoding gene disrupted or deleted, and our analysis *in vivo* was limited to a single animal model and route of infection. It is probable that the deletion or disruption of two, three, or more AT-encoding genes will result in reduced virulence, and performing such studies would likely reveal redundant or synergistic functions for some ATs in infection. As *B. pseudomallei* infects not only animals, but can be found in the rhizosphere and even within the roots and foliage of several plant species

(64), fully understanding the role of trimeric ATs may require the use of diverse model systems.

Table 1. Strains and plasmids used in this study.

Strain or Plasmid	Description	Source or reference
Strains		
E. coli		
DH5α	Molecular cloning strain	(65)
RHO3	Conjugation strain; Km^s, Δ*asd*, Δ*aphA*	(31)
B. pseudomallei		
Bp340	Δ*amrRAB-oprA* derivative of *B. pseudomallei* 1026b	(32)
Bp340::pD*boaA*	Bp340 with *boaA* disrupted by pCC1; Km^r	This study
Bp340::pD*boaB*	Bp340 with *boaB* disrupted by pCC2; Km^r	This study
Bp340::pD*bpaA*	Bp340 with *bpaA* disrupted by pCC3; Km^r	This study
Bp340::pD*bpaB*	Bp340 with *bpaB* disrupted by pCC4; Km^r	This study
Bp340::pD*bpaC*	Bp340 with *bpaC* disrupted by pCC5; Km^r	This study
Bp340::pD*bpaD*	Bp340 with *bpaD* disrupted by pCC6; Km^r	This study
Bp340::pD*bpaE*	Bp340 with *bpaE* disrupted by pCC7; Km^r	This study
Bp340::pD*bpaEds1*	Bp340 with *bpaEds1* disrupted by pCC7; Km^r	This study
Bp340::pD*bpaF*	Bp340 with *bpaE* disrupted by pCC8; Km^r	This study
Bp340Δ*boaB*	Bp340 with an in-frame, nonpolar *boaB* deletion	This study
Bp340Δ*bpaE*	Bp340 with an in-frame, nonpolar *bpaE* deletion	This study
Bp340Δ*bpaF*	Bp340 with an in-frame, nonpolar *bpaF* deletion	This study
Bp340Δ*bpaFds1/2*	Bp340 with an in-frame, nonpolar *bpaF*ds1/2 deletion	This study
Plasmids		
pEXKm5	Allelic exchange vector; Ap^r, Km^r, $sacB^+$, $gusA^+$	(31)
pCC1	pCC with an ~300 bp internal fragment of *boaA*; Km^r	This study
pCC2	pCC with an ~300 bp internal fragment of *boaB*; Km^r	This study
pCC3	pCC with an ~300 bp internal fragment of *bpaA*; Km^r	This study
pCC4	pCC with an ~300 bp internal fragment of *bpaB*; Km^r	This study
pCC5	pCC with an ~300 bp internal fragment of *bpaC*; Km^r	This study
pCC6	pCC with an ~300 bp internal fragment of *bpaD*; Km^r	This study
pCC7	pCC with an ~300 bp internal fragment of *bpaE*; Km^r	This study
pCC*bpaEds1*	pCC with an ~300 bp internal fragment of *bpaEds1*; Km^r	This study
pCC8	pCC with an ~300 bp internal fragment of *bpaF*; Km^r	This study
pCCX3	pEXKm5 with *bpaE* flanking sequences; Ap^r, Km^r	This study
pMBX1	pEXKm5 with *bpaF* flanking sequences; Ap^r, Km^r	This study
pMBX2	pEXKm5 with *bpaFds1/2* flanking sequences; Ap^r, Km^r	This study
pMBX3	pEXKm5 with *boaB* flanking sequences; Ap^r, Km^r	This study

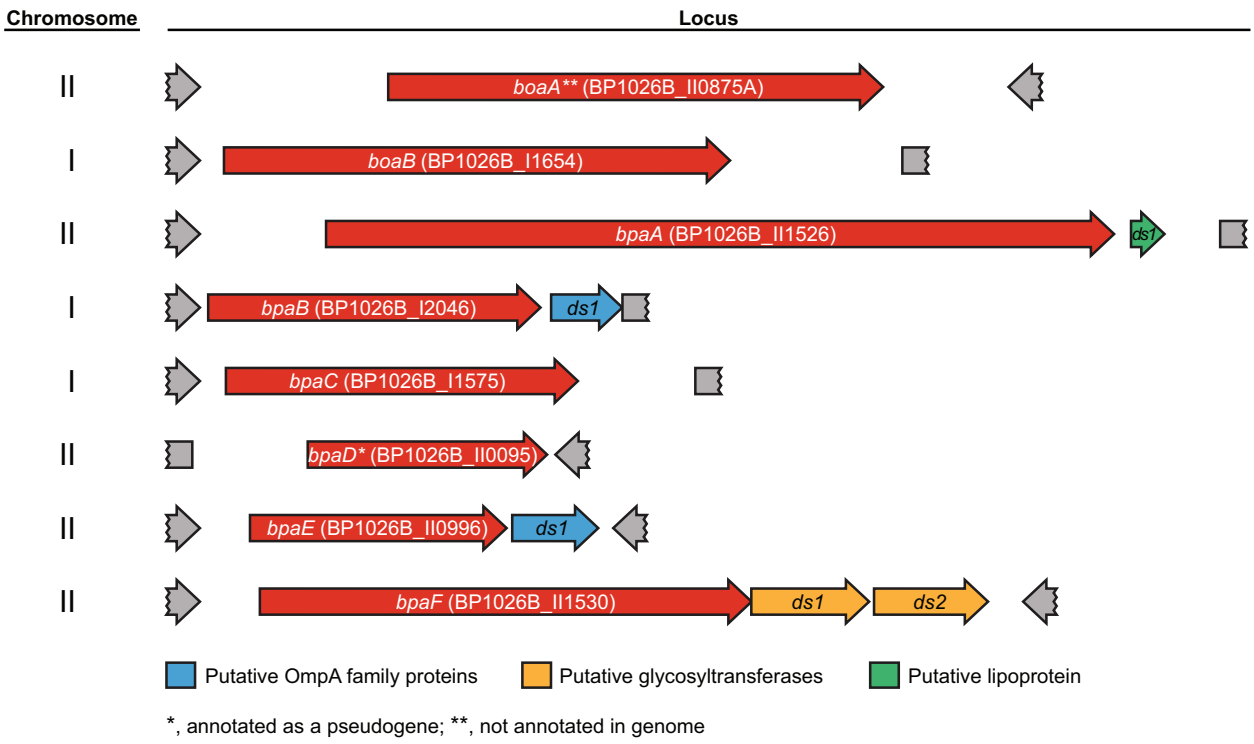

Fig. 1. *B. pseudomallei* 1026b putative trimeric AT gene loci. Genomic context of each putative trimeric AT gene drawn to scale, with the predicted function of immediate 3′ genes indicated, if present. The chromosome on which each trimeric AT gene is present is indicated by (I) or (II).

Fig. 2. *B. pseudomallei* 1026b putative trimeric AT protein domains. Domains predicted by daTAA (domain annotation of trimeric autotransporter adhesins) are indicated in the legend. The characteristic C-terminal β-barrel domain is shown in yellow, and predicted coiled-coil regions are underlined. White regions are sequences with limited homology to known AT proteins, and in BoaA, BoaB, BpaA, BpaB, and BpaF, contain repeats of 11 (SLSTSTSTGTG), 14 (SLSTGLSTTNS(N/T/S)(V/L)(A/T)), and 18 (SLSTSTSTGLSSA(N/T/Q)SS(I/V)A) amino acids.

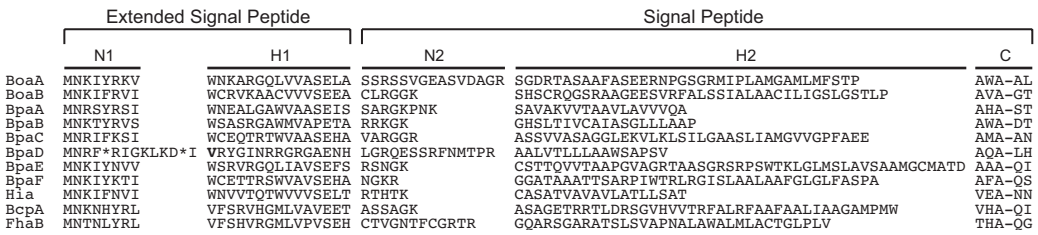

Fig. 3. ESPRs of putative *B. pseudomallei* 1026b trimeric AT proteins. Extended signal peptide and conventional signal peptide are indicated. N1, N-terminal charged region of the ESPR; H1, C-terminal hydrophobic region of the ESPR; N2, N-terminal charged region of the conventional signal peptide; H2, central hydrophobic region of the conventional signal peptide; C, signal peptidase recognition site with putative cleavage sites indicated with a hyphen. N1, H1, N2, H2, and C regions are defined according to (39). For BpaD, **V** indicates the predicted start codon.

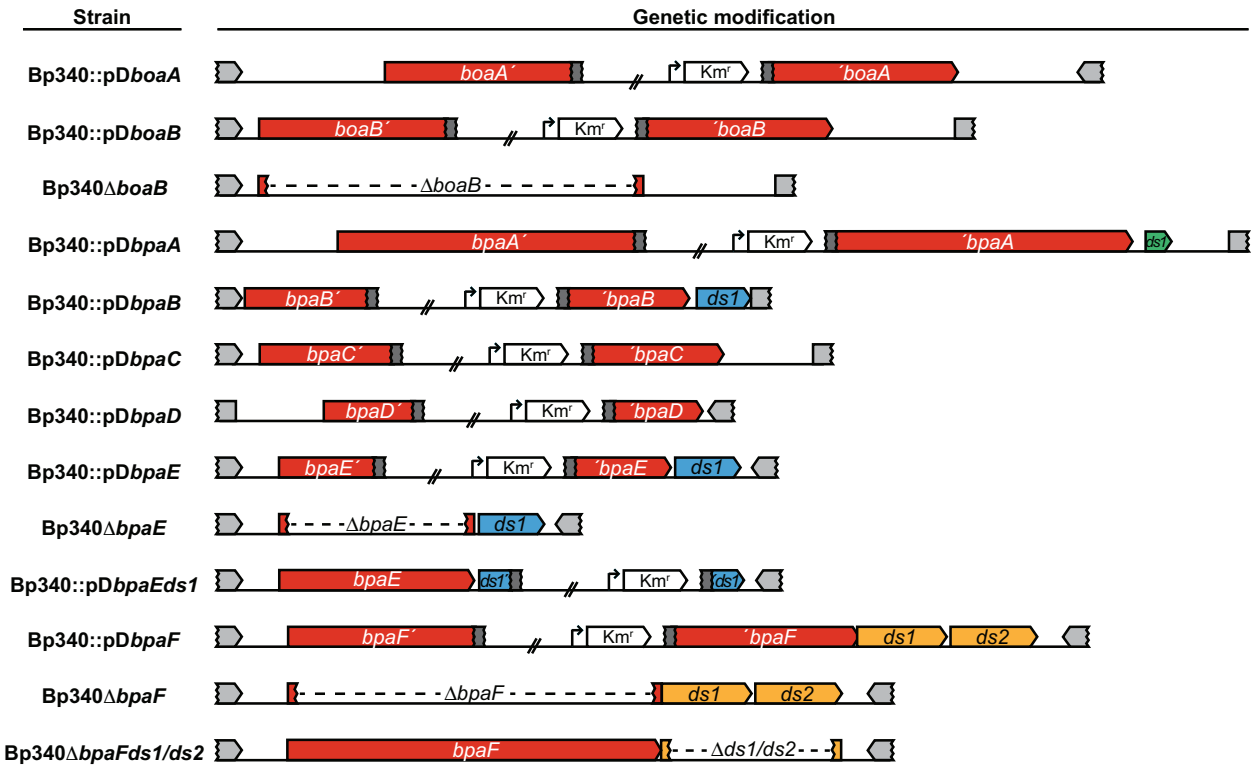

Fig. 4. Schematic of deletion and disruption mutations used in this study.

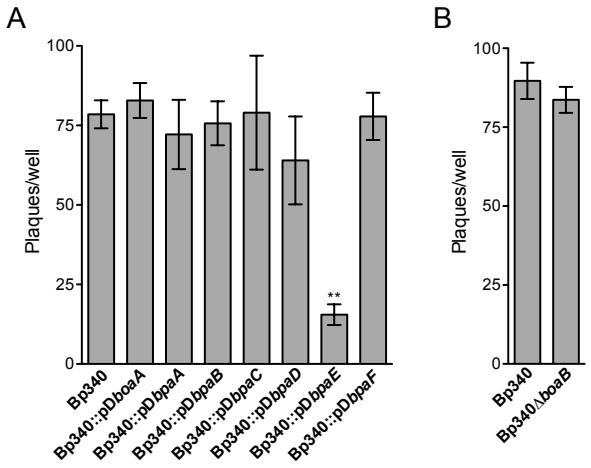

Fig. 5. Plaque formation by *B. pseudomallei* 1026b trimeric AT disruption mutants. A549 cells (approximately 1×10^6 cells per well in a 6-well plate) were inoculated with *B. pseudomallei* trimeric AT disruption mutants at an MOI of 0.1, and plates were incubated for 2 h at 37ºC. Plates were washed thoroughly with fresh medium and were overlaid with a mixture containing F12K medium, low-melting agarose, gentamicin and neutral red. Plates were incubated for 24 h at 37ºC with 5% CO_2, and plaques were enumerated in each well. Data are mean ± SEM for two experiments performed in triplicate. Significance is compared to Bp340. **, $p < 0.01$ by Tukey's multiple comparison test following a one-way ANOVA.

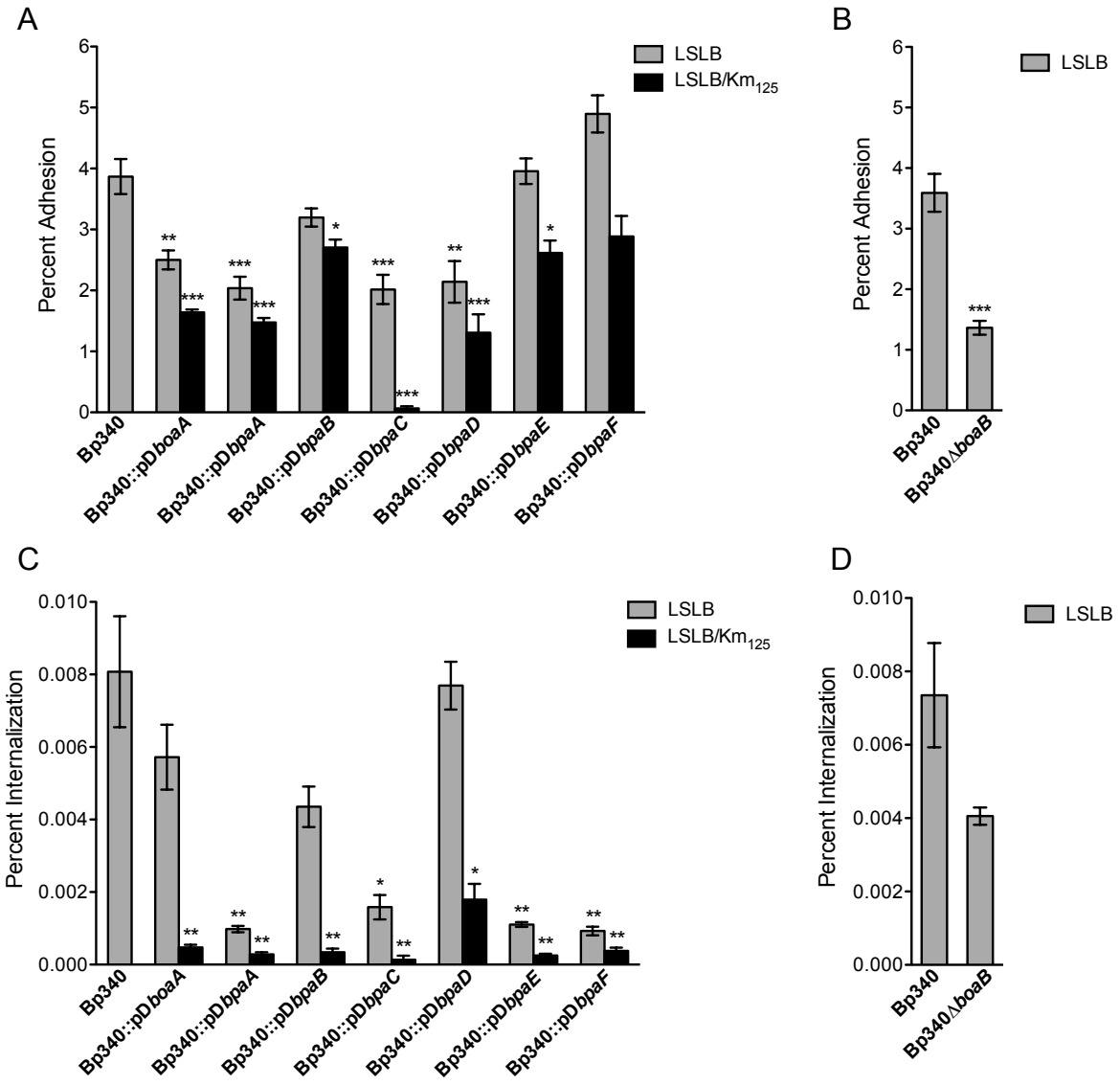

Fig. 6. Contribution of trimeric AT proteins to adherence and invasion. A549 cells were grown as described for plaque formation experiments and were inoculated with the indicated strains at an MOI of 100. Plates were incubated for 2 h, and each well was washed thoroughly with fresh culture medium. For adherence of the trimeric AT disruption mutants (A) and Bp340Δ*boaB* (B), cells were immediately lysed using 1% Triton X-100 and lysates were diluted and plated to determine the total CFU. For invasion of the trimeric AT disruption mutants (C) and Bp340Δ*boaB* (D), cells were

incubated an additional 90 min. in the presence of gentamicin, washed with fresh culture medium, and lysed using 1% Triton X-100. Lysates were diluted and plated to determine the total CFU. For both assays, lysates were plated on LSLB and LSLB containing Km to assess plasmid loss. Data are the mean ± SEM of the percentage of adherent or internalized bacteria compared to the inoculum and represent two experiments performed in triplicate. Significance is compared to Bp340. *, $p < 0.05$; **, $p < 0.01$; ***, $p < 0.001$ by Tukey's multiple comparison test following a one-way ANOVA.

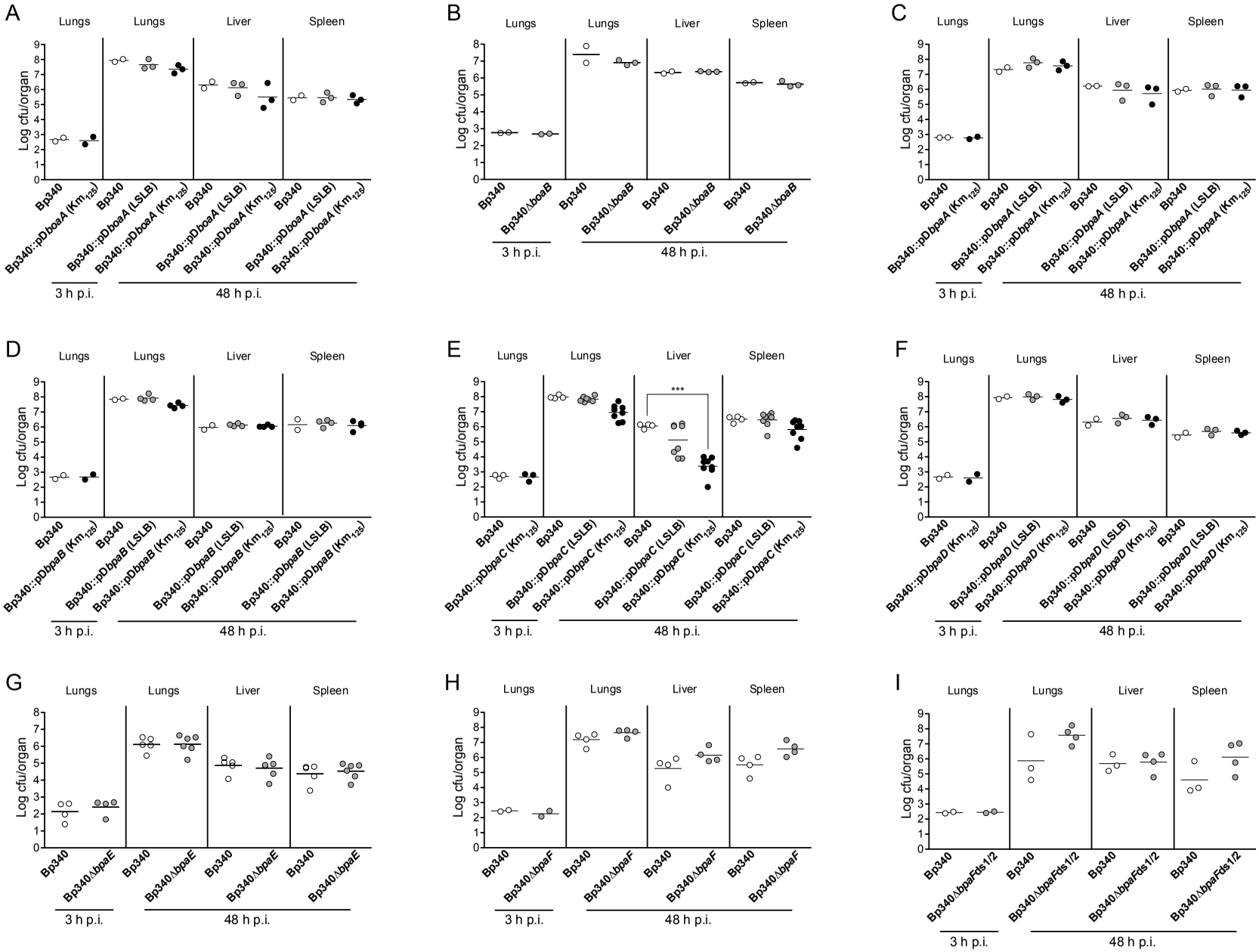
A
B
C
D
E
F
G
H
I
Lungs
Liver
Spleen
Log cfu/organ
3 h p.i.
48 h p.i.
***
Bp340
Bp340::pDboaA (Km125)
Bp340::pDboaA (LSLB)
Bp340ΔboaB
Bp340::pDbpaA (Km125)
Bp340::pDbpaA (LSLB)
Bp340::pDbpaB (Km125)
Bp340::pDbpaB (LSLB)
Bp340::pDbpaC (Km125)
Bp340::pDbpaC (LSLB)
Bp340::pDbpaD (Km125)
Bp340::pDbpaD (LSLB)
Bp340ΔbpaE
Bp340ΔbpaF
Bp340ΔbpaFds1/2

Fig. 7. Contribution of *B. pseudomallei* 1026b trimeric ATs to virulence *in vivo*. Six- to eight-week-old female BALB/c mice were anesthetized with Avertin by intraperitoneal injection and were inoculated intranasally with 500 CFU of *B. pseudomallei* trimeric AT disruption (A, C, D–F) and deletion (B, G–I) mutation strains. Mice were euthanized by CO_2 overdose at the indicated time points and the lungs, liver, and spleen were aseptically harvested and homogenized. For each organ, the bacterial burden was determined by plating serial dilutions of the homogenates. For disruption mutants (A), (C), and (D–F), homogenates were plated on both LSLB and LSLB containing Km to assess plasmid loss. Significance is compared to Bp340. **, $p < 0.01$; ***, $p < 0.001$ by Tukey's multiple comparison test following a one-way ANOVA.

References

1. **Chaowagul W, White NJ, Dance DA, Wattanagoon Y, Naigowit P, Davis TM, Looareesuwan S, Pitakwatchara N. 1989. Melioidosis: a major cause of community-acquired septicemia in northeastern Thailand. J. Infect. Dis. 159:890–899.**

2. **White NJ. 2003. Melioidosis. Lancet 361:1715–1722.**

3. **Currie BJ, Fisher DA, Howard DM, Burrow JNC, Lo D, Selva nayagam S, Anstey NM, Huffam SE, Snelling PL, Marks PJ, Stephens DP, Lum GD, Jacups SP, Krause VL. 2000. Endemic melioidosis in tropical northern Australia: a 10-year prospective study and review of the literature. Clin. Infect. Dis. 31:981–986.**

4. **Dance DA. 2000. Melioidosis as an emerging global problem. Acta. Trop. 74:115–119.**

5. **Dance DA. 1991. Melioidosis: the tip of the iceberg? Clin. Microbiol. Rev. 4:52–60.**

6. **Moore RA, DeShazer D, Reckseidler S, Weissman A, Woods DE. 1999. Efflux-mediated aminoglycoside and macrolide resistance in *Burkholderia pseudomallei*. Antimicrob. Agents Chemother. 43:465–470.**

7. **Godfrey AJ, Wong S, Dance DA, Chaowagul W, Bryan LE. 1991. *Pseudomonas pseudomallei* resistance to beta-lactam antibiotics due to alterations in the chromosomally encoded beta-lactamase. Antimicrob. Agents Chemother. 35:1635–1640.**

8. **Jones AL, Beveridge TJ, Woods DE. 1996. Intracellular survival of *Burkholderia pseudomallei*. Infect. Immun. 64:782–790.**

9. **Kespichayawattana W, Rattanachetkul S, Wanun T, Utaisincharoen P, Sirisinha S. 2000. *Burkholderia pseudomallei* induces cell fusion and actin-associated membrane protrusion: a possible mechanism for cell-to-cell spreading. Infect. Immun. 68:5377–5384.**

10. **Cheng AC. 2010. Melioidosis: advances in diagnosis and treatment. Curr. Opin. Infect. Dis. 23:554–559.**

11. **Brown NF, Boddey JA, Flegg CP, Beacham IR. 2002. Adherence of *Burkholderia pseudomallei* cells to cultured human epithelial cell lines is regulated by growth temperature. Infect. Immun. 70:974–980.**

12. **Jones AL, DeShazer D, Woods DE. 1997. Identification and characterization of a two-component regulatory system involved in invasion of eukaryotic cells and heavy-metal resistance in *Burkholderia pseudomallei*. Infect. Immun. 65:4972–4977.**

13. **Kespichayawattana W, Intachote P, Utaisincharoen P, Sirisinha S. 2004. Virulent *Burkholderia pseudomallei* is more efficient than avirulent *Burkholderia thailandensis* in invasion of and adherence to cultured human epithelial cells. Microb. Pathog. 36:287–292.**

14. **Muangsombut V, Suparak S, Pumirat P, Damnin S, Vattanaviboon P, Thongboonkerd V, Korbsrisate S. 2008. Inactivation of *Burkholderia pseudomallei bsaQ* results in decreased invasion efficiency and delayed escape of bacteria from endocytic vesicles. Arch. Microbiol. 190:623–631.**

15. **Stevens MP, Stevens JM, Jeng RL, Taylor LA, Wood MW, Hawes P, Monaghan P, Welch MD, Galyov EE. 2005. Identification of a bacterial factor required for actin-based motility of *Burkholderia pseudomallei*. Mol. Microbiol. 56:40–53.**

16. **Burtnick MN, Brett PJ, Nair V, Warawa JM, Woods DE, Gherardini FC. 2008. *Burkholderia pseudomallei* type III secretion system mutants exhibit delayed vacuolar escape phenotypes in RAW 264.7 murine macrophages. Infect. Immun. 76:2991–3000.**

17. **Burtnick MN, Brett PJ, Harding SV, Ngugi SA, Ribot WJ, Chantratita N, Scorpio A, Milne TS, Dean RE, Fritz DL, Peacock SJ, Prior JL, Atkins TP, DeShazer D. 2011. The cluster 1 type VI secretion system is a major virulence determinant in *Burkholderia pseudomallei*. Infect. Immun. 79:1512–1525.**

18. **Suparak S, Kespichayawattana W, Haque A, Easton A, Damnin S, Lertmemongkolchai G, Bancroft GJ, Korbsrisate S. 2005. Multinucleated giant cell formation and apoptosis in infected host cells is mediated by *Burkholderia pseudomallei* type III secretion protein BipB. J. Bacteriol. 187:6556–6560.**

19. **Suwannasaen D, Mahawantung J, Chaowagul W, Limmathurotsakul D, Felgner PL, Davies H, Bancroft GJ, Titball RW, Lertmemongkolchai G. 2010. Human immune responses to *Burkholderia pseudomallei* characterized by protein microarray analysis. J. Infect. Dis. 203:1002–1011.**

20. **Dowling AJ, Wilkinson PA, Holden MT, Quail MA, Bentley SD, Reger J, Waterfield NR, Titball RW, Ffrench-Constant RH. 2010. Genome-wide analysis reveals loci encoding anti-macrophage factors in the human pathogen *Burkholderia pseudomallei* K96243. PLoS ONE 5:e15693.**

21. Balder R, Lipski S, Lazarus JJ, Grose W, Wooten RM, Hogan RJ, Woods DE, Lafontaine ER. 2010. Identification of *Burkholderia mallei* and *Burkholderia pseudomallei* adhesins for human respiratory epithelial cells. BMC Microbiol. 10:250.

22. Essex-Lopresti AE, Boddey JA, Thomas R, Smith MP, Hartley MG, Atkins T, Brown NF, Tsang CH, Peak IR, Hill J, Beacham IR, Titball RW. 2005. A type IV pilin, PilA, contributes to adherence of *Burkholderia pseudomallei* and virulence *in vivo*. Infect. Immun. 73:1260–1264.

23. Dautin N, Bernstein HD. 2007. Protein secretion in gram-negative bacteria via the autotransporter pathway. Annu. Rev. Microbiol. 61:89–112.

24. Henderson IR, Navarro-Garcia F, Desvaux M, Fernandez RC, Ala'Aldeen D. 2004. Type V protein secretion pathway: the autotransporter story. Microbiol. Mol. Biol. Rev. 68:692–744.

25. Cotter SE, Surana NK, St Geme JW3. 2005. Trimeric autotransporters: a distinct subfamily of autotransporter proteins. Trends Microbiol. 13:199–205.

26. Cotter SE, Surana NK, Grass S, St Geme JW3. 2006. Trimeric autotransporters require trimerization of the passenger domain for stability and adhesive activity. J. Bacteriol. 188:5400–5407.

27. Tahir El Y, Skurnik M. 2001. YadA, the multifaceted *Yersinia* adhesin. Int. J. Med. Microbiol. 291:209–218.

28. Laarmann S, Cutter D, Juehne T, Barenkamp SJ, St Geme JW. 2002. The *Haemophilus influenzae* Hia autotransporter harbours two adhesive pockets that reside in the passenger domain and recognize the same host cell receptor. Mol. Microbiol. 46:731–743.

29. DeShazer D, Brett PJ, Carlyon R, Woods DE. 1997. Mutagenesis of *Burkholderia pseudomallei* with Tn5-OT182: isolation of motility mutants and molecular characterization of the flagellin structural gene. J. Bacteriol. 179:2116–2125.

30. Edwards TE, Phan I, Abendroth J, Dieterich SH, Masoudi A, Guo W, Hewitt SN, Kelley A, Leibly D, Brittnacher MJ, Staker BL, Miller SI, Van Voorhis WC, Myler PJ, Stewart LJ. 2010. Structure of a *Burkholderia pseudomallei* trimeric autotransporter adhesin head. PLoS ONE 5:e12803.

31. Lopez CM, Rholl DA, Trunck LA, Schweizer HP. 2009. Versatile dual-technology system for markerless allele replacement in *Burkholderia pseudomallei*. Appl. Environ. Microbiol. 75:6496–6503.

32. Mima T, Schweizer HP. 2010. The BpeAB-OprB efflux pump of *Burkholderia pseudomallei* 1026b does not play a role in quorum sensing, virulence factor production, or extrusion of aminoglycosides but is a broad-spectrum drug efflux system. Antimicrob. Agents Chemother. 54:3113–3120.

33. Edwards RA, Keller LH, Schifferli DM. 1998. Improved allelic exchange vectors and their use to analyze 987P fimbria gene expression. Gene 207:149–157.

34. French CT, Toesca IJ, Wu T-H, Teslaa T, Beaty SM, Wong W, Liu M, Schröder I, Chiou P-Y, Teitell MA, Miller JF. 2011. Dissection of the *Burkholderia* intracellular life cycle using a photothermal nanoblade. Proc. Natl. Acad. Sci. U. S. A. 108:12095–12100.

35. Babu MM, Priya ML, Selvan AT, Madera M, Gough J, Aravind L, Sankaran K. 2006. A database of bacterial lipoproteins (DOLOP) with functional assignments to predicted lipoproteins. J. Bacteriol. 188:2761–2773.

36. Okuda S, Tokuda H. 2011. Lipoprotein sorting in bacteria. Annu. Rev. Microbiol. 65:239–259.

37. Tiyawisutsri R, Holden MT, Tumapa S, Rengpipat S, Clarke SR, Foster SJ, Nierman WC, Day NP, Peacock SJ. 2007. *Burkholderia* Hep_Hag autotransporter (BuHA) proteins elicit a strong antibody response during experimental glanders but not human melioidosis. BMC Microbiol. 7:19.

38. Holden MTG, Titball RW, Peacock SJ, Cerdeño-Tárraga AM, Atkins T, Crossman LC, Pitt T, Churcher C, Mungall K, Bentley SD, Sebaihia M, Thomson NR, Bason N, Beacham IR, Brooks K, Brown KA, Brown NF, Challis GL, Cherevach I, Chillingworth T, Cronin A, Crossett B, Davis P, DeShazer D, Feltwell T, Fraser A, Hance Z, Hauser H, Holroyd S, Jagels K, Keith KE, Maddison M, Moule S, Price C, Quail MA, Rabbinowitsch E, Rutherford K, Sanders M, Simmonds M, Songsivilai S, Stevens K, Tumapa S, Vesaratchavest M, Whitehead S, Yeats C, Barrell BG, Oyston PCF, Parkhill J. 2004. Genomic plasticity of the causative agent of melioidosis, *Burkholderia pseudomallei*. Proc. Natl. Acad. Sci. U. S. A. 101:14240–14245.

39. Leyton DL, Rossiter AE, Henderson IR. 2012. From self sufficiency to dependence: mechanisms and factors important for autotransporter biogenesis. Nat. Rev. Microbiol. 10:213–225.

40. Szczesny P, Lupas A. 2008. Domain annotation of trimeric autotransporter adhesins--daTAA. Bioinformatics 24:1251–1256.

41. Tahir YE, Kuusela P, Skurnik M. 2000. Functional mapping of the *Yersinia enterocolitica* adhesin YadA. Identification of eight NSVAIG - S motifs in the amino-terminal half of the protein involved in collagen binding. Mol.

Microbiol. 37:192–206.

42. Benz I, Schmidt MA. 2001. Glycosylation with heptose residues mediated by the *aah* gene product is essential for adherence of the AIDA-I adhesin. Mol. Microbiol. 40:1403–1413.

43. Galyov EE, Brett PJ, DeShazer D. 2010. Molecular insights into *Burkholderia pseudomallei* and *Burkholderia mallei* pathogenesis. Annu. Rev. Microbiol., 2010(null) ed. 64:495–517.

44. Pilatz S, Breitbach K, Hein N, Fehlhaber B, Schulze J, Brenneke B, Eberl L, Steinmetz I. 2006. Identification of *Burkholderia pseudomallei* genes required for the intracellular life cycle and *in vivo* virulence. Infect. Immun. 74:3576–3586.

45. Bliska JB, Copass MC, Falkow S. 1993. The *Yersinia pseudotuberculosis* adhesin YadA mediates intimate bacterial attachment to and entry into HEp-2 cells. Infect. Immun. 61:3914–3921.

46. Yang Y, Isberg RR. 1993. Cellular internalization in the absence of invasin expression is promoted by the *Yersinia pseudotuberculosis yadA* product. Infect. Immun. 61:3907–3913.

47. Alamuri P, Lower M, Hiss JA, Himpsl SD, Schneider G, Mobley HL. 2010. Adhesion, invasion, and agglutination mediated by two trimeric autotransporters in the human uropathogen *Proteus mirabilis*. Infect. Immun. 78:4882–4894.

48. Mil-Homens D, Fialho AM. 2012. A BCAM0223 mutant of *Burkholderia cenocepacia* is deficient in hemagglutination, serum resistance, adhesion to epithelial cells and virulence. PLoS ONE 7:e41747.

49. Ruiz-Ranwez V, Posadas DM, Van der Henst C, Estein SM, Arocena GM, Abdian PL, Martin FA, Sieira R, De Bolle X, Zorreguieta A. 2013. BtaE, an adhesin that belongs to the trimeric autotransporter family, is required for full virulence and defines a specific adhesive pole of *Brucella*. Infect. Immun. IAI.01241-12.

50. Schutz M, Weiss EM, Schindler M, Hallstrom T, Zipfel PF, Linke D, Autenrieth IB. 2010. Trimer stability of YadA is critical for virulence of *Yersinia enterocolitica*. Infect. Immun. 78:2677–2690.

51. Bentancor LV, Camacho-Peiro A, Bozkurt-Guzel C, Pier GB, Maira-Litrán T. 2012. Identification of Ata, a multifunctional trimeric autotransporter of *Acinetobacter baumannii*. J. Bacteriol. 194:3950–3960.

52. Skurnik M, Tahir El Y, Saarinen M, Jalkanen S, Toivanen P. 1994. YadA mediates specific binding of enteropathogenic *Yersinia enterocolitica* to human intestinal submucosa. Infect. Immun. 62:1252–1261.

53. Barenkamp SJ, St Geme JW. 1996. Identification of a second family of high-molecular-weight adhesion proteins expressed by non-typable *Haemophilus influenzae*. Mol. Microbiol. 19:1215–1223.

54. Hill DJ, Virji M. 2003. A novel cell-binding mechanism of *Moraxella catarrhalis* ubiquitous surface protein UspA: specific targeting of the N-domain of carcinoembryonic antigen-related cell adhesion molecules by UspA1. Mol. Microbiol. 48:117–129.

55. Felgner PL, Kayala MA, Vigil A, Burk C, Nakajima-Sasaki R, Pablo J, Molina DM, Hirst S, Chew JS, Wang D, Tan G, Duffield M, Yang R, Neel J, Chantratita N, Bancroft G, Lertmemongkolchai G, Davies DH, Baldi P, Peacock S, Titball RW. 2009. A *Burkholderia pseudomallei* protein microarray reveals serodiagnostic and cross-reactive antigens. Proc. Natl. Acad. Sci. U. S. A. 106:13499–13504.

56. Ruiz-Perez F, Henderson IR, Leyton DL, Rossiter AE, Zhang Y, Nataro JP. 2009. Roles of periplasmic chaperone proteins in the biogenesis of serine protease autotransporters of *Enterobacteriaceae*. J. Bacteriol. 191:6571–6583.

57. Desvaux M, Scott-Tucker A, Turner SM, Cooper LM, Huber D, Nataro JP, Henderson IR. 2007. A conserved extended signal peptide region directs posttranslational protein translocation via a novel mechanism. Microbiology 153:59–70.

58. Szabady RL, Peterson JH, Skillman KM, Bernstein HD. 2005. An unusual signal peptide facilitates late steps in the biogenesis of a bacterial autotransporter. Proc. Natl. Acad. Sci. U. S. A. 102:221–226.

59. Desvaux ML, Cooper LM, Filenko NA, Scott-Tucker A, Turner SM, Cole JA, Henderson IR. 2006. The unusual extended signal peptide region of the type V secretion system is phylogenetically restricted. FEMS Microbiol. Lett. 264:22–30.

60. Benz I, Schmidt MA. 2002. Never say never again: protein glycosylation in pathogenic bacteria. Mol. Microbiol. 45:267–276.

61. Sherlock O, Dobrindt U, Jensen JB, Munk Vejborg R, Klemm P. 2006. Glycosylation of the self-recognizing *Escherichia coli* Ag43 autotransporter protein. J. Bacteriol. 188:1798–1807.

62. Chua KL, Chan YY, Gan YH. 2003. Flagella are virulence determinants of

***Burkholderia pseudomallei*. Infect. Immun. 71:1622–1629.**

63. Leakey AK, Ulett GC, Hirst RG. 1998. BALB/c and C57Bl/6 mice infected with virulent *Burkholderia pseudomallei* provide contrasting animal models for the acute and chronic forms of human melioidosis. Microb. Pathog. 24:269–275.

64. Kaestli M, Schmid M, Mayo M, Rothballer M, Harrington G, Richardson L, Hill A, Hill J, Tuanyok A, Keim P, Hartmann A, Currie BJ. 2011. Out of the ground: aerial and exotic habitats of the melioidosis bacterium *Burkholderia pseudomallei* in grasses in Australia. Environ. Microbiol. 14:2058–2070.

65. Inatsuka CS, Xu Q, Vujkovic-Cvijin I, Wong S, Stibitz S, Miller JF, Cotter PA. 2010. Pertactin is required for *Bordetella* species to resist neutrophil-mediated clearance. Infect. Immun. 78:2901–2909.

CHAPTER IV

Discussion and Future Directions

B. pseudomallei has one of the most complex bacterial genomes sequenced to date; 7.24 Mb pairs of highly dynamic DNA that can show up to 14% of variability across isolates (21). Variable regions that contain multiple genomic islands with DNA acquired from other bacteria that could be associated with virulence are often found, and the connection of these acquired genes with clinical outcome is still unknown (23). Genotyping of *B. pseudomallei* colonies from several tissues of a single patient with melioidosis can show significant genetic diversity, showing that while within the host, this organism can rapidly evolve (14). However, very little is known about how *B. pseudomallei* causes disease.

B. pseudomallei can invade, and spread from cell to cell without exiting the cytoplasm. Unknown invasins facilitate actin-dependent internalization of *B. pseudomallei* into eukaryotic cells primary endosomes. The activity of $T3SS_{Bsa}$ (7, 8) is required for escape from these primary endosomes, and subsequent entry into the eukaryotic cell cytoplasm. Once in the cytoplasm the trimeric autotransporter BimA allows for actin based motility, which is required for efficient cell to cell spread, and T6SS-1 (4) facilitates intracellular spread and MNGC formation, possibly through fusion of host cell membranes. T6SS-1, one of the six T6SS found in *B. pseudomallei*, is believed to be a major virulence factor in the Syrian hamster, and BALB/c model of melioidosis (4). A few other potential virulence factors such as capsular polysaccharides

(15), LPS and flagella (1, 10) have been described, however their role in pathogenesis is still unknown.

Autotransporter proteins are part of the largest family of extracellular proteins found in Gram-negative bacteria and many have been shown to be virulence factors, playing crucial roles in how bacteria cause disease (9). *B. pseudomallei* contains genes predicted to encode two classical ATs and nine trimeric ATs, however only the trimeric AT encoded by *bimA* has been well characterized. *bimA* has been shown to have an important role in the formation of actin tails, which allows the bacteria to spread from cell to cell through actin-mediated motility (18). Our goal was to determine if any of the remaining putative autotransporters played a role in *B. pseudomallei* pathogenesis.

In chapter 2, our data show that the classical AT protein encoded by *bcaA* contributes to non-phagocytic cell invasion, and to dissemination to or survival of *B. pseudomallei* in the spleen in a BALB/c intranasal model of infection. *bcaA* and *bcaB* (a gene found immediately 3′ of *bcaA*) appear to form an operon, and although *bcaB* also plays a role in cell invasion, no phenotype for *bcaB in vivo* was observed using the BALB/c intranasal model of infection.

BcaA is predicted to have an approximately 80 KDa passanger domain containing a serine protease domain belonging to the Peptidase S8 or Subtilase family. Subtilisins are characterized by having a well conserved Asp, Ser and His catalytic triad and they have been shown to play a role in cellular nutrition, mediating host cell invasion and maturation of other polypeptides (20). BcaA contains the same well conserved catalytic triad found in other subtilisins, and appears to be proteolyzed into smaller polypeptides of approximately 21KDa and 28 kDa present in whole cell lysates, but not in supernatants.

The smaller polypeptides were not detected in western blots of concentrated supernatant fractions, suggesting that they remain associated with the bacterial cell. Further studies will include characterization of these polypeptides, and determining if they are generated by auto-proteolysis or if another protein is involved in processing. After such studies, further analysis of BcaA function should be conducted to determine its role, as well as its active domains and whether it interacts with other proteins, such as BcaB.

BcaB is predicted to have a prolyl 4-hydroxylase domain. In bacteria, these domains are believed to hydroxylate peptidyl prolines, but although some of these hydroxylases have been identified in bacteria, their functions and substrates remain unknown. Further studies should include determining if BcaB has a role in hydroxylating any of the fifty-two prolines found in BcaA, since it is possible that BcaA is the physiological substrate for BcaB, which would be consistent with their operon structure.

Although *bcaA* and *bcaB* are each required for cell invasion and plaque formation, only *bcaA* had a phenotype *in vivo*. There is a possibility that the lack of phenotype for *bcaB in vivo*, reflects the limitations of the tools we used in our study. Although the BALB/c model has been broadly used as an acute model for *B. pseudomallei* infection (12), it may not be sensitive enough to reveal phenotypes for all factors that contribute to disease, depending on the step and stage of disease in which they function. Future experiments will include development of additional animal models that will expand the repertoire of *B. pseudomallei* disease stages and processes that we are able to study in our laboratory.

Chapter 3 outlines the extensive work we performed characterizing eight of the nine trimeric AT found in *B. pseudomallei*, we did not include the previously

characterized trimeric AT protein BimA (18). Our study included bioinformatic gene synteny analysis, N-terminal extension characterization, protein domain annotation, as well as *in vitro* studies designed to determine the role of these genes in adherence, invasion and plaque formation. We also performed the first animal experiments using any *B. pseudomallei* strains defective for the production of trimeric ATs and found that one trimeric AT, BpaC (BPSL1631), is required for efficient dissemination or survival of bacteria to the liver in a BALB/c intranasal model of infection.

We determined that three of the trimeric ATs (*bpaB*, *bpaA,* and *bpaE*) have genes 3′ that are predicted to be lipidated, and localized to the outer membrane suggesting they may function as accessory proteins for their corresponding ATs. Accessory proteins have recently been shown to be required for AT biogenesis (13, 16). The Bam complex has been suggested to be necessary for trimeric AT insertion in the outer membrane through an unknown mechanism, while periplasmic chaperones have been shown to be required for AT passage through the periplasm (13). However, further characterization of these putative accessory proteins will be necessary to determine their role, if any, in the production and function of *B. pseudomallei* trimeric ATs.

Seven of the eight trimeric AT-encoding genes in our study had an extended signal peptide region (ESPR), which has been suggested to regulate the rate of translocation across the inner membrane to avoid accumulation of misfolded proteins in the periplasm (5, 13, 19). In addition to ESPRs in the majority of *B. pseudomallei* trimeric ATs, five of these proteins (BoaA, BoaB, BpaA, BpaB and BpaF) contain "SLST" repeat regions that are unique to the *Burkholderia* species. Although these repeats have no predicted structure or function, there is a possibility that these serine- and

threonine-rich repeats are glycosylation sites and therefore may be important for AT function. Protein glycosylation is prokaryotes has been extensively documented and shown to be important for the function of several virulence factors (2, 3, 9, 17).

Adhesion and internalization studies in A549 cell monolayers, showed that the eight trimeric ATs fell into one of four categories: having a phenotype in adherence only (BoaA, BoaB, and BpaD), in internalization only (BpaE and BpaF), in both adherence and internalization (BpaA and BpaC), or in neither adherence nor invasion (BpaB). However, when using a BALB/c mouse model of infection we only observed a phenotype for *bapC*, which had a dissemination or survival defect in the liver.

Our study was the first study to systematically evaluate a class of genes (those encoding trimeric ATs) in *B. pseudomallei* both *in vivo* and *in vitro*. While we demonstrated that nearly all tested ATs have a function in adherence or invasion of non-phagocytic cells, and that BapC is important for efficient dissemination or survival to the liver in a BALB/c model of infection, we only evaluated strains containing a single trimeric AT-encoding gene disrupted or delete, and our analysis was limited to a single animal model and route of infection. It is possible that multiple genes must be deleted for a reduction in virulence to be observed. These genes may have redundant or synergistic functions during infection, and since *B. pseudomallei* infects not only animals but a variety of other organisms, including plants (11), the use of diverse model systems will most likely be required for fully understanding the role of trimeric ATs.

References

1. **Anuntagool, N., T. Panichakul, P. Aramsri, and S. Sirisinha. 2000. Shedding of lipopolysaccharide and 200-kDa surface antigen during the in vitro growth of virulent Ara- and avirulent Ara+ Burkholderia pseudomallei. Acta tropica 74:221-228.**

2. **Benz, I., and M. A. Schmidt. 2001. Glycosylation with heptose residues mediated by the aah gene product is essential for adherence of the AIDA-I adhesin. Mol Microbiol 40:1403-1413.**

3. **Benz, I., and M. A. Schmidt. 2002. Never say never again: protein glycosylation in pathogenic bacteria. Mol Microbiol 45:267-276.**

4. **Burtnick, M. N., P. J. Brett, S. V. Harding, S. A. Ngugi, W. J. Ribot, N. Chantratita, A. Scorpio, T. S. Milne, R. E. Dean, D. L. Fritz, S. J. Peacock, J. L. Prior, T. P. Atkins, and D. Deshazer. The cluster 1 type VI secretion system is a major virulence determinant in Burkholderia pseudomallei. Infection and immunity 79:1512-1525.**

5. **Desvaux, M., A. Scott-Tucker, S. M. Turner, L. M. Cooper, D. Huber, J. P. Nataro, and I. R. Henderson. 2007. A conserved extended signal peptide region directs posttranslational protein translocation via a novel mechanism. Microbiology 153:59-70.**

6. **Essex-Lopresti, A. E., J. A. Boddey, R. Thomas, M. P. Smith, M. G. Hartley, T. Atkins, N. F. Brown, C. H. Tsang, I. R. Peak, J. Hill, I. R. Beacham, and R. W. Titball. 2005. A type IV pilin, PilA, Contributes To Adherence of Burkholderia pseudomallei and virulence in vivo. Infection and immunity 73:1260-1264.**

7. **French, C. T., I. J. Toesca, T. H. Wu, T. Teslaa, S. M. Beaty, W. Wong, M. Liu, I. Schroder, P. Y. Chiou, M. A. Teitell, and J. F. Miller. Dissection of the Burkholderia intracellular life cycle using a photothermal nanoblade. Proceedings of the National Academy of Sciences of the United States of America 108:12095-12100.**

8. **Gong, L., M. Cullinane, P. Treerat, G. Ramm, M. Prescott, B. Adler, J. D. Boyce, and R. J. Devenish. The Burkholderia pseudomallei type III secretion system and BopA are required for evasion of LC3-associated phagocytosis. PLoS One 6:e17852.**

9. **Henderson, I. R., F. Navarro-Garcia, M. Desvaux, R. C. Fernandez, and D. Ala'Aldeen. 2004. Type V protein secretion pathway: the autotransporter story. Microbiol Mol Biol Rev 68:692-744.**

10. **Inglis, T. J., T. Robertson, D. E. Woods, N. Dutton, and B. J. Chang. 2003. Flagellum-mediated adhesion by Burkholderia pseudomallei precedes invasion of Acanthamoeba astronyxis. Infection and immunity 71:2280-2282.**

11. **Kaestli, M., M. Schmid, M. Mayo, M. Rothballer, G. Harrington, L. Richardson, A. Hill, J. Hill, A. Tuanyok, P. Keim, A. Hartmann, and B. J. Currie. Out of the ground: aerial and exotic habitats of the melioidosis bacterium Burkholderia pseudomallei in grasses in Australia. Environ Microbiol 14:2058-2070.**

12. **Leakey, A. K., G. C. Ulett, and R. G. Hirst. 1998. BALB/c and C57Bl/6 mice infected with virulent Burkholderia pseudomallei provide contrasting animal models for the acute and chronic forms of human melioidosis. Microb Pathog 24:269-275.**

13. **Leyton, D. L., A. E. Rossiter, and I. R. Henderson. From self sufficiency to dependence: mechanisms and factors important for autotransporter biogenesis. Nat Rev Microbiol 10:213-225.**

14. **Price, E. P., H. M. Hornstra, D. Limmathurotsakul, T. L. Max, D. S. Sarovich, A. J. Vogler, J. L. Dale, J. L. Ginther, B. Leadem, R. E. Colman, J. T. Foster, A. Tuanyok, D. M. Wagner, S. J. Peacock, T. Pearson, and P. Keim. Within-host evolution of Burkholderia pseudomallei in four cases of acute melioidosis. PLoS Pathog 6:e1000725.**

15. **Reckseidler-Zenteno, S. L., R. DeVinney, and D. E. Woods. 2005. The capsular polysaccharide of Burkholderia pseudomallei contributes to survival in serum by reducing complement factor C3b deposition. Infection and immunity 73:1106-1115.**

16. **Ruiz-Perez, F., I. R. Henderson, D. L. Leyton, A. E. Rossiter, Y. Zhang, and J. P. Nataro. 2009. Roles of periplasmic chaperone proteins in the biogenesis of serine protease autotransporters of Enterobacteriaceae. J Bacteriol 191:6571-6583.**

17. **Sherlock, O., U. Dobrindt, J. B. Jensen, R. Munk Vejborg, and P. Klemm. 2006. Glycosylation of the self-recognizing Escherichia coli Ag43 autotransporter protein. J Bacteriol 188:1798-1807.**

18. **Stevens, M. P., J. M. Stevens, R. L. Jeng, L. A. Taylor, M. W. Wood, P. Hawes, P. Monaghan, M. D. Welch, and E. E. Galyov. 2005. Identification of a bacterial factor required for actin-based motility of Burkholderia pseudomallei. Mol Microbiol 56:40-53.**

19. Szabady, R. L., J. H. Peterson, K. M. Skillman, and H. D. Bernstein. 2005. An unusual signal peptide facilitates late steps in the biogenesis of a bacterial autotransporter. Proceedings of the National Academy of Sciences of the United States of America 102:221-226.

20. Tripathi, L. P., and R. Sowdhamini. 2008. Genome-wide survey of prokaryotic serine proteases: analysis of distribution and domain architectures of five serine protease families in prokaryotes. BMC Genomics 9:549.

21. Tumapa, S., M. T. Holden, M. Vesaratchavest, V. Wuthiekanun, D. Limmathurotsakul, W. Chierakul, E. J. Feil, B. J. Currie, N. P. Day, W. C. Nierman, and S. J. Peacock. 2008. Burkholderia pseudomallei genome plasticity associated with genomic island variation. BMC Genomics 9:190.

22. Ulrich, R. L., D. Deshazer, E. E. Brueggemann, H. B. Hines, P. C. Oyston, and J. A. Jeddeloh. 2004. Role of quorum sensing in the pathogenicity of Burkholderia pseudomallei. J Med Microbiol 53:1053-1064.

23. Wiersinga, W. J., T. van der Poll, N. J. White, N. P. Day, and S. J. Peacock. 2006. Melioidosis: insights into the pathogenicity of Burkholderia pseudomallei. Nat Rev Microbiol 4:272-282.

APPENDICES

This session highlights collaborative work that led to scientific publications performed by our laboratory with Dr. Edward A. Miao of the Department of Microbiology and Immunology at UNC, Chapel Hill; and Dr. Timothy J. Hagen of the Department of Chemistry and Biochemistry at Northern Illinois University. In both cases our contributions included, but were not limited to, *in vitro* and *in vivo* ABSL-3 work with virulent *Burkholderia pseudomallei* strains.

Caspase-11 protects against bacteria that escape the vacuole[1]

Introduction

Canonical inflammasomes, such as NLRP3, NLRC4, and AIM2, are cytosolic sensors that detect pathogens or danger signals and activate Caspase-1, leading to secretion of the proinflammatory cytokines interleukin (IL)-1β and IL-18, and pyroptosis, a form of programmed cell death (*1*). Pyrin domain-containing inflammasomes, including NLRP3, signal through the ASC adaptor protein to recruit Caspase-1 (Fig. S1). Many diverse agonists cause cytosolic perturbations that are detected through NLRP3; however the underlying mechanisms remain obscure (*2*). In contrast, the CARD domain-containing inflammasome NLRC4 can signal directly to Caspase-1 resulting in pyroptosis, as well as indirectly through ASC to promote IL-1β and IL-18 secretion (Fig. S1) (*1*, *3*). NLRC4 detects bacterial flagellin and type III secretion system (T3SS) rod or needle components within the macrophage cytosol (*4*-*6*). Together, NLRC4 and the ASC dependent inflammasomes account for all known canonical Caspase-1 activation pathways.

Burkholderia pseudomallei is a Gram-negative bacterium endemic to Southeast Asia that causes mellioidosis and is a potential biologic weapon (*7*). *B. pseudomallei* uses

[1] Adapted for this dissertation from: Youssef Aachoui, Irina A. Leaf, Jon A. Hagar, Mary F. Fontana, Cristine G. Campos, Daniel E. Zak, Michael H. Tan, Peggy A. Cotter, Russell E. Vance, Alan Aderem, and Edward A. Miao. Caspase-11 protects against bacteria that escape the vacuole. 2013. Science. 339 (6122):975-978.

a T3SS to escape the phagosome and replicate in the cytosol. NLRC4 and NLRP3 both detect *B. pseudomallei*, promoting IL-1β secretion from murine bone marrow-derived macrophages (BMM) ((*8*) and Fig. 1A). Despite encoding many of the same virulence factors as *B. pseudomallei*, including T3SS and T6SS, the closely related *B. thailandensis* is far less virulent (*9*). We therefore hypothesized that NLPR3 and NLRC4 also detect *B. thailandensis*, and indeed, NLRP3 and NLRC4 accounted for all IL-1β secretion in response to *B. thailandensis* (Fig. 1B). We next determined whether inflammasome activation is critical to survival following *B. thailandensis* challenge using Caspase-1 deficient mice. Kayagaki et al. recently showed that all existing Caspase-1 deficient mice also lack Caspase-11 due to the backcrossing of a mutant *Casp11* allele from 129 into C57BL/6 mice (*10*). Inflammasome detection was critical for resistance to *B. thailandensis*, as *Casp1*$^{-/-}$*Casp11*$^{-/-}$ animals succumbed to the infection (Fig. 1C, S2A). In contrast, wild type C57BL/6 mice survived high dose intraperitoneal or intranasal challenge (Fig. 1C, S2A). Surprisingly, *Nlrc4*$^{-/-}$*Asc*$^{-/-}$ mice that are deficient in all known canonical inflammasomes were also resistant (Fig. 1D, S2B). This indicated that an unknown signaling pathway provides protection via either Caspase-1 or -11 (see pathway schematic Fig. S1). Resistance to *B. thailandensis* was at least partially independent of IL-1β and IL-18, depending on the route of infection (Fig. 1E, S2C), suggesting that both cytokines and pyroptosis can contribute to protection. We therefore examined pyroptosis *in vitro*, and found that cytotoxicity in response *B. thailandensis* was impaired in *Casp1*$^{-/-}$ *Casp11*$^{-/-}$ BMM (Fig. 1F). Consistent with our *in vivo* data, pyroptosis *in vitro* did not require *Nlrc4* or *Asc* (Fig. 1F). *B. pseudomallei* similarly triggered pyroptosis in *Nlrc4*$^{-/-}$ *Asc*$^{-/-}$ macrophages (Fig. 1G). These results indicate that a pyroptosis-inducing pathway

distinct from all known canonical inflammasomes detects *B. thailandensis* and protects against lethal infection.

Inflammasomes discriminate pathogens from non-pathogens by detecting contamination or perturbation of the cytosolic compartment (*11*). The *B. thailandensis* T3SS facilitates bacterial access to the cytosol, and was required for induction of pyroptosis, whereas the virulence-associated T6SS was dispensable (Fig. 2A). We therefore hypothesized that macrophages detect vacuolar lysis or release of bacteria into the cytosol.

In order to establish their intracellular vacuolar growth niche, *Salmonella typhimurium* and *Legionella pneumophila* use T3SS and T4SS, respectively, to translocate effector proteins that work in concert to maintain the stability of these altered bacteria-containing vacuoles (*12-14*). Loss of the *S. typhimurium* SifA or *L. pneumophila* SdhA effectors causes rupture of the vacuole and release of bacteria into the cytosol (*15-17*). *S. typhimurium* uses two distinct T3SS encoded by the *Salmonella* pathogenicity island 1 (SPI1) and SPI2; these two T3SS translocate distinct batteries of effectors, such as SifA by SPI2 (*18*). While *S. typhimurium*-expressing SPI1 and flagellin are readily detected by NLRC4 (*19*, *20*), bacteria grown under conditions that mimic the vacuolar environment express SPI2 and repress flagellin, minimizing canonical inflammasome detection (*1*, *11*, *21*). Infection of BMMs with *S. typhimurium* that lacked *sifA*, however, significantly increased IL-1β secretion and pyroptosis (Fig. 2B-C). IL-1β secretion was dependent on canonical inflammasomes (Fig. 2B), whereas pyroptosis was still observed in *Nlrc4*$^{-/-}$*Asc*$^{-/-}$ and *Nlrp3*$^{-/-}$*Nlrc4*$^{-/-}$ macrophages (Fig. 2C). Furthermore, the NLRC4 inflammasome agonist flagellin was not required for these

responses (Fig. 2D, 2E). Thus, macrophages detect *S. typhimurium* when it aberrantly enters the cytosol, activating pyroptosis independent of all known canonical inflammasomes.

L. pneumophila also translocates flagellin through its T4SS. Thus, *L. pneumophila* mutants lacking flagellin (Δ*flaA*) evaded NLRC4 detection (Fig. 2F) (*2*). In contrast, *L. pneumophila* Δ*flaA* Δ*sdhA* mutants induce Caspase-1 activation (*16*, *17*), IL-1β secretion (*17*), and pyroptosis (Fig. 2F; (*17*)). The AIM2-ASC canonical inflammasome has been implicated in *L. pneumophila* Δ*flaA* Δ*sdhA*-induced IL-1β secretion, likely by detecting DNA released from bacteria lysing in the cytosol; however, the role of AIM2-ASC in pyroptosis was not examined (*17*). Analogous to *S. typhimurium* Δ*sifA*, *L. pneumophila* Δ*flaA* Δ*sdhA* induced pyroptosis in the absence of flagellin and ASC (Fig. 2G), ruling out all canonical inflammasomes in triggering pyroptosis under these infection conditions. These data demonstrate that diverse bacteria are detected in the cytosol.

Because IL-1β secretion required the canonical inflammasomes whereas pyroptosis did not, we hypothesized that cell death is triggered by a distinct mechanism mediated by Caspase-11. Like Caspase-1, Caspase-11 is an inflammatory caspase that can directly trigger pyroptosis (Fig. S1). Caspase-11 can also promote IL-1β secretion dependent upon NLRP3, ASC, and Caspase-1 (*10*, *22-24*). Because Caspase-1 is activated by recruitment to an oligomerized platform known as the inflammasome, Kayagaki et al. hypothesized that a similar oligomeric structure would activate Caspase-11, which they termed the non-canonical inflammasome (*10*). Although the cholera toxin B subunit and many different Gram-negative bacteria can trigger Caspase-11 activation

in vitro (*10*, *22-24*), the nature of the physiologic stimulus that activates Caspase-11 during infection remains uncertain.

Caspase-11 activation requires priming through a Toll like receptor 4 (TLR4)-TRIF-STAT1 pathway (*10*, *22-24*). Consistent with this, *Tlr4*$^{-/-}$ and *Trif*$^{-/-}$ macrophages did not undergo pyroptosis after *S. typhimurium* Δ*sifA* infection, whereas cell death was observed in macrophages deficient in the other TLR4 adaptor, Myd88 (Fig. 3A). This dependence could be overcome by priming the macrophages with interferon (IFN)-γ (Fig. 3A), which signals through STAT1. Interestingly, IFN-γ or LPS priming significantly increased the sensitivity of macrophages to *S. typhimurium* Δ*sifA* (Fig. 3A, S3A). These priming effects correlated with increased Caspase-11 expression (Fig. S3B-C), but could also be mediated by enhancing aberrant vacuolar rupture. We used retroviruses to complement *Casp1*$^{-/-}$*Casp11*$^{-/-}$ macrophages with either *Casp1* or *Casp11* in order to determine which was involved. Caspase-11 alone promoted pyroptosis without IL-1β secretion after *B. thailandensis* infection, whereas Caspase-1 enabled both responses (Fig. 3B). This is consistent with *B. thailandensis* detection through NLRC4 and/or NLRP3 activating Caspase-1 (*8*) and an additional pathway activating Caspase-11. In contrast, the responses to *S. typhimurium* Δ*sifA* or *L. pneumophila* Δ*flaA* Δ*sdhA* acted through Caspase-11, and not Caspase-1 (Fig. 3C-D). We further confirmed that Caspase-11 was responsible for the cell death observed in *Nlrc4*$^{-/-}$*Asc*$^{-/-}$ macrophages using short hairpin (sh)RNAmir (Fig. 3E-F, S3E). Finally, *Casp11*$^{-/-}$ BMM revealed that Caspase-11 was required for pyroptosis after *B. thailandensis*, *S. typhimurium* Δ*sifA*, and *L. pneumophila* Δ*flaA* Δ*sdhA* (Fig. 3G-I). Although a previous report suggested that NLRC4 signals through Caspase-11 to alter phagosomal trafficking (*25*), we saw no evidence that

NLRC4 contributes to Caspase-11 dependent cell death (Fig. 1F, 2D, S4). Pyroptosis initiated by Caspase-11 was morphologically similar to pyroptosis triggered by Caspase-1 (Fig. S5A-B). Therefore, macrophages activate Caspase-11 in response to cytosolic *B. thailandensis*, *S. typhimurium*, or *L. pneumophila* (Fig. S1).

S. typhimurium Δ*sifA* is attenuated (*15*), attributed to the role of SifA in coordinating intracellular trafficking of the *Salmonella*-containing vacuole. We hypothesized that this attenuation was actually due to innate immune detection though Caspase-11. Indeed, *S. typhimurium* Δ*sifA* was mildly attenuated in C57BL/6 mice as expected, but this was not replicated in $Casp1^{-/-}Casp11^{-/-}$ mice (Fig. 4A-B). We next determined the relative clearance of *S. typhimurium* Δ*sifA* during co-infection with wild type *S. typhimurium*, a more quantitative measure of virulence than lethal challenge. 16-fold fewer *S. typhimurium* Δ*sifA* were recovered from C57BL/6 mice 48h post infection. However, only a 4-fold reduction was seen in $Casp11^{-/-}$ mice (Fig. 4C), indicating that Caspase-11 clears *S. typhimurium* Δ*sifA in vivo*; in contrast, wild type *S. typhimurium* effectively evades Caspase-11 (*23*) by remaining within the vacuole. The remaining *S. typhimurium* Δ*sifA* attenuation likely reflects the role of *sifA* as a virulence factor promoting intracellular replication. Moreover, all known canonical inflammasomes were dispensable for *S. typhimurium* Δ*sifA* clearance, as were IL-1β and IL-18 (Fig. 4D), implicating pyroptosis as the mechanism of clearance. Clearance of bacteria after pyroptosis is mediated by neutrophils through generation of reactive oxygen (*21*). Consistent with this, NADPH oxidase deficient $p47phox^{-/-}$ mice were also defective for clearance of *S. typhimurium* Δ*sifA* (Fig. 4D). Interestingly, TLR4 and IFN-γ were not required (Fig. 4E), suggesting that there is redundant priming of Caspase-11 pathways *in*

vivo. Therefore, Caspase-11 protects mice from *S. typhimurium* Δ*sifA*, and because IL-1β and IL-18 are not required, pyroptosis is likely to be the mechanism of bacterial clearance in this case.

We next examined the susceptibility of *Casp11*$^{-/-}$ mice to the naturally cytosolic pathogens *B. thailandensis* and *B. pseudomallei*. While C57BL/6 mice are resistant to *B. thailandensis* infection, *Casp11*$^{-/-}$ mice succumbed (Fig. 4F). Likewise, *Casp11*$^{-/-}$ succumbed to *B. pseudomallei* infection, whereas C57BL/6 mice survived (Fig. 4G). Since *Nlrc4*$^{-/-}$ mice are also susceptible to *B. pseudomallei* infection (*8*), we conclude that both Caspase-1 and Caspase-11 play critical roles in limiting *B. pseudomallei* infection.

Collectively, these data demonstrate, for the first time, that Caspase-11 protects animals from lethal infection by bacteria that have the ability to invade the cytosol. This could be critical for defense against ubiquitous environmental bacteria such as *B. thailandensis* that encode virulence factors, but have not evolved to evade Caspase-11 detection. It will be interesting to determine whether Caspase-11 is activated in response to the process of vacuolar rupture or the presence of bacteria within the cytosol. Caspase-11 also responds to vacuolar bacteria under delayed kinetics, but such responses have not been shown to provide protection from infection *in vivo* (*10*, *22-24*). LPS-induced septic shock is mediated by Caspase-11 (*10*), suggesting that Caspase-11 can be activated by other mechanisms besides cytosol-localized bacteria. Thus, we propose that Caspase-11 provides protection against pathogens, but is dysregulated during overwhelming infection, contributing to septic shock and mortality. It will be interesting to determine if Caspase-11 triggers eicosanoid secretion as is seen for Caspase-1, and whether these

mediators contribute to septic shock (*26*). The identity of the hypothesized non-canonical inflammasome(s) that activate Caspase-11 and the precise nature of the activating signal will shed more light on the mechanisms by which Caspase-11 can both promote innate immunity and exacerbate immunopathology. These insights may lead to novel therapies to treat infection and sepsis.

References

1. E. A. Miao, J. V. Rajan, A. Aderem, Caspase-1-induced pyroptotic cell death, *Immunol Rev* 243, 206–214 (2011).

2. L. Franchi, R. Muñoz-Planillo, G. Núñez, Sensing and reacting to microbes through the inflammasomes, *Nature Immunology* 13, 325–332 (2012).

3. P. Broz, J. Von Moltke, J. W. Jones, R. E. Vance, D. M. Monack, Differential requirement for Caspase-1 autoproteolysis in pathogen-induced cell death and cytokine processing, *Cell Host Microbe* 8, 471–483 (2010).

4. E. A. Miao *et al.*, From the Cover: Innate immune detection of the type III secretion apparatus through the NLRC4 inflammasome, *Proceedings of the National Academy of Sciences* 107, 3076–3080 (2010).

5. Y. Zhao *et al.*, The NLRC4 inflammasome receptors for bacterial flagellin and type III secretion apparatus, *Nature* 477, 596–600 (2011).

6. E. M. Kofoed, R. E. Vance, Innate immune recognition of bacterial ligands by NAIPs determines inflammasome specificity, *Nature* 477, 592–595 (2011).

7. W. J. Wiersinga, B. J. Currie, S. J. Peacock, Melioidosis, *N Engl J Med* 367, 1035–1044 (2012).

8. I. Ceballos-Olvera, M. Sahoo, M. A. Miller, L. D. Barrio, F. Re, D. J. Philpott, Ed. Inflammasome-dependent Pyroptosis and IL-18 Protect against Burkholderia pseudomallei Lung Infection while IL-1β Is Deleterious, *PLoS Pathog* 7, e1002452 (2011).

9. W. J. Wiersinga, T. Van Der Poll, N. J. White, N. P. Day, S. J. Peacock, Melioidosis: insights into the pathogenicity of Burkholderia pseudomallei, *Nat Rev Micro* 4, 272–282 (2006).

10. N. Kayagaki *et al.*, Non-canonical inflammasome activation targets caspase-11, *Nature* 479, 117–121 (2011).

11. E. A. Miao, J. V. Rajan, Salmonella and Caspase-1: A complex Interplay of Detection and Evasion, *Front Microbiol* 2, 85 (2011).

12. N. Schroeder, L. J. Mota, S. Méresse, Salmonella-induced tubular networks, *Trends Microbiol* 19, 268–277 (2011).

13. S. Shoma *et al.*, Critical involvement of pneumolysin in production of interleukin-1alpha and caspase-1-dependent cytokines in infection with

Streptococcus pneumoniae in vitro: a novel function of pneumolysin in caspase-1 activation, *Infect Immun* 76, 1547–1557 (2008).

14. J. Ge, F. Shao, Manipulation of host vesicular trafficking and innate immune defence by Legionella Dot/Icm effectors, *Cell Microbiol* 13, 1870–1880 (2011).

15. C. R. Beuzón *et al.*, Salmonella maintains the integrity of its intracellular vacuole through the action of SifA, *EMBO J* 19, 3235–3249 (2000).

16. E. A. Creasey, R. R. Isberg, The protein SdhA maintains the integrity of the Legionella-containing vacuole, *Proceedings of the National Academy of Sciences* 109, 3481–3486 (2012).

17. J. Ge, Y.-N. Gong, Y. Xu, F. Shao, Preventing bacterial DNA release and absent in melanoma 2 inflammasome activation by a Legionella effector functioning in membrane trafficking, *Proceedings of the National Academy of Sciences* (2012), doi:10.1073/pnas.1117490109.

18. J. van der Heijden, B. B. Finlay, Type III effector-mediated processes in Salmonellainfection, *Future Microbiology* 7, 685–703 (2012).

19. L. Franchi *et al.*, Cytosolic flagellin requires Ipaf for activation of caspase-1 and interleukin 1β in salmonella-infected macrophages, *Nature Immunology* 7, 576–582 (2006).

20. E. A. Miao *et al.*, Cytoplasmic flagellin activates caspase-1 and secretion of interleukin 1β via Ipaf, *Nature Immunology* 7, 569–575 (2006).

21. E. A. Miao *et al.*, Caspase-1-induced pyroptosis is an innate immune effector mechanism against intracellular bacteria, *Nature Immunology* 11, 1136–1142 (2010).

22. P. Gurung *et al.*, TRIF-mediated caspase-11 production integrates TLR4- and Nlrp3 inflammasome-mediated host defense against enteropathogens, *Journal of Biological Chemistry* (2012), doi:10.1074/jbc.M112.401406.

23. P. Broz *et al.*, Caspase-11 increases susceptibility to Salmonella infection in the absence of caspase-1, *Nature* (2012), doi:10.1038/nature11419.

24. V. A. K. Rathinam *et al.*, TRIF Licenses Caspase-11-Dependent NLRP3 Inflammasome Activation by Gram-Negative Bacteria, *Cell* 150, 606–619 (2012).

25. A. Akhter *et al.*, Caspase-11 Promotes the Fusion of Phagosomes Harboring Pathogenic Bacteria with Lysosomes by Modulating Actin Polymerization, *Immunity* (2012), doi:10.1016/j.immuni.2012.05.001.

26. J. Von Moltke *et al.*, Rapid induction of inflammatory lipid mediators by the inflammasome in vivo, *Nature* (2012), doi:10.1038/nature11351.

Acknowledgments:

The authors thank V. Dixit sharing mice (under a materials transfer agreement) and M. Heise for sharing mice, and S. Miller, J. Mougous, and H. Schweizer for sharing bacterial strains. We also thank D. Rodriguez and L. Zhou for managing mouse colonies. The data presented in this manuscript are tabulated in the main paper and in the supplementary materials. This work was supported by NIH grants AI097518 (EAM) and AI057141 (EAM and AA), AI065359 (PAC), AI075039 (REV), AI080749 (REV), and AI063302 (REV), Investigator Awards from the Burroughs Welcome Fund and Cancer Research Institute (REV), and an NSF graduate fellowship (MFF).

Figure 1

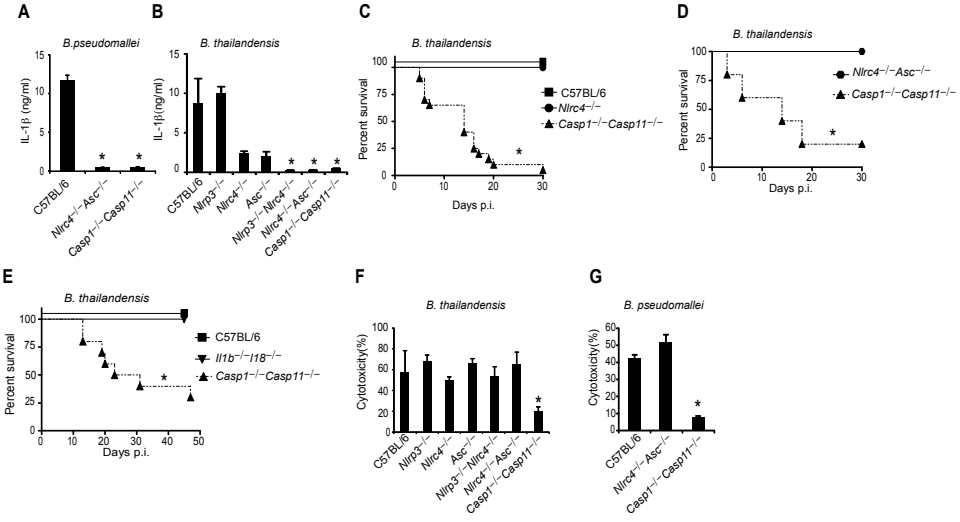

Fig. 1. *Burkholderia* detection and protection conferred by Casp1/11 is independent of all known canonical inflammasomes. Lipopolysaccharide (LPS) primed BMMs were infected with *B. pseudomallei* (**A**, **G**) or *B. thailandensis* (**B**, **F**) for 4h. (**A**, **B**) IL-1 secretion was determined by ELISA or (**F**, **G**) cytotoxicity was determined by LDH release assay. (**C**, **D**, **E**) Survival curves of wild type C57BL/6 or the indicated knockout mice infected i.p. with *B. thailandensis* . Data are representative of at least 3 (**A**, **B**, **F**, **G**) or 2 (**D**, **E**) experiments. (**C**) Data are pooled from 3 experiments. For number of mice in each panel see Table S2. Statistically significant differences with respect to controls are indicated (Student's T-test or log rank test for survival; * = $p \leq 0.05$, n.s. = $p > 0.05$).

Figure 2

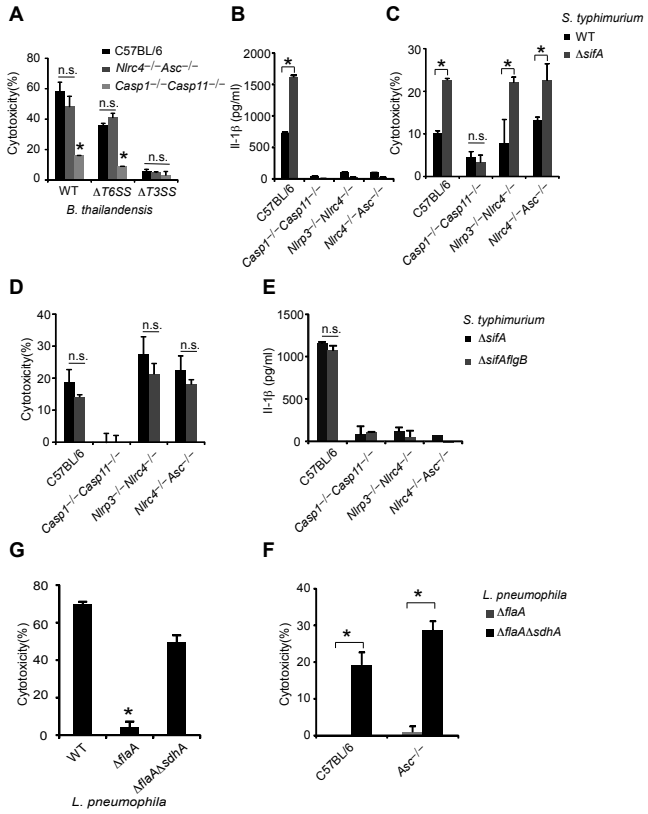

Fig. 2. Diverse cytosolic bacteria activate pyroptosis independent of NLRC4, NLRP3 and ASC. (**A**) LPS-primed BMMs were infected for 4h with either *B. thailandensis* or the indicated mutants and cytotoxicity was determined. BMMs were infected for 8h with (**B**) *S. typhimurium* or *S. typhimurium* Δ*sifA*, (**D**) *S. typhimurium* Δ*sifA* or *S. typhimurium* Δ*sifA* Δ*flgB* (**D**) and cytotoxicity was determined. LPS-primed BMM were infected for 8h with *S. typhimurium* or *S. typhimurium* Δ*sifA* (**C**), *S. typhimurium* Δ*sifA* or *S. typhimurium* Δ*sifA* Δ*flgB* (**E**) and IL-1β secretion was determined. (**F**, **G**) Cytotoxicity in wild type or *Asc*$^{-/-}$ BMMs infected for 4h with *L. pneumophila*, *L. pneumophila* Δ*flaA* or *L. pneumophila* Δ*sdhA* Δ*flaA*. Cytotoxicity was determined by LDH release and IL-1β secretion by ELISA. Data are representative of at least 3 experiments. Statistically significant differences with respect to controls are indicated (Student's T-test; * = $p \leq 0.05$, n.s. = $p > 0.05$).

Figure 3

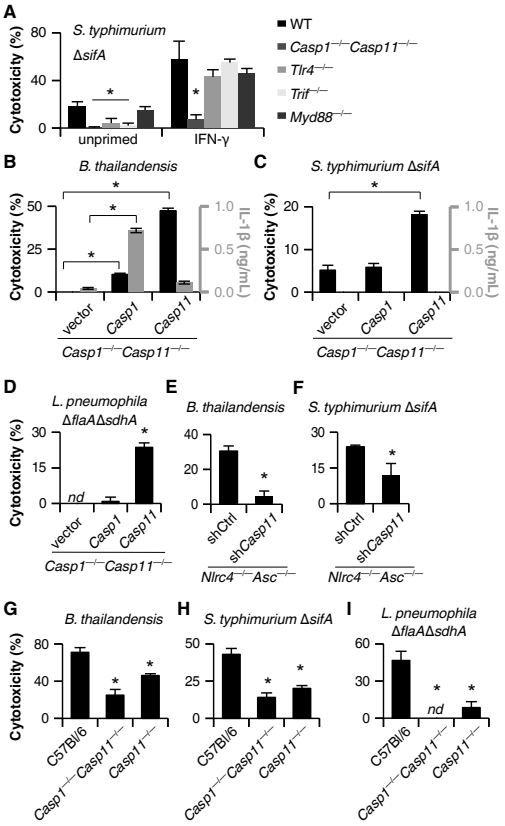

Fig. 3. Caspase-11 mediates pyroptosis after infection by cytosolic bacteria. (**A-I**) Macrophage cytotoxicity and IL-1β secretion were determined after infection with *S. typhimurium* Δ*sifA* (8h), *L. pneumophila* Δ*flaA* Δ*sdhA* (4h), or *B. thailandensis* (4h). (**A**) C57BL/6, *Casp1*$^{-/-}$*Casp11*$^{-/-}$, *Tlr4*$^{-/-}$, *Trif*$^{-/-}$, and *Myd88*$^{-/-}$ BMM infected with *S. typhimurium* Δ*sifA* with or without IFN-γ priming prior to infection. (**B-C**) Retroviral transduction was used to complement *Casp1* or *Casp11* in *Casp1*$^{-/-}$*Casp11*$^{-/-}$ iBMM. Macrophages were primed with LPS (**B**) or IFN-γ (**C**) and responses to *B. thailandensis* (**B**) or *S. typhimurium* Δ*sifA* (**C**) infection were examined. (**D**) Control or complemented *Casp1*$^{-/-}$*Casp11*$^{-/-}$ BMM infected with *L. pneumophila* Δ*flaA* Δ*sdhA*. (**E-F**) Retroviral transduction was used to introduce control or *Casp11*-targeting shRNAmir into *Nlrc4*$^{-/-}$*Asc*$^{-/-}$ iBMM. Macrophages were primed overnight with LPS (**E**) or IFN-γ (**F**) and then infected as indicated. (**G-I**) C57BL/6, *Casp1*$^{-/-}$*Casp11*$^{-/-}$, and *Casp11*$^{-/-}$ BMM infected with *B. thailandensis* (**G**), *S. typhimurium* Δ*sifA* (**H**), or *L. pneumophila* Δ*flaA* Δ*sdhA* (**I**). Data are representative of at least 3 (**A-C**, **E**, **G**, **H**) or 2 (**D**, **F**, **I**) independent experiments. Statistically significant differences with respect to controls are indicated (Student's T-test; * = $p \leq 0.05$). nd, none detected.

Figure 4

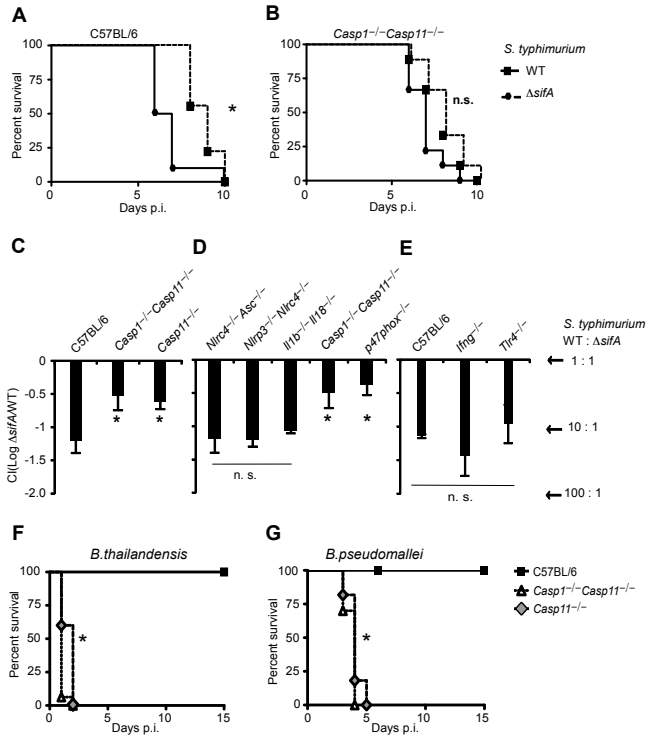

Fig. 4. Caspase-11 protects against cytosolic bacteria in vivo. (**A**, **B**) *S. typhimurium* or *S. typhimurium* Δ*sifA* were injected i.p. into C57BL/6 (1000 cfu) or *Casp*1−/−*Casp*11−/−mice (250 cfu) and survival was monitored. (**C**-**E**) The indicated mice were infected with 5x104 cfu of both wild type *S. typhimurium* and *S. typhimurium* Δ*sifA* marked with ampicillin or kanamycin resistance, respectively. Bacterial loads were determined 48h later and competitive index calculated (CI = log (*S. typhimurium* Δ*sifA*/ *S. typhimurium*). A CI of -1 corresponds to 10 cfu of *S. typhimurium* for every 1 cfu of *S. typhimurium* Δ*sifA* . (**F**-**G**) C57BL/6, *Casp*1−/−*Casp*11−/−, or *Casp*11−/− mice were infected with (F) 2x107 cfu mouse passaged *B. thailandensis* i.p. or (**G**) 100 cfu *B. pseudomallei* i.n. (**A**, **B**, **F**, **G**) Data are pooled from two independent experiments. (**C**) Representative of 3 experiments. (**D**, **E**) Representative of 2 experiments. For number of mice in each panel see Table S2. Statistically significant differences with respect to controls are indicated (Student's T-test or log rank test for survival; * = $p \leq 0.05$, n.s. = $p > 0.05$).

Supplementary Materials

Materials and Methods

Figures S1-S3

Tables S1-S2

References (26-48)

Supplementary Materials and Methods

Mice and *in vivo* infections

Wild-type C57BL/6 (Jackson Laboratory), *Asc*$^{-/-}$(*27*), *Nlrp3*$^{-/-}$ (*28*), *Nlrc4*$^{-/-}$ (*27*), *Nlrp3*$^{-/-}$*Nlrc4*$^{-/-}$, *Nlrc4*$^{-/-}$*Asc*$^{-/-}$, *Il1b*$^{-/-}$*Il18*$^{-/-}$ (*29*, *30*), *Casp1*$^{-/-}$*Casp11*$^{129mt/129mt}$ referred to as *Casp1*$^{-/-}$*Casp11*$^{-/-}$ (*31*), *Casp11*$^{-/-}$ (*10*), *Ifng*$^{-/-}$ (Jackson # 002287) (*32*), *Tlr4*$^{lps-del/lps-del}$ referred to as *Tlr4*$^{-/-}$ (Jackson # 007227), *Trif*$^{Lps2/Lps2}$ referred to as *Trif*$^{-/-}$ (Jackson # 005037), *Myd88*$^{-/-}$ (Jackson # 009088), and *Ncf1*$^{m1J/m1J}$ referred to as *p47phox*$^{-/-}$ (Jackson # 004742) (*33*) mice were used in this study. Mice were housed in a specific pathogen–free facility. All protocols were approved by the Institutional Animal Care and Use Committee at the University of North Carolina at Chapel Hill, the Institute for Systems Biology, Seattle Biomedical Research Institute, or The University of California at Berkeley and met guidelines of the US National Institutes of Health for the humane care of animals.

For study of lethal *B. thailandensis* challenge, mice were infected via intraperitoneal (i.p.) injection with 2×10^7 cfu (except Fig. 1D at 2 x 10^6 cfu) or intranasal (i.n.) inoculation with $1x10^4$ cfu. For Figure 4F, mice were infected with 2 x

10^7 cfu i.p. of *B. thailandensis* that was passaged through as *Casp1*$^{-/-}$*Casp11*$^{-/-}$ mouse (strain E264-1); this strain displays more synchronized infection kinetics than the parental E264. For *B. pseudomallei* infection studies, mice were infected with 100 cfu i.n. For monotypic *S. typhimurium* and *S. typhimurium* Δ*sifA* challenges, C57BL/6 mice were infected via i.p. injection with 1000 cfu. Because *Casp1*$^{-/-}$*Casp11*$^{-/-}$ mice have a mild innate susceptibility to *S. typhimurium* infection, a lower dose of 250 cfu was used, which yielded more comparable infection kinetics in comparison to C57BL/6 mice. For numbers of mice used in lethal challenges see Table S3. For studies of coinfection with *S. typhimurium* and *S. typhimurium* Δ*sifA*, 4 or 5 mice were infected with $5x10^4$ cfu each of *S. typhimurium* pWSK29 (ampicillin resistant) and *S. typhimurium* Δ*sifA* pWSK129 (kanamycin resistant). Spleens were harvested 2 days post infection and homogenized in sterile PBS. Viable cfu in homogenates were enumerated by plating serial dilutions on agar containing ampicillin (100μg/mL) or kanamycin (40μg/mL). Bacterial competitive indices were calculated as the log of (*S. typhimurium* Δ*sifA* cfu / *S. typhimurium* cfu).

Bacterial growth conditions

Burkholderia strains were grown in Luria-Bertani medium (LB) overnight at 37°C. For *in vitro* infections, bacteria were pelleted from 1mL of culture were opsonized with 50μL of mouse sera for 30 min at 37°C and then suspended in 1 ml of DMEM. *Salmonella* strains were grown in LB overnight at 37°C. For induction of SPI2 expression, bacteria were cultured as previously described (*34*). Briefly, freshly streaked bacterial colonies were used to inoculate LB. After 16-20h growth at 37°C, bacteria were pelleted, washed with PBS 3X, and then back-diluted to an OD_{600} of 0.026 in SPI2 media

and grown 16-18h at 37°C. SPI2 media: 0.1% w/v casamino acids, 38mM glycerol, 5mM KCl, 7.5mM $(NH_4)_2SO_4$, 0.5mM K_2SO_4, 1mM KH_2PO_4, 100mM Tris, 100mM BisTris, 200uM $MgCl_2$, 100mM Hepes; pH to 6.5. *Legionella* strains were grown overnight at 37°C in buffered yeast extract supplemented with $FeNO_3$, thymidine, and cysteine (*35*).

Macrophage culture, infection, and analysis of inflammasome activation

BMMs were prepared as described (*20*). For infections, macrophages were seeded into 96-well tissue culture treated plates at a density of $5x10^4$ cells/well (*B. thailandensis*, *B. pseudomallei*, *S. typhimurium*) or $1x10^5$ cells/well (*L. pneumophila*). When indicated, macrophages were primed with lipopolysaccharide (50 ng/ml) or IFN-γ (8 ng/ml) overnight. Bacteria were added to BMMs at MOI 50 (*B. thailandensis*, *B. pseudomallei*, *S. typhimurium*) or MOI 1 (*L. pneumophila*), centrifuged for 5 min at 200 xg (*B. thailandensis*, *B. pseudomallei*, *S. typhimurium*) or 10 min at 400 xg (*L. pneumophila*), and then incubated at 37°C for 1hr. After 1 hour extracellular bacterial growth was stopped by addition of 15 μg/ml gentamicin (*S. typhimurium*) or 300 μg/ml kanamycin (*B. thailandensis*). Supernatant samples were collected at the indicated time points. Cytotoxicity was defined as the percentage of total lactate dehydrogenase released into the supernatant and was determined as described (*36*) or using the CytoTox 96 assay kit (Promega). IL-1β secretion was determined by enzyme-linked immunosorbent assay (ELISA) (R&D Systems).

Complementation and knockdown of *Casp1* and *Casp11*

Bone marrow derived macrophages were immortalized (iBMM) as described (*37*). For complementation of *Casp1* and *Casp11* in *Casp1*$^{-/-}$*Casp11*$^{-/-}$ iBMMs, macrophages were transduced with pMXsIP (*38*) derived retrovirus carrying *Casp1* or *Casp11*; for complementation of primary BMMs, macrophages were transduced with MSCV derived retroviruses (*39*). For knockdown of *Casp11* expression in immortalized *Nlrc4*$^{-/-}$*Asc*$^{-/-}$ iBMMs, macrophages were transduced with LMP retrovirus carrying shRNAmir seed sequences targeting *Casp11* transcripts or scrambled control sequence (Open Biosystems, UNC Lenti-shRNA Core Facility).

Caspase-11 mRNA and protein expression

Total RNA was extracted using TRIzol solution (Invitrogen) and overall RNA quality was analyzed with an Agilent 2100 Bioanalyzer. Sample mRNA was amplified, labeled and hybridized to GeneChip Mouse Genome 430 2.0 arrays according to the array manufacturer's instructions (Affymetrix). Probe intensities were measured and then processed with Affymetrix GeneChip operating software into image analysis (.CEL) files. The Affymetrix CEL files were normalized with robust multi-array average expression measure (*40*) and baseline scaling using the software Bioconductor (*41*). Plotted are average $\log_2$ normalized expression intensities, computed from 2-3 biological replicates/condition.

Caspase-11 protein expression in macrophages was determined after incubation with LPS (50ng/mL) or IFN-γ (8ng/mL) overnight. Protein from $1x10^5$ cells was analyzed by Western blot using anti-Caspase-11 antibody (17D9, Novus) diluted 1:500.

Blots were stripped and equivalent loading of protein was ensured by Western blot using anti-β-actin HRP antibody (Cat. # 20272, AbCam) diluted 1:20,000.

Fluorescence Microscopy

Nlrc4$^{-/-}$*Asc*$^{-/-}$ and *Casp11*$^{-/-}$ BMMs were seeded onto glass cover slips in 24-well plates at a density of 2.78×10^5 cells/well. Macrophage were primed with IFN-γ (8 ng/ml) overnight then infected with *S. typhimurium* Δ*sifA*. At 8 hours post infection, cells were washed with PBS and then incubated for 15 min on ice with Hoechst (0.12 μg/ml) and Propidium Iodide (PI) (1 μg/ml). Images were acquired using an EVOS *florescent microscope*.

Statistical analysis

Error bars indicate the standard deviation of technical replicates. For mouse survival experiments, statistically significant differences between samples were determined using log rank (Mantel Cox). For all other experiments, statistically significant differences between samples were determined using a two-tailed, unpaired Student's T-test. * = $p \leq 0.05$, n.s. = $p > 0.05$.

Supplementary Tables:

Table S1. Strain and plasmid list

Name of Strain	Designation	Notes	Reference
S. typhimurium	ATCC 14028s	wild type	www.atcc.org
S. typhimurium	CS401	14028s strep^R, *phoN*::Tn10dCm	Samuel I Miller
S. typhimurium Δ*sifA*	JAF57	CS401 Δ*sifA*	(*42*)
S. typhimurium Δ*sifA flgB*	JAF57 *flgB*	CS401 Δ*sifA flgB44*::Tn*10*	S. Yamaguchi
B. thailandensis	E264	wild type	www.atcc.org
B. thailandensis	E264-1	mouse passaged wild type	this study
B. thailandensis T3SS mutant			Joseph Mougous
B. thailandensis T6SS mutant			Joseph Mougous
B. pseudomallei	Bp340	1026b amrRAB-oprA	(*43*)
B. pseudomallei Δ*purM*	Bp82	purine auxotroph	(*44*)
L. pneumophila	LP02	wild type; Philadelphia-1 *rpslL hsdR thyA*$^-$	(*46*)
L. pneumophila Δ*flaA*		flagellin mutant	(*47*)
L. pneumophila Δ*flaA* Δ*sdhA*		flagellin, *sdhA* mutant	(*48*)

Plasmids	Resistance	Notes	
pWSK29	Amp	Low copy vector	(*45*)
pWSK129	Kan	Low copy vector	(*45*)

Table S2. Numbers of mice used in survival experiments

Figure	Mice genotype	Number of mice
Fig.1C	C57Bl/6	21
	Nlrc4$^{-/-}$	15
	Casp1$^{-/-}$*Casp11*$^{-/-}$	21
Fig.1d	Nlrc4$^{-/-}$Asc$^{-/-}$	10
	Casp1$^{-/-}$*Casp11*$^{-/-}$	5
Fig.1E	C57Bl/6	10
	Il1b$^{-/-}$*Il18*$^{-/-}$	10
	Casp1$^{-/-}$*Casp11*$^{-/-}$	10
Fig.4A	C57Bl/6 – *S. typhimurium*	10
	C57Bl/6 – *S. typhimurium* Δ*sifA*	9
Fig.4B	*Casp1*$^{-/-}$*Casp11*$^{-/-}$ – *S. typhimurium*	9
	Casp1$^{-/-}$*Casp11*$^{-/-}$ – *S. typhimurium* Δ*sifA*	9
Fig.4F	C57Bl/6	7
	Casp1$^{-/-}$*Casp11*$^{-/-}$	16
	Casp11$^{-/-}$	17
Fig.4G	C57Bl/6	8
	Casp1$^{-/-}$*Casp11*$^{-/-}$	10
	Casp11$^{-/-}$	11
Fig. S2A	C57Bl/6	5
	Casp1$^{-/-}$*Casp11*$^{-/-}$	5
Fig. S2B	C57Bl/6	5
	Casp1$^{-/-}$*Casp11*$^{-/-}$	8
	Nlrc4	10
	Asc$^{-/-}$	7
	Nlrp3$^{-/-}$	9
	Nlrc4$^{-/-}$Asc$^{-/-}$	9
Fig. S2C	*Il1b*$^{-/-}$*Il18*$^{-/-}$	19
	Casp1$^{-/-}$*Casp11*$^{-/-}$	10

Supplemental References

27. S. Mariathasan *et al.*, Differential activation of the inflammasome by caspase-1 adaptors ASC and Ipaf, *Nature* 430, 213–218 (2004).

28. S. Mariathasan *et al.*, Cryopyrin activates the inflammasome in response to toxins and ATP, *Nature* 440, 228–232 (2006).

29. L. P. Shornick *et al.*, Mice deficient in IL-1beta manifest impaired contact hypersensitivity to trinitrochlorobenzone, *J Exp Med* 183, 1427–1436 (1996).

30. K. Takeda *et al.*, Defective NK cell activity and Th1 response in IL-18-deficient mice, *Immunity* 8, 383–390 (1998).

31. K. Kuida *et al.*, Altered cytokine export and apoptosis in mice deficient in interleukin-1 beta converting enzyme, *Science* 267, 2000–2003 (1995).

32. D. K. Dalton *et al.*, Multiple defects of immune cell function in mice with disrupted interferon-gamma genes, *Science* 259, 1739–1742 (1993).

33. C. K. Huang, L. Zhan, M. O. Hannigan, Y. Ai, T. L. Leto, P47(phox)-deficient NADPH oxidase defect in neutrophils of diabetic mouse strains, C57BL/6J-m db/db and db/, *Journal of Leukocyte Biology* 67, 210–215 (2000).

34. E. A. Miao, J. A. Freeman, S. I. Miller, Transcription of the SsrAB regulon is repressed by alkaline pH and is independent of PhoPQ and magnesium concentration, *J Bacteriol* 184, 1493–1497 (2002).

35. B. Byrne, M. S. Swanson, Expression of Legionella pneumophila virulence traits in response to growth conditions, *Infect Immun* 66, 3029–3034 (1998).

36. T. Decker, M. L. Lohmann-Matthes, A quick and simple method for the quantitation of lactate dehydrogenase release in measurements of cellular cytotoxicity and tumor necrosis factor (TNF) activity, *J. Immunol. Methods* 115, 61–69 (1988).

37. S. E. Warren *et al.*, Cutting Edge: Cytosolic Bacterial DNA Activates the Inflammasome via Aim2, *The Journal of Immunology* 185, 818–821 (2010).

38. T. Kitamura *et al.*, Retrovirus-mediated gene transfer and expression cloning: powerful tools in functional genomics, *Exp Hematol* 31, 1007–1014 (2003).

39. R. G. Hawley, F. H. Lieu, A. Z. Fong, T. S. Hawley, Versatile retroviral vectors for potential use in gene therapy, *Gene Ther* 1, 136–138 (1994).

40. R. A. Irizarry *et al.*, Exploration, normalization, and summaries of high density oligonucleotide array probe level data, *Biostatistics* 4, 249–264 (2003).

41. R. C. Gentleman *et al.*, Bioconductor: open software development for computational biology and bioinformatics, *Genome Biol* 5, R80 (2004).

42. J. A. Freeman, M. E. Ohl, S. I. Miller, The Salmonella enterica serovar typhimurium translocated effectors SseJ and SifB are targeted to the Salmonella-containing vacuole, *Infect Immun* 71, 418–427 (2003).

43. T. Mima, H. P. Schweizer, The BpeAB-OprB efflux pump of Burkholderia pseudomallei 1026b does not play a role in quorum sensing, virulence factor production, or extrusion of aminoglycosides but is a broad-spectrum drug efflux system, *Antimicrob. Agents Chemother.* 54, 3113–3120 (2010).

44. K. L. Propst, T. Mima, K.-H. Choi, S. W. Dow, H. P. Schweizer, A Burkholderia pseudomallei purM Mutant Is Avirulent in Immunocompetent and Immunodeficient Animals: Candidate Strain for Exclusion from Select-Agent Lists, *Infect Immun* 78, 3136–3143 (2010).

45. R. F. Wang, S. R. Kushner, Construction of versatile low-copy-number vectors for cloning, sequencing and gene expression in Escherichia coli, *Gene* 100, 195–199 (1991).

46. K. H. Berger, R. R. Isberg, Two distinct defects in intracellular growth complemented by a single genetic locus in Legionella pneumophila, *Mol Microbiol* 7, 7–19 (1993).

47. T. Ren, D. S. Zamboni, C. R. Roy, W. F. Dietrich, R. E. Vance, Flagellin-Deficient Legionella Mutants Evade Caspase-1- and Naip5-Mediated Macrophage Immunity, *PLoS Pathog* 2, e18 (2006).

48. R. K. Laguna, E. A. Creasey, Z. Li, N. Valtz, R. R. Isberg, A Legionella pneumophila-translocated substrate that is required for growth within macrophages and protection from host cell death, *Proc Natl Acad Sci USA* 103, 18745–18750 (2006).

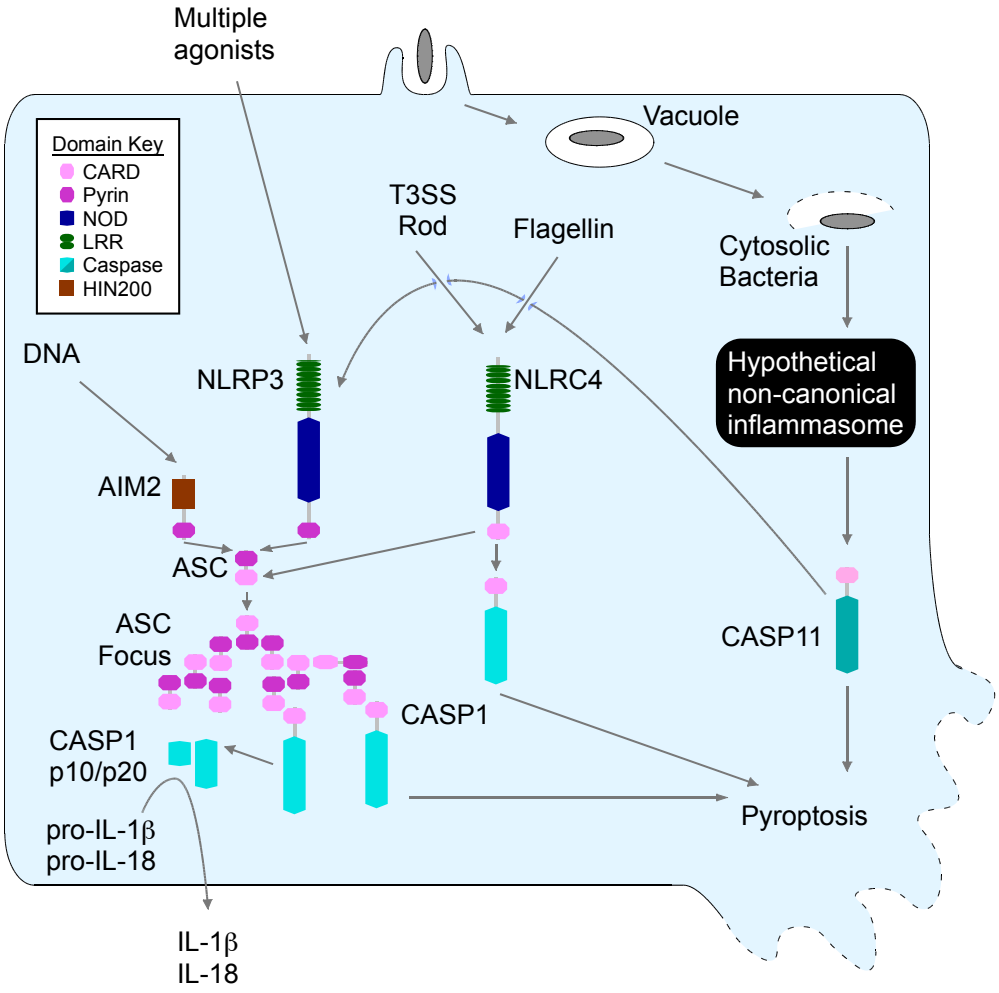

Figure S1. Schematic of inflammasome detection pathways. Canonical inflammasomes including NLRP3, AIM2, and NLRC4 activate caspase-1. NLRC4 contains a CARD domain that can bind to the CARD of caspase-1 directly through homotypic interaction, triggering pyroptosis. The NLRC4 also binds ASC through CARD homotypic interactions, resulting in recruitment of the entire complement of cellular ASC into a single ASC focus. The Pyrin domain of NLRP3 or AIM2 cannot bind directly to caspase-1, but triggers formation of the ASC focus via Pyrin-Pyrin homotypic interactions. The ASC focus recruits and activates caspase-1, resulting in its proteolytic maturation to the p10 and p20 fragments, and subsequent IL-1 and IL-18 cleavage and secretion. Therefore, cells that are deficient in both *Nlrc4* and *Asc* cannot signal through any known canonical inflammasome. The activating platform for caspase-11 remains unknown; nevertheless, the hypothetical activator was named the non-canonical inflammasome. Our data indicate that cytosolic bacteria are detected through this hypothetical non-canonical inflammasome, resulting in caspase-11-dependent pyroptosis. Caspase-11 activation also triggers NLRP3 activation via an unknown mechanism (denoted by an arrow through tunnels).

Figure S2

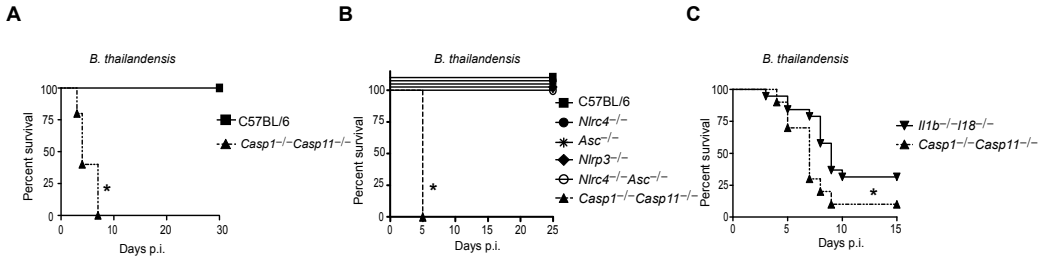

Fig. S2. Burkholderia protection conferred by Casp1/11 is independent of all known canonical inflammasomes (**A**-**C**) Wild type C57BL/6 or the indicated knockout mice were infected i.n. with *B*. *thailandensis* and survival was monitored. Data are representative of 4 (**A**), 1 (**B**) or pooled from 2 (**C**) experiments. For number of mice in each panel see Table S2. Statistically significant differences with respect to controls are indicated (log rank test for survival; * = $p \leq 0.05$).

Figure S3

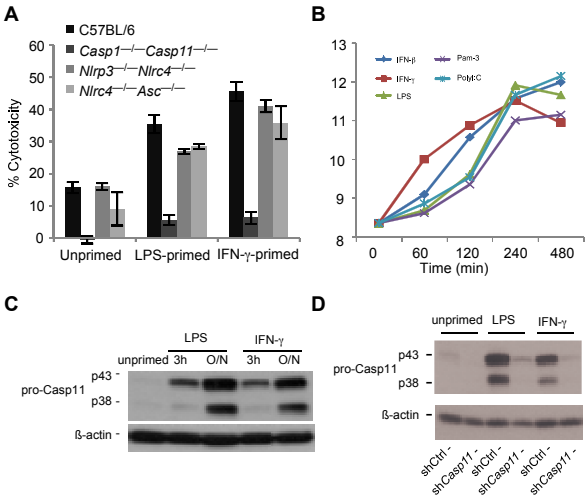

Fig. S3. TLR ligands and IFN-γ enhance *Casp11* expression and Caspase-11-dependent cell death. (**A**) Untreated, LPS-primed, or IFN-γ-primed BMMs were infected with *S. typhimurium* Δ*sifA* and cytotoxicity was determined. (**B**) Transcriptional upregulation of *Casp11* in C57BL/6 BMMs after priming with the indicated molecules was determined using Affymetrix GeneChip technology. (**C**) Caspase-11 expression in untreated, LPS-primed, and IFN-γ-primed C57BL/6 BMMs was determined by immunoblot. Blots were stripped and β-actin expression was determined as a loading control. (**D**) Caspase-11 expression in untreated, LPS-primed, and IFN-γ-primed control or *Casp11* shRNA-expressing *Nlrc4-Asc* iBMMs was determined by immunoblot. Loading controls were performed as in (**C**). Results are representative of more than 3 (**A**, **B**), 2 (**C**), or 1 (**D**) experiments. Statistically significant differences with respect to controls are indicated (Student's T-test; * = $p < 0.05$).

Figure S4

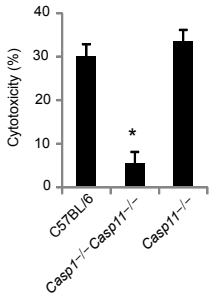

Fig. S4. Caspase-11 is not required for pyroptosis induced by flagellin expressing wild type *L. pneumophila*. Wild type *L. pneumophila* inadvertently translocate flagellin into the macrophage cytosol, resulting in detection through NLRC4, which activates Caspase-1. We investigated whether this response was altered in the absence of Caspase-11. C57BL/6, *Casp*1−/−*Casp*11−/−, and *Casp*11−/−BMM infected with *L. pneumophila* at an MOI of 1 and cytotoxicity was determined 4 hours later; C57BL/6 and *Casp*11−/− BMMs showed similar cytotoxicity, indicating that Caspase-11 is not required for NLRC4-induced pyroptosis. Data are representative of at least 3 independent experiments. Statistically significant differences with respect to controls are indicated (Student's T-test; * = $p \leq 0.05$).

Figure S5

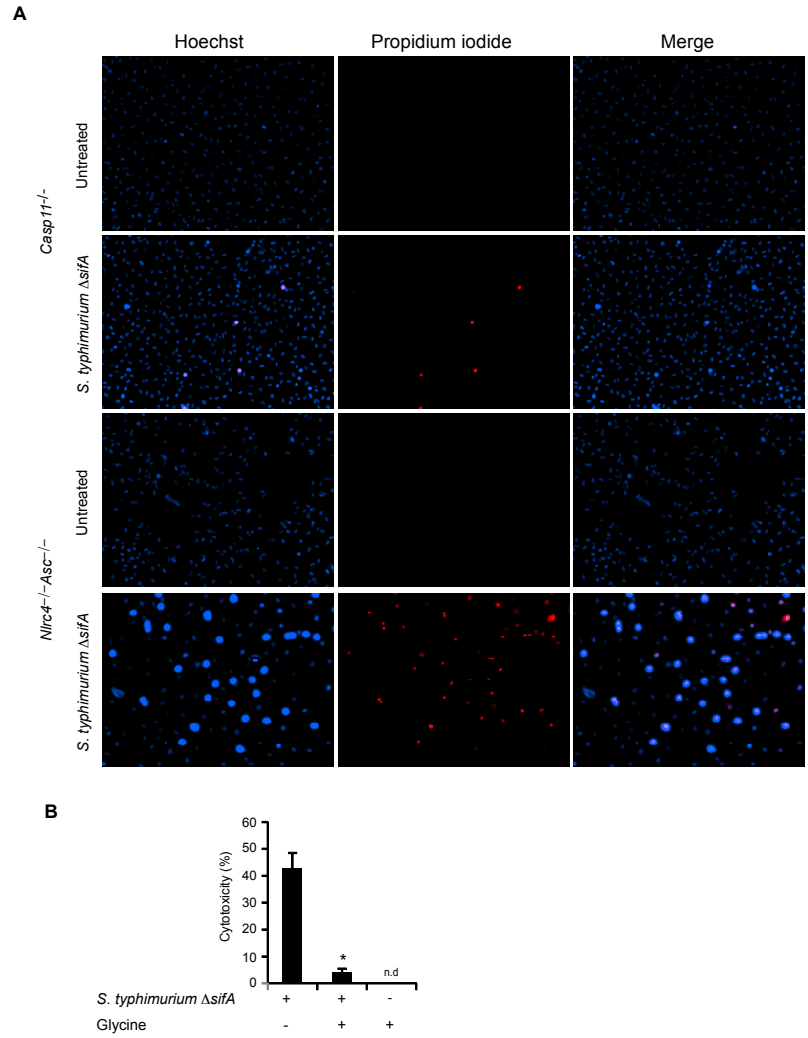

Fig. 5S. Morphology of *S. typhimurium* Δ*sifA*-induced pyroptosis. IFN-γ-primed *Nlrc*4$^{-/-}$ *Asc*$^{-/-}$ or *Casp11*$^{-/-}$ BMMs were infected for 8h with *S. typhimurium* Δ*sifA* (MOI 50) (**A**) Representative fluorescence microscopy images of BMM stained with membrane permeant Hoechst and membrane impermeant propidium iodide (PI) 8 hours post infection as a measure of cell death in addition to LDH release. Although Hoechst is a membrane permeant dye, its staining intensity significantly increased in pyroptotic cell due afer membrane rupture; in order to visualize both intact and pyroptotic cells the image is over-exposed for lysed cells, making their nucleus appear larger in the Hoechst channel. (**B**) Caspase-1-dependent pyroptotic cell death is known to be inhibited by addition of glycine to the media. In order to determine if Caspase-11-dependent cell death was occurring through a morphologically similar pathway, we added 20mM glycine at 4h post *S. typhimurium* Δ*sifA* infection. LDH release was determined 4h later (total of 8h infection).

Discovery of Inhibitors of *Burkholderia pseudomallei* methionine aminopeptidase with Antibacterial Activity[1]

Burkholderia pseudomallei is the causative agent of melioidosis, a severe and often fatal infection that manifests as pneumonia or septicemia.[1] Melioidosis is endemic to Southeast Asia and Northern Australia, where it is a significant cause of morbidity and mortality, and can also be found in other tropical regions.[2] The Centers for Disease Control and Prevention consider *B. pseudomallei* to be a bioterrorism risk and have thus listed the organism as a Category B priority agent that could potentially cause a large-scale public health crisis if used in an attack.[3] Although it is critical to identify antimicrobial agents active against *B. pseudomallei*, the process of drug discovery has been challenging. The current standard treatment for melioidosis is intensive administration of the third-generation cephalosporin antibiotic ceftazidime followed by a regimen of trimethoprim-sulfamethoxazole or amoxicillin-clavulanic acid for 3–6 months.[2] Ceftazidime is highly active *in vitro* and was shown to be safe for clinical use;

---

[1] Authored by: Phumvadee Wangtrakuldee, Matthew S. Byrd, Cristine G. Campos, Michael W. Henderson, Zheng Zhang, Ali Masoudi, Peter J. Myler, James R. Horn, Peggy A. Cotter, Timothy J. Hagen

however, resistance to this drug is possible, and the long treatment duration in combination with other antibiotics results in substantial patient non-compliance.[2,4] In addition, *B. pseudomallei* is intrinsically resistant to several classes of antibiotics, including aminoglycosides and macrolides, due to a multi-drug efflux pump that transports drugs out of the cell.[5] This intrinsic resistance creates an even greater challenge for the scientific community to find alternative treatments that act via novel mechanisms.

Methionine Aminopeptidase (MetAP) is a dinuclear metalloprotease that removes the N-terminal methionine from nascent proteins.[6] MetAP is conserved in all life forms from bacteria to humans. Genetic studies have shown that deleting the MetAP-encoding gene in numerous prokaryotes results in either a slow-growth or lethal phenotype.[6] These studies reveal the critical role of MetAPs in prokaryote survival and suggest these enzymes are promising targets for the discovery of new antibiotics.

Early studies by Lu *et al.* targeting *M. tuberculosis* MetAP enzymes demonstrated that potent inhibitors of MtMe tAP1a and MtMetAP1c inhibited the growth of mycobacteria in culture.[7] Similarly, potent inhibitors of Human MetAP2 were also shown to exhibit activities against HMVEC proliferation.[8] While possessing only limited sequential identity and similarity to MtMetAP1 (37% identity /46% similarity) and human MetAP2 (12% identity /18% similarity), the MetAP of *B. pseudomallei* contains key amino acid residues at the active sites (Asp 131, Asp 142, His 205, Glu 238, and Glu 269) identical to those in *M. tuberculosis* MetAP1 and Human MetAP2 (Figure 1). This observation suggests that the various types of inhibitors effective against MetAP1 from both *M. tuberculosis* and humans might also be effective inhibitors of *B. pseudomallei* MetAP1.

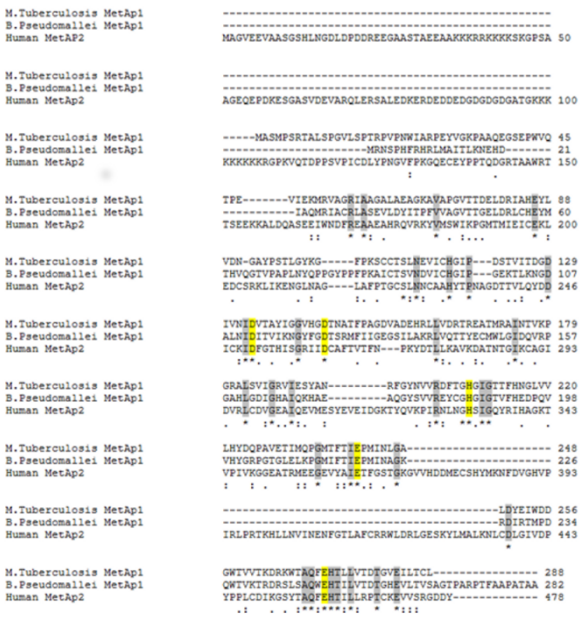

Figure 1. Alignment of the amino acid sequences of *B. pseudomallei* MetAP1, human (*Homo sapiens*) MetAP2 and *M. tuberculosis* MetAP1. There are five conserved metal-ligating residues (highlighted in yellow). Other identical residues among all three MetAPs are highlighted.

Several inhibitors of methionine aminopeptidase have been reported over the past several years. Triazole compounds were reported to be potent MetAP inhibitors, demonstrating activity in many organisms through the interaction of each of the triazole nitrogen atoms in positions 1 and 2 with divalent cobalt ions.[9] Furan-type compounds displayed sub-micromolar inhibitory activity against *Escherichia coli* methionine aminopeptidase.[10] The carboxyl group in these compounds coordinates with the metal ions at the enzyme active site pocket. Derivatives of anthranilic acid sulfonamide were reported to have potent MetAP inhibition activities against human MetAP2, with the shape of the backbone allowing both aromatic rings to reside in a hydrophobic pocket.[8]

Moreover, the chlorosubstitution at the para-position on the sulfonyl phenyl contributes to a tight binding due to a narrow hydrophobic region within the enzyme. Nitroxoline(NIT), or 5-nitro-8-hydroxyquinoline, exhibited activity against human MetAP2 *in vitro* in the nanomolar range.[11] The phenolic group at the 8-position dissociates to O^- at physiological pH. The O^- and the nitrogen atom at the 1 position participate in binding to the metal ion.[12] Here, representative compounds from each chemical series of MetAP inhibitor were selected for evaluation of their inhibition potencies against BpMetAP1 (Table 1).

Compounds **1**, **5**, and **6** were purchased from Sigma-Aldrich. Compound **2** was synthesized from alkylation of 3-amino-5-thio-1,2,4-triazole to 1-(bromomethyl)-4-methylbenzene. The synthesis of compound **2** is shown in Scheme 1. The final compound after recrystallization resulted in an approximately 67% yield. Compounds **3** and **4** were synthesized in a similar procedure using 4-flurobenzyl bromide and 1-(bromomethyl)-2,4-dichlorobenzene as the starting materials, likewise resulting in relatively considerate yields. Compound **7** was synthesized from 2-amino-5-bromobenzoic acid and 4-methylbenzene-1-sulfonyl chloride, providing a product with a 76% yield. Following a similar procedure, compound **8** was synthesized using 4-chlorobenzene-1-sulfonyl chloride as a starting material with a yield of 92%.

Scheme 1. Syntheses of Compounds 2-4 and 7-8[a]

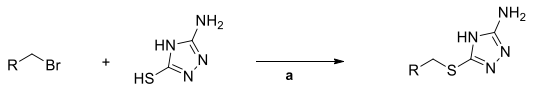

Compound	R	Yield
2	C_7H_8	67%
3	C_6H_5F	47%
4	$C_6H_4Cl_2$	92%

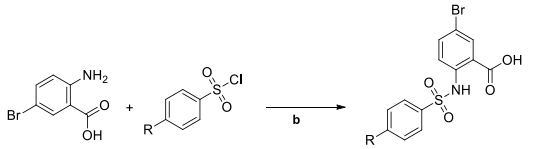

Compound	R	Yield
7	CH_3	76%
8	Cl	92%

[a]**Reagents and conditions: (a) NaOH, EtOH, 70 °C, 20 min (b) 1 M Na_2CO_3, pH 8.**

The four chemical series of compounds (**1**-**8**) were profiled for *in vitro* BpMetAP1 activity using an established activity inhibition assay (Table 1).[13] This assay used the fluorescent substrate, H-Met-Gly-Pro-AMC, along with a coupled secondary enzyme, rhDPPIV. The hydrolysis of H-Met-Gly-Pro-AMC (MetAP1), followed by Gly-Pro-AMC hydrolysis (rhDPPIV) can be conveniently monitored by the fluorescence of the aminomethylcoumarin product. Overall, these compounds exhibited a wide range of inhibition potencies. Nitroxoline (**1**) was found to significantly inhibit BpMetAP1 activity compared to other compounds, with an IC_{50} value of 60 nM respectively (Table 1). The triazole-type compounds **2**, **3**, and **4** demonstrated inhibition of BPMetAp1 in the low micromolar range. Different substituents at the C2 and C4 position on the phenyl

ring did not alter the inhibitory effect of these compounds. Furan type compounds **5** and **6** displayed IC_{50} values of more than 250 μM, indicating that they are not potent inhibitors of BpMetAP1. Sulfonamide compound **7** was shown to exhibit partial inhibition profile. The IC_{50} value was determined to be in the micromolar range. The substitution of a chlorine group from a methyl group reduces the inhibition potency of the sulfonamide compounds against BPMetAP1.

Table 1. Inhibition of Enzymatic Activity of Purified BpMetAp1 by various types of MetAP Inhibitors

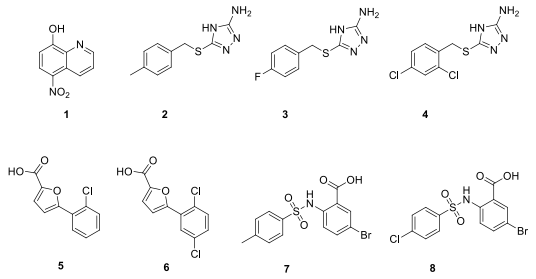

Compound	Type of compound	IC_{50}(μM)[a]
1	Nitroxoline	0.06 ± 0.03
2	1,2,4 triazole	3.1 ± 0.26
3	1,2,4 triazole	7.0 ± 3
4	1,2,4 triazole	1.0 ± 0.1
5	furan	>250[b]
6	furan	>250
7	sulfonamide	44 ± 9[c]
8	sulfonamide	>250

[a]Assay details are in the Supporting information.[b]250 μM is the highest limit regarding solubility of most of the compounds in DMSO. [d]Partial Inhibition observed.

Docking experiments were performed to examine the binding modes of the two compounds with the most potent inhibition of BpMetAP1 activity. Initially, a homology model of the BpMetAP1 was constructed from MtMetAP1 (PDB code: 3IU9). Using the

Sybyl docking suite compounds **1** and **4** were docked into the active site of BpMeAP1 by constraining to the position of 8-quinolinol binding to the chelated metal of *Aeromonas proteolytica* aminopeptidase (PDB code: 3VH9). Compound **1** contains a phenolic group that donates its proton at physiological pH. This process consequently assigned a full negative charge to the oxygen. Docking results showed that this compound chelates the metal ions by forming a complex with the negative charge from the oxygen and the nitrogen atom at the 1 position (Figure 2). Analysis of triazole-type compound **4** suggested that its inhibitory effect is dependent upon the presence of nitrogen atoms at positions 1 and 2. These nitrogen atoms coordinate with the metal ions in a manner similar to other triazole-type compounds that bind at the active site of MetAP.[9] The phenyl group of compound **4** fits in the hydrophobic pocket, thus enhancing its inhibitory effect.

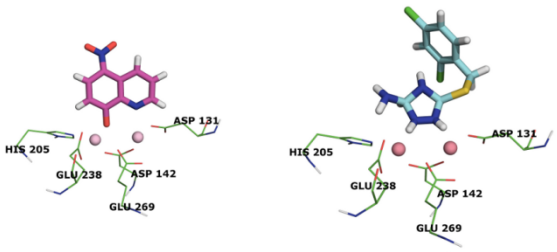

Figure 2. Proposed binding modes for **1** (left, magenta) and **4** (right, cyan) in the BpMetAp1 binding site.

Compounds **1**-**8** were subsequently evaluated for the ability to inhibit the growth of *Burkholderia thailandensis*. *B. thailandensis* is closely related to *B. pseudomallei*, displaying 98% sequence identity at the nucleotide level. However, *B. thailandensis* is not select agent pathogen, which allows for its use as a model without the requirement of

a BSL-3 facility.[14] Cells were grown in the presence of 1 mM inhibitor, 0.5 mM kanamycin (Km), or DMSO alone for approximately 24 h. Km was used as a positive control for growth inhibition because previous studies have demonstrated its efficacy against both *B. thailandensis* and *B. pseudomallei*, and it is one of only four antibiotics approved for use in the BSL-3 laboratory.[5,15,16] Growth was monitored by reading the absorbance at 600 nm every 15 min, and the area under the curve was calculated for cells grown in each condition (Supplemental Table 1). Treatment with compound **1** resulted in complete growth inhibition, similar to the Km control, while compounds **2**, **3**, **4**, **7**, and **8** showed partial inhibition of bacterial growth (approximately 15–30%; Figure 3). Compounds **5** and **6** exhibited essentially no cell growth inhibition, consistent with the high IC_{50} values observed in the activity inhibition assay. It was previously reported that triazole-derived compounds do not exhibit antibacterial activity.[8] While treatment with compounds **2**, **3**, and **4** did result in a modest reduction in growth over 24 h, the inhibition was not complete; our results, therefore, are consistent with earlier findings.

The *in vitro* and *in vivo* inhibition results for the tested compounds are largely in agreement. Compound **1** was the most potent inhibitor of both purified BpMetAp1 and of *B. thailandensis* growth, while compound **4** was the second most potent inhibitor in both assays. *In vitro*, compound **2** displayed greater inhibition than compound **8**, but *in vivo*, the inhibitory effects of these two compounds were nearly indistinguishable.

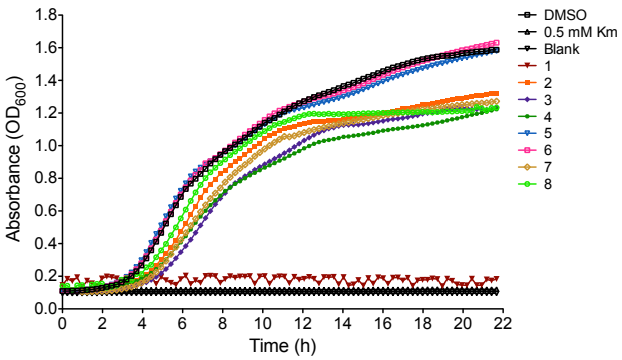

Figure 3. *B. thailandensis* growth inhibition assay.

Following this initial assessment of potential inhibitors against *B. thailandensis*, we evaluated compound **1** at different concentrations in an attempt to establish the minimum inhibitory concentration (MIC) that would prevent growth. We observed complete growth inhibition at the lowest concentration tested (62.5 μM), indicating that we had likely not reached the MIC (Figure 4A). Although testing these compounds in *B. thailandensis* is a simple and effective process, it is possible that *B. pseudomallei*-specific resistance mechanisms may reduce or eliminate the effectiveness of compound **1** in the growth inhibition assay. Therefore, we tested compound **1** against the virulent *B. pseudomallei* strain Bp340, a derivative of the clinical melioidosis isolate 1026b that lacks an aminoglycoside/macrolide-specific multidrug efflux pump (to facilitate antibiotic selection in the laboratory).[5] As with *B. thailandensis*, treatment with compound **1** resulted in the complete growth inhibition of *B. pseudomallei* Bp340 at the lowest tested concentration (31.25 μM; Figure 4B). A subsequent test of compound **1** against 1026b revealed no difference in inhibition compared to Bp340, suggesting that the lack of the multidrug efflux pump does not affect the activity of this compound (data not shown).

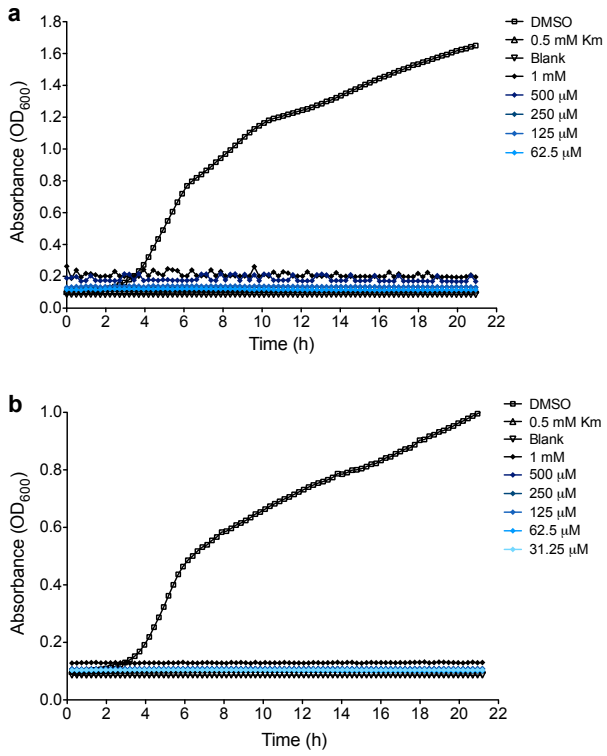

Figure 4. *B. thailandensis* **(a)** and *B. pseudomallei* **(b)** growth inhibition by compound 1.

In conclusion, we evaluated a set of small molecule inhibitors of *B. pseudomallei* MetAP1 in an enzyme activity assay. A homology model of the BpMetAP1 was generated from MtMetAP1, and the proposed binding mechanisms of two of the most potent compounds in the *in vitro* assay were illustrated through molecular docking. These compounds showed a range of MetAP1 inhibition. Assessment of the antibacterial cell-growth inhibition reveal that five of the compounds had modest to high cell growth inhibitory effects, while others had minimal effects. Compound **1** is the most potent inhibitor in the enzyme activity assay and shows nearly complete cell growth inhibition *in vivo*. The efficiency of this molecule in inhibiting BpMetAP1 activity and in arresting cell growth suggests that nitroxoline-derived compounds may be useful candidates for potential melioidosis therapeutics.

ASSOCIATED CONTENT

Supporting Information. Experimental procedures for the synthesis and characterization of the compounds, the *in vitro* activity assay, the *in vivo* antibacterial assay, and the ^{1}H NMR and ^{13}C NMR spectra of the reported compounds. This material is available free of charge via the Internet at http://pubs.acs.org.

ACKNOWLEDGMENT

We acknowledge Northern Illinois University for supporting this work. This project has been funded in part with Federal funds from the National Institute of Allergy and Infectious Diseases, National Institutes of Health, Department of Health and Human Services, under Contract Nos. HHSN272200700057C and HHSN272201200025C. We appreciate comments and advice regarding homology model and docking studies from Dr. Michael Clare. We also thank Mr. Sriram Jakkaraju for technical assistance regarding surface plasmon resonance work. Dr. Herbert Schweizer kindly provided *Burkholderia* strains.

ABBREVIATIONS

BpMetAP, *Burkholderia pseudomallei* methionine aminopeptidase; DMSO, dimethyl sulfoxide; HMVEC, human microvascular endothelial cell; Km, kanamycin; MetAP, methionine aminopeptidase; Met-Gly-Pro-AMC, methionine-glycine-proline-7-amino-4-methylcoumarin; rhDPPIV, human DPPIV/CD26.

References

1. **Limmathurotsakul, D.; Peacock, S.J. Melioidosis: A Clinical Overview. *Br. Med. Bull.* 2011, *99,* 125-139 .**

2. **Wiersinga, W. J.; Curie, B.J.; Peacock, S.J. Melioidosis. *N. Engl. J. Med.* 2012, *367*, 1035-1044.**

3. **Rotz, L.D.; Khan, S. K.; Lillibridge, S. R.; Ostroff, S. M.; Hughes, J. M. Public Health Assessment of Potential Biological Terrorism Agents. *Em. Infect. Dis*. 2002, *8*, 225-229.**

4. **Chantratita, N.; Rholl, D.A.; Sim, B.; Wuthiekanun, V.; Limmathurotsakul, D.; Amornchai, P.; Thanwisai, A.; Chua, H.H.; Ooi, W.F.; Holden, M.T.G.; Day, N.P.; Tan, P.; Schweizer, H.P.; Peacock, S.J. Antimicrobial Resistance to Ceftazidime Involving Loss of Penicillin-Binding Protein 3 in *Burkholderia pseudomallei*. *Proc. Natl. Acad. Sci. U.S.A.* 2011, *108*, 17165-17170.**

5. **Mima, T.; Schweizer, H. P. The BpeAB-OprB Efflux Pump of *Burkholderia pseudomallei* 1026b Does Not Play a Role in Quorum Sensing, Virulence Factor Production, or Extrusion of Aminoglycosides but Is a Broad-Spectrum Drug Efflux System. *Antimicrob. Agents Chemother.* 2010, *54*, 3113-3120.**

6. **Giglione, C.; Boularot, A.; Meinnel, T. Protein N-terminal methionine excision. *Cell. Mol. Life Sci.* 2004, *61*, 1455-1474.**

7. **Lu, J.; Chai, S. C.; Ye, Q. Catalysis and Inhibition of *Mycobacterium tuberculosis* Methionine Aminopeptidase. *J. Med. Chem*. 2010, *53*, 1329-1337.**

8. **Kawai, M.; BaMaung, N. Y.; Fidanze, S. D.; Erickson, S. A.; Comess, K. M.; Kalvin, D.; Wang, J.; Zhang, Q.; Lou, P.; Tucker-Garcia, L.; Bouska, J.; Bell, R. L.; Lesniewski, R.; Henkin, J.; Sheppard, G. S.; Development of sulfonamide compounds as potent methionine aminopeptidase type II inhibitors with antiproliferative properties. *Bioorg. Med. Chem. Lett.* 2006, *16*, 3574-3577.**

9. **Oefner, C.; Douangamath, A.; D'Arcy, A.; Häfeli, S.; Mareque, D.; Sweeney, A. M.; Padilla, J.; Pierau, S.; Schulz, H.; Thormann, M.; Wadman, S.; Dale, G. E. The 1.15 Å Crystal Structure of the Staphylococcus aureus Methionyl-aminopeptidae and Complexes with Triazole Based Inhibitors. *J. Mol. Biol.* 2003, *332,* 13-21.**

10. **Huang, Q.; Huang, M.; Nan, F.; Ye, Q. Metalloform-selective inhibition: Synthesis and structure-activity analysis of Mn(II)-form-selective inhibitors**

of *Escherichia Coli* methionine aminopeptidase. *Bioorg. Med. Chem. Lett*. 2005, *15*, 5386-5391.

11. Shim, J. S.; Matsui, Y.; Bhat, S.; Nacev, B. A.; Xu, J.; Bhange, H. C.; Dhara, S.; Han, K. C.; Chong, C. R.; Pomper, M. G.; So, A.; Liu, J. O. Effect of Nitrooxline on Angiogenesis and Growth of Human Bladder Cancer. *J. Natl. Cancer Inst*. 2010, *102*, 1855-1873.

12. Pelletier, C.; Prognon, P.; Bourlioux, P. Roles of divalent cations and pH in mechanism of action of nitroxoline against *Escherichia coli* strains. *Antimicrob. Agents Chemother*. 1995, *39*, 707-712.

13. Zhou, Y.; Guo, X.; Yi, T.; Yoshimoto, T.; Pei, D. Two Continuous Spectrophotometric Assays for Methionine Aminopeptidase. *Anal. Biochem.* 2000, 280, 159-165.

14. Yu, Y.; Kim, H. S.; Chua, H. H.; Lin, C. H.; Sim, S. H.; Lin, D.; Derr, A.; Engels, R.; DeShazer, D.; Birren, B.; Nierman, W. C.; Tan, P. Genomic patterns of pathogen evolution revealed by comparison of *Burkholderia pseudomallei*, the causative agent of melioidosis, to avirulent *Burkholderia thailandensis*. *BMC Microbiol.* 2006, *6*, 46.

15. Anderson, M.S.; Garcia, E.C.; Cotter, P.A. The *Burkholderia bcpAIOB* Genes Define Unique Classes of Two-Partner Secretion and Contact Dependent Growth Inhibition Systems. *PLoS Genetics*. 2012, *8*, e1002877.

16. Schweizer, H.P.; Peacock, S.J. Antimicrobial Drug-Selection Markers for *Burkholderia pseudomallei* and *B. mallei*. *Em. Infect. Dis.* 2008, *14*, 1689-1692.